博士学位論文

レーザーフラッシュフォトリシスおよび光電気化学技術による DNA 内過剰電子移動の構造–特性関連に関する研究

林　士勛

2016 年 1 月

大阪大学大学院工学研究科

Preface

The studies presented in this dissertation were carried out under the direction of Professor Tetsuro Majima, the institute of Scientific and Industrial Research (SANKEN), Osaka University during April 2013 to March 2016.

The object of the dissertation is studies on excess-electron transfer in DNA by using femtosecond laser flash photolysis and the photoelectrochemical technique. The aim of the research is to determine the rate constants of excess-electron transfer and to investigate the mechanism of excess-electron transfer in DNA. The author hopes that these results and conclusion presented in this dissertation contributes to further understanding of excess-electron transfer in DNA and the development of bioelectronics applications such as DNA sensors and so on.

Shih-Hsun Lin

Department of Applied Chemistry
Graduate School of Engineering
Osaka University
2016

Contents

General Introduction

DNA, considered as a polymer established by alternating deoxyribose, phosphate groups, and the nucleobases, attracts attention of scientists from all kinds of research field. The sequence of paired nucleobases, which are π-aromatic compounds with H-bonds, forms a double helical structure with π stacking. Due to the well-ordered continuous π-π stacking, the charge transfer (CT) in DNA has been observed by Eley and Spivey over 40 years ago.[1] Since then, CT in DNA has attracted considerable attention from researchers. It is possible to apply DNA to nanoelectronics[2-4] or DNA sensor[5-7] and so on in the nanotechnological viewpoints. In a biological viewpoint, DNA is incessantly reacted with oxidants or reductants in environment. It is well-known that the oxidation of DNA promotes oxidative damage.[8,9] In contrast, the reduction of DNA can repair DNA lesions such as cyclobutane thymine−thymine (T−T) dimers.[10-13] These electron transfer (ET) between DNA and the oxidants or reductants is well-studied but our understanding of CT in DNA through nucleobases is limited.[14]

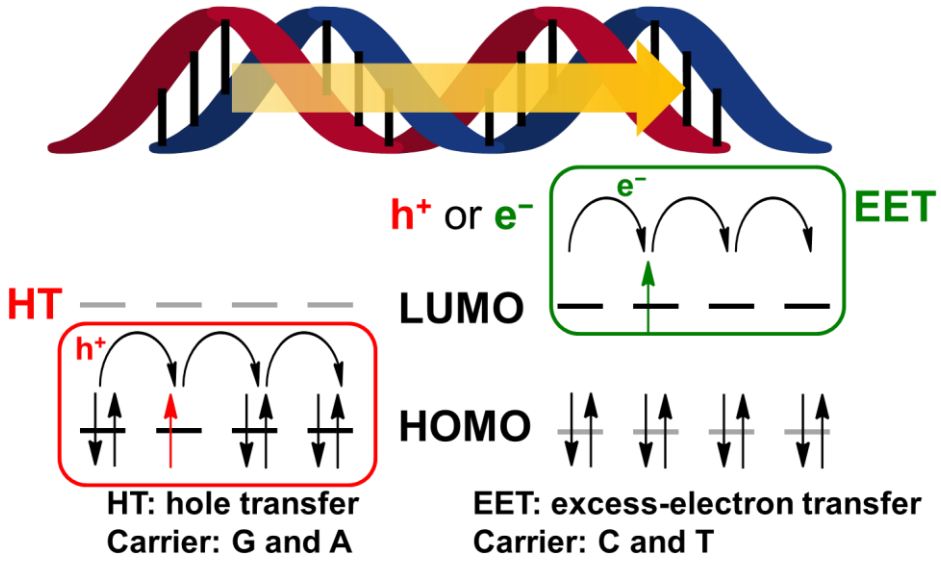

Figure 1. Comparison of photo-induced hole transfer and excess-electron transfer in DNA. The hole transfer is that the positive charge migrates through guanine (G) or Adenine (A) on the HOMO energy level. The excess-electron transfer is that the negative charge migrates through thymine (T) or cytosine (C) on the LUMO energy level.

To date, charge transfer in DNA can be classified to hole transfer as oxidation of a nucleobase by an adjacent radical cation and excess-electron transfer as reduction of a nucleobase by an adjacent radical anion from the mechanistic viewpoint.[15-17] Thus, “excess-

electron" means one additional electron in DNA, and has been used for differentiating from hole for long time. HT mainly occurs at guanine (G) and adenine (A) nucleotides and thus positive charge migrates through the HOMOs in DNA from a mechanistic viewpoint.[17] On the other hand, excess electron should migrate through the LUMOs of cytosine (C) and thymine (T) in DNA (Figure 1).[17] Thus, both processes, HT and EET transfer, are actually electron transfer reactions. However, it should be noted that both HT and EET processes are classified in regard to orbital energy level. These intrinsic differences between HT and EET is one of the reasons that numerous reviews have provided detailed summaries of HT in DNA but only limited data are available on EET in DNA.

Most researchers initiated their work on the oxidation of DNA, which relates to DNA damage as mentioned above, and, furthermore, on the mobility of the generated positively charged radical in the DNA. To study the dynamics of HT in DNA, photo-induced electron transfer (PET) has been commonly used. One of the common methods for study HT is measuring the hole transfer product generation after light irradiation in donor–DNA–acceptor system. Product analysis of oxidative reactions of DNA has provided valuable information on CT in DNA.[18,19] Moreover, investigations on HT in DNA by using laser flash photolysis have also provided deeply information on dynamics of HT in DNA including rate constants for single-step tunneling, or superexchange, and multistep hopping process, which was proposed by several groups such as Schuster,[20] Jortner,[21] Giese,[19] and Lewis,[22] by a random walk model and widely accepted (Figure 2). Thus, dynamics of HT have been studied in detail for decades, while the dynamics of EET in have just become clearer more recently.

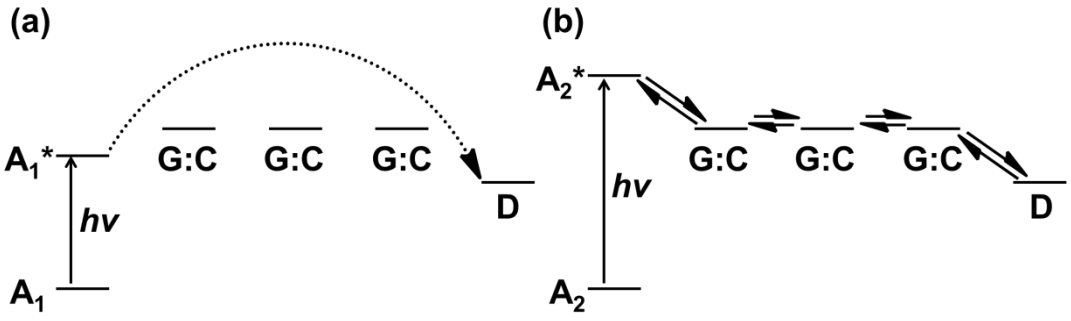

Figure 2. (a) Tunneling and (b) hopping mechanisms for photo-induced HT in DNA.

Because the tunneling process is expected to be strongly distance dependent and the hopping process weakly distance dependent, hopping mechanism for HT in DNA is expected to dominate long-distances HT and has been observed in several donor–DNA–acceptor

systems.[20,23,24] For quantitative investigation on the rate constants of HT in DNA, rate constants of HT can be expressed as an exponential function of the donor–acceptor distance (R_{DA}) as described by eq (1),[23-26]

$$k_{HT} = k_0 \times \exp(-\beta R_{DA}) \quad (1)$$

where β is the damping factor and k_0 is a temperature-dependent factor. When multistep hopping mechanism is operative (Figure 2b), β values as small as 0.1 $Å^{-1}$ have been reported.[19,24-29] For a deeper investigation, the laser flash photolysis technique has revealed detailed rate constants of single-step hole hopping in DNA. [24,30] In 2004, our lab have determined the rate constant of single-step hole hopping through a consecutive A sequence as 2×10^{10} s^{-1} in a donor–DNA–acceptor system by the nanosecond laser flash photolysis.[23] Lewis et al. also reported G-to-G and A-to-A hole hopping rate constants as 4.3×10^9 and 1.2×10^9 s^{-1}, respectively, in 2010.[30] Thus, single-step hole hopping takes several tens to hundreds picoseconds.

Although the study of HT in DNA has been conducted by several research groups with detailed kinetic information, the study of EET in DNA based on a suitable donor–DNA–acceptor system for time-resolved spectroscopic measurements is still limited. Sevilla and coworkers used γ-ray radiolysis to investigate the contribution of tunneling and hopping mechanisms of EET in DNA;[31,32] however, the site-selectivity of excess-electron injection and trapping processes cannot be confirmed in this experiment. In 2002, Carell et al. reported EET from photoexcited reduced flavin to TT dimer through DNA.[33,34] After UV irradiation, a cyclobutane TT dimer lesion will be generated in a consecutive T DNA sequence. The TT dimer can be repaired by DNA photolyase enzymes by the electron injection from reduced and deprotonated $FADH^-$ cofactor to TT dimer.[10] Thus, Carell and coworkers studied EET in dye-modified DNA which mimics the DNA repair process by DNA photolyase. From the generation yield of DNA fragment from the cycloreversion of TT dimer, they determined the β value to be 0.11 $Å^{-1}$, indicating EET by hopping mechanism. Furthermore, several research groups also employed product analysis to study EET in DNA and reported that hopping mechanism dominates EET in DNA.[35-39] Similar β values have been determined by photochemical product analysis of EET using reduced-flavin-sensitized cleavage of thymine oxetane (0.16 $Å^{-1}$, by Diederichsen et al.),[36] Ir(III)-sensitized loss of bromide from 5-bromouracil (0.12 $Å^{-1}$, by Barton et al.),[37] and pyrene-derivatives-sensitized loss of bromide from 5-bromouracil (0.22–0.26 $Å^{-1}$, by Lewis et al.).[38,39] Such small values indicate that the multistep hopping mechanism is operative. [33-39] The hopping mechanism indicates the

occurrence of multiple electron tunneling processes through DNA.[18] However, this principal setup is limited to understand dynamics of EET in DNA or to determinate rate constants of excess-electron hopping. Nevertheless, estimation of excess-electron hopping rate constants have been reported from the studies based on product analysis. By comparing with the debromination of 5-bromouracil radical anion, Lewis and co-workers suggested that the single-step excess-electron hopping rate constant between two 5-bromouracil separated by T is no faster than 10^7 s^{-1}.[38,39] From the comparison with the cycloreversion of TT dimer rate and debromination rate of 5-bromouracil radical anion, Carell group also reported that the electron-transfer rate along four A:T base pairs is within 1.8×10^7 to 1.4×10^8 s^{-1}.[40]

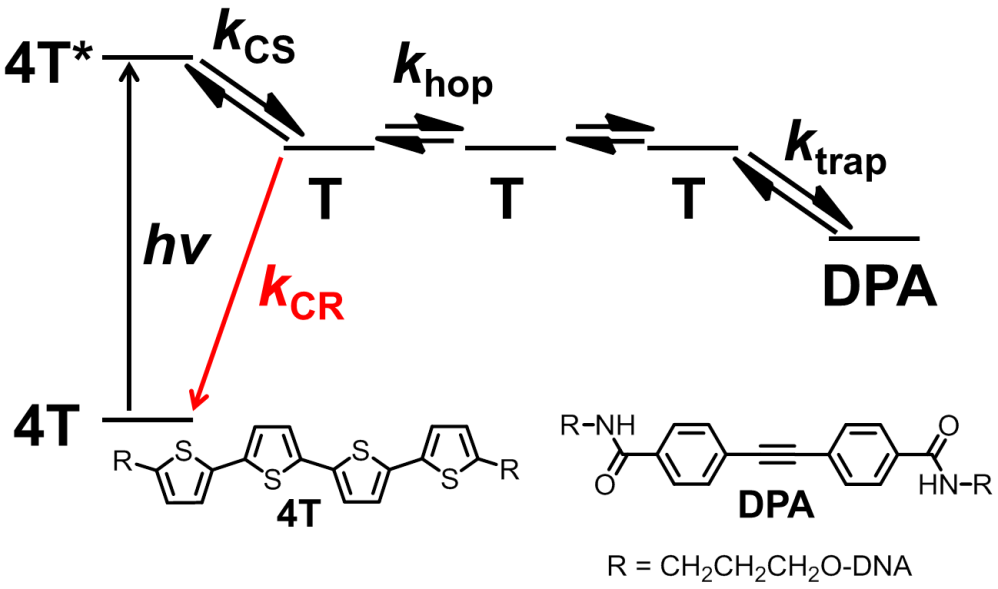

Figure 3. Illustration of EET in DNA by hopping mechanism in the **4T**−DNA−**DPA** system.

In 2011, our lab investigated EET in donor–DNA–acceptor system, in which tetrathiophene, **4T**, have been employed as a photosensitizing electron donor and diphenylacetylene derivative **DPA** as electron acceptor, using femtosecond laser flash photolysis (Figure 3). The rate constants of single-step excess-electron hopping (k_{hop}) among nucleobases were determined for the first time.[41] Furthermore, our lab also investigated the dynamics of EET in T consecutive sequences by *N*,*N*-dimethylaminopyrene (**APy**) and **DPA** as a photosensitizing electron donor and acceptor, respectively, in hairpin sturcture.[42] From a series of the studies on the basis of donor–DNA–acceptor system, the rate constant of excess-electron hopping among consecutive Ts was determined to be in the order of 10^{10}–10^{11} s^{-1}.[41,42] One of the key steps in the study of EET in DNA by using femtosecond laser flash

photolysis techniques is injection of excess electrons to DNA (charge separation, CS, with the rate constant k_{CS}) from a photo-sensitizing electron donor. For the transient absorption measurements, generation of the donor radical cation with a strong absorption band is preferable. The injected excess electrons are expected to migrate through the DNA by hopping mechanism, and then are trapped by an electron acceptor (electron trapping by **DPA**, with the rate constant k_{trap}) attached to the DNA to generate a detectable reduced acceptor. However, observation of long-distance EET was still difficult in donor–DNA–acceptor system with the nicked-dumbbell structure, due to the rapid charge recombination (CR, with the rate constant k_{CR}, the red arrow shown in Figure 3) which caused efficient regeneration of ground-state electron donor. Thus, for a detailed investigation of EET in DNA, an electron donor realizes slow charge recombination has to be employed.

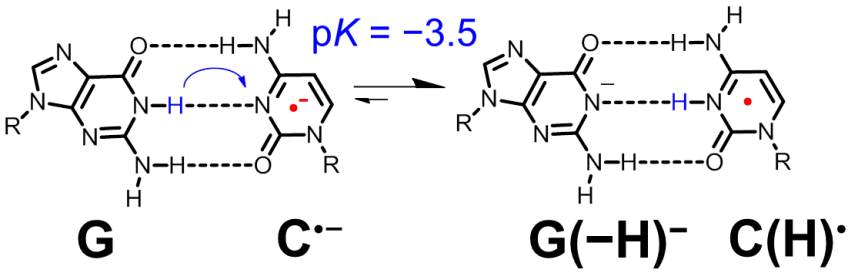

Scheme 1. Proposed proton-transfer reaction pathway for G:C$^{\bullet-}$ base pair.[40]

In addition, several issues are still under debate such as sequence dependence of EET in DNA. Although several groups including our lab have reported the dynamics of intrastrand EET in DNA through consecutive A:T sequences, however, it has been also noted that pH affects the dynamics of EET in DNA because the protonated C radical anion (C$^{\bullet-}$), which can be generated by proton transfer from the complementary base, G (Scheme 1), or from surrounding water molecules, will limit or terminate EET.[43] The sequence dependence of EET in DNA has also been investigated by means of product analysis by several researchers. In 2004, Ito and Rokita reported the sequence dependence of the debromination yield of 5-bromouracil as a consequence of EET in DNA. By comparing of the generation yield, they reported the contribution of C in EET is limited by protonation of C radical anion over T radical anion.[44] Wagenknecht group also reported that EET is highly sequence dependent and occurs more efficiently over A:T base pairs than over G:C base pairs on the basis of product analysis.[45] However, there was no kinetics information reported in these reports. Moreover, although the rate constant of proton transfer in G:C$^{\bullet-}$ base pairs (k_{PT}) was theoretically

calculated to be 10^{11} s^{-1},[46] it has not been determined directly. Thus, limited information is available on the effect of G:C base pairs on EET dynamics based on direct measurements. In addition, investigations on interstrand EET in alternating A:T sequences in DNA, in which interaction between the LUMOs of Ts does not exist, are still limited. For example, Carell and coworkers reported an interstrand EET in PNA:DNA double strands based on product analysis, which means an indirect measurement of interstrand EET in PNA:DNA double strands.[47] According to their results, the distance dependence of interstand EET efficiency was similar to that of intrastrand EET in DNA, indicating that both intrastrand and interstrand EET in DNA are efficient.

As mentioned above, there are unsolved issues in EET in DNA for researchers of this field. First, the distance of EET in donor–DNA–acceptor is still limited by using laser flash photolysis technique compared to that of HT. Although long-distance EET was proposed in the measurements based on photochemical product analysis methods, the rate constants for EET in DNA have not been clearly determined. Second, it is still under debate whether EET in DNA is sequence-dependent or not. In the product analysis experiments, the changes of EET efficiencies have been found; however, the rate constants of competitive processes such as proton transfer have not been determined experimentally. For a quantitative investigation on EET in DNA, determination for rate constants of each process is inevitable.

In order to study long-distance EET in donor–DNA–acceptor system with the nicked-dumbbell structure and explore the sequence dependence of EET in DNA quantitatively, a new photosensitizing electron donor with strongly electron donating ability is necessary. In addition, on the basis of our knowledge about thiophene-based materials, the author proposes to use oligomers based on EDOT (3,4-ethylenedioxythiophene), **2E** and **3E** in Figure 4, because of its high electron donating ability and well-known photochemical properties.[48] On the other hand, electrochemical studies on CT in DNA developed DNA sensors, which are highly sensitive to DNA structures such as mismatches and lesions that perturb the π-stacking between base pairs *in vitro*.[5-7] Furthermore, as seen in the state of the arts of organic solar cells, photon-to-electron conversions in π-stacking multichromophores have provided a new mode of signal transduction of DNA sensors based on the photoelectrochemistry.[7,49-51] Thus, by using the photoelectrochemical technique, a further understanding of long-distance EET in DNA can be investigated (Figure 4).

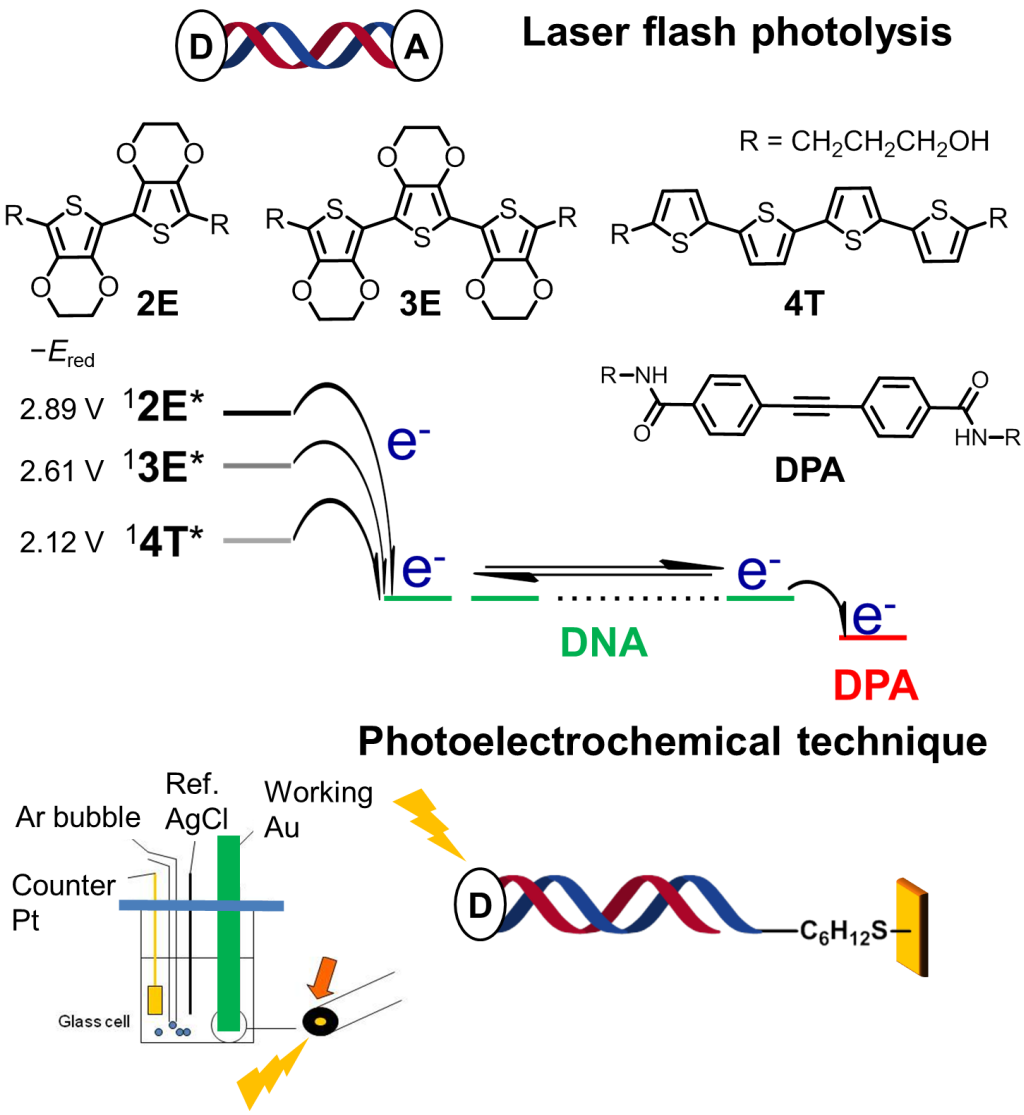

Figure 4. Simplified illustration of the strategies used in the present studies on EET in DNA.

To study the dynamics of EET in DNA, the author aimed to establish donor−DNA−acceptor system using femtosecond laser flash photolysis and photoelectrochemical technique (Figure 4). A quantitative investigation of EET in DNA has great potential for fundamental importance to fabricate DNA-based electronics and so on. The context of this dissertation consists of three chapters on the studies of EET in DNA. Introduction of each chapter is shown below.

In Chapter 1, the dynamics of excess-electron injection and charge recombination processes in the dyad molecules of oligothiophenes and nucleobases were clarified by using femtosecond laser flash photolysis.

In Chapter 2, a trimer of 3,4-ethylenedioxythiophene (EDOT) derivative was used as electron donor to study the sequence dependence of EET in DNA. From the DNA oligomers

contained G:C base pairs, dynamics in G:C$^{\bullet-}$ base pairs is estimated experimentally to clarify its role in EET in DNA in Chapter 2-1. In Chapter 2-2, the author clarified the role of LUMO interaction in the dynamics of EET in DNA by comparing intrastrand and interstrand EET in consecutive and alternating A:T sequences, respectively. In Chapter 2-3, the author used photoelectrochemical technique to study the dynamics of EET in DNA.

In Chapter 3, the author aimed to clarify energetic aspects of EET dynamics in donor–DNA–acceptor systems by employing various electron donors including a dimer of EDOT. The role of structural fluctuation in the excess-electron transfer in DNA is also discussed.

References

(1) Eley, D. D.; Spivey, D. I. *Trans. Faraday Soc.* **1962**, *58*, 411.

(2) Porath, D.; Bezryadin, A.; de Vries, S.; Dekker, C. *Nature* **2000**, *403*, 635.

(3) Fink, H. W.; Schonenberger, C. *Nature* **1999**, *398*, 407.

(4) Priyadarshy, S.; Risser, S. M.; Beratan, D. N. *J. Phy. Chem.* **1996**, *100*, 17678.

(5) Drummond, T. G.; Hill, M. G.; Barton, J. K. *Nat. Biotech.* **2012**, *21*, 1192.

(6) Paleček, E. Bartošík, M. *Chem. Rev.* **2012**, *112*, 3427.

(7) Zhao, W.-W.; Xu, J.-J.; Chen, H.-Y. *Chem. Rev.* **2014**, *114*, 7421.

(8) Burrows, C. J.; Muller, J. G. *Chem. Rev.* **1998**, *98*, 1109

(9) Armitage, B. *Chem. Rev.* **1998**, *98*, 1171.

(10) Carell, T. *Angew. Chem. Int. Ed.* **1995**, *34*, 2491.

(11) Sancar, A. *Biochemistry* **1994**, *33*, 2.

(12) Taylor, J. S. *Acc. Chem. Res.* **1994**, *27*, 76.

(13) Kneuttinger, A.C.; Kashiwazaki, G.; Prill, S.; Heil, K.; Müller, M.; Carell, T. *Photochem Photobiol.* **2014**, *90*, 1.

(14) Genereux, J. C.; Barton, J. K. *Chem. Rev.* **2010**, *110*, 1642.

(15) Wagenknecht, H.-A. *Nat. Prod. Rep.* **2006**, *23*, 973.

(16) Fujitsuka, M.; Majima, T. *Phys. Chem. Chem. Phys.* **2012**, *14*, 11234.

(17) Seidel, C. A. M.; Schulz, A.; Sauer, M. H. M. *J. Phys. Chem.* **1996**, *100*, 5541.

(18) Giese, B. *Acc. Chem. Res.* **2000**, *33*, 631.

(19) Giese, B.; Amaudrut, J.; Kohler, A.-K.; Spormann, M.; Wessely, S. *Nature* **2001**. 412, 318.

(20) Lewis, F. D.; Zhu, H. Daublain, P.; Fiebig, T.; Raytchev, M. Wang, Q. Shafirovich, V. *J. Am. Chem. Soc.* **2006**, *128*, 791.

(21) Jortner, J.; Bixon, M.; Langenbacher, T.; Michel-Beyerle, M. E. *Proc. Natl. Acad. Sci. U.S.A.* **1998**, *95*, 12759.

(22) Henderson, P. T.; Jones, D.; Hampikian, G.; Kan, Y.; Schuster, G. B. *Proc. Natl. Acad. Sci. U.S.A.* **1999**, *96*, 8353.

(23) Takada, T.; Kawai, K.; Cai, X.; Sugimoto, A.; Fujitsuka, M.; Majima, T. *J. Am. Chem. Soc.* **2004**, *126*, 1125.

(24) Kawai, K.; Majima, T. *Acc. Chem. Res.* **2013**, *46*, 2616

(25) Meggers, E.; Michel-Beyerle, M. E.; Giese, B. *J. Am. Chem. Soc.* **1998**, *120*, 12950.

(26) Marcus, R. A. *Angew. Chem. Int. Ed.* **1993**, *32*, 1111.

(27) Murphy, C.; Arkin, M.; Jenkins, Y.; Ghatlia, N.; Bossmann, S.; Turro, N.; Barton, J. *Science* **1993**, *262*, 1025.

(28) Berlin, Y. A.; Burin, A. L.; Ratner, M. A. *J. Phys. Chem. A* **2000**, *104*, 443.

(29) Berlin, Y. A.; Burin, A. L.; Ratner, M. A. *J. Am. Chem. Soc.* **2001**, *123*, 260.

(30) Conron, S. M. M.; Thazhathveetil, A. K.; Wasielewski, M. R.; Burin, A. L.; Lewis, F. D. *J. Am. Chem. Soc.* **2010**, *132*, 14388-14390.

(31) Cai, Z.; Gu, Z.; Sevilla, M. D. *J. Phy. Chem. B* **2000**, *104*, 10406.

(32) Messer, A.; Carpenter, K.; Forzley, K.; Buchanan, J.; Yang, S.; Razskazovskii, Y.; Cai, Z.; Sevilla, M. D. *J. Phy. Chem. B* **2000**, *104*, 1128.

(33) Behrens, C.; Burgdorf, L. T.; Schwögler, A.; Carell, T. *Angew. Chem. Int. Ed.* **2002**, *41*, 1763.

(34) Behrens, C.; Carell, T. *Chem. Commun.* **2003**, *14*, 1632.

(35) Ito, T.; Rokita, S. E. *J. Am. Chem. Soc.* **2003**, *125*, 11480.

(36) Stafforst, T.; Diederichsen, U. *Angew. Chem. Int. Ed.* **2006**, *45*, 5376.

(37) Elias, B.; Shao, F.; Barton, J. K. *J. Am. Chem. Soc.* **2008**, *130*, 1152.

(38) Daublain, P.; Thazhathveetil, A. K.; Wang, Q.; Trifonov, A.; Fiebig, T.; Lewis, F. D. *J. Am. Chem. Soc.* **2009**, *131*, 16790.

(39) Daublain, P.; Thazhathveetil, A. K.; Shafirovich, V.; Wang, Q.; Trifonov, A.; Fiebig, T.; Lewis, F. D. *J. Phys. Chem. B* **2010**, *114*, 14265.

(40) Fazio, D.; Trindler, C.; Heil, K.; Chatgilialoglu, C.; Carell, T. *Chem.—Eur. J.* **2011**, *17*, 206.

(41) Park, M. J.; Fujitsuka, M.; Kawai, K.; Majima, T. *J. Am. Chem. Soc.* **2011**, *133*, 15320.

(42) Park, M. J.; Fujitsuka, M.; Nishitera, H.; Kawai, K.; Majima, T. *Chem. Commun.* **2012**, *48*, 11008.

(43) Steenken, S.; Telo, J. P.; Novais, H. M.; Candeias, L. P. *J. Am. Chem. Soc.* **1992**, *114*,

4701.

(44) Ito, T.; Rokita, S. E. *Angew. Chem., Int. Ed.* **2004**, *43*, 1839.

(45) Wagner, C.; Wagenknecht, H.-A. *Chem.— Eur. J.* **2005**, *11*, 1871.

(46) Chen, H.-Y.; Kao, C.-L.; Hsu, S. C. N. *J. Am. Chem. Soc.* **2009**, *131*, 15930.

(47) Cichon, M. K.; Haas, H. C.; Grolle, F.; Mees, A.; Carell, T. *J. Am. Chem. Soc.* **2002**, *124*, 13984.

(48) Turbiez, M.; Frère, P.; Roncali, J. *J. Org. Chem.* **2003**, *68*, 5357.

(49) Okamoto, A.; Kamei, T.; Tanaka, K.; Saito, I. *J. Am. Chem. Soc.* **2004**, *126*, 14732.

(50) Tanabe, K.; Iida, K.; Haruna, K.-i.; Kamei, T.; Okamoto, A.; Nishimoto, S.-i. *J. Am. Chem. Soc.* **2006**, *128*, 692

(51) Takada, T.; Lin, C.; Majima, T. *Angew. Chem. Int. Ed.* **2007**, *46*, 6681.

Chapter 1. Driving Force Dependence of Charge Separation and Recombination: Driving Force Dependence of Charge Separation and Recombination Processes in Dyads of Nucleotides and Strongly Electron-Donating Oligothiophenes

Abstract

Charge transfer in DNA has attracted great attention of scientists because of its importance in biological processes. However, our knowledge on excess-electron transfer in DNA still remains limited when compared to numerous studies of hole transfer in DNA. To clarify the dynamic of excess-electron transfer in DNA by photochemical techniques, new electron-donating photosensitizers should be developed. Herein, a terthiophene and two 3,4-ethylenedioxythiophene oligomers were used as photosensitizers in dyads including natural nucleobases as electron acceptors. The charge separation and recombination processes in the dyads were investigated by femtosecond laser flash photolysis, and the driving force dependence of these rate constants was discussed on the basis of the Marcus theory. From this study, the conformation effect on charge recombination process was found. The author expect that 3,4-ethylenedioxythiophene oligomers are useful in investigation of excess-electron transfer dynamics in DNA.

Introduction

Charge transfer (CT) in DNA by hopping and tunneling processes through the nucleobases with well-ordered continuously π-π stacking has attracted attention of scientists for decades. From the mechanistic viewpoint, CT in DNA can be classified to hole transfer (HT) as oxidation of a nucleobase by an adjacent radical cation and excess-electron transfer (EET) as reduction of a nucleobase by an adjacent radical anion. In the HT in DNA, it has been well established that guanine (G) and adenine (A), which exhibit relatively low oxidation potentials, act as hole carriers; in contrast, in the EET in DNA, thymine (T) and cytosine (C) are expected to be the excess electron carriers due to their high reduction potentials.[1-3] One of the key steps in the study of EET in DNA by photochemical techniques is an excess electron injection to DNA from a photosensitizing electron donor, which possesses sufficiently low oxidation potential in the excited state (E_{OXS1}) to reduce a nucleobase. Various photosensitizers, such as stilbenediether,[4,5] pyrene and its derivatives,[6-9] and phenothiazine,[10] have been used to investigate the electron injection to DNA by femtosecond laser flash photolysis. In the previous reports, the author used dimer and tetramer of thiophene (**2T** and **4T**) as the photosensitizing electron donors because of their high electron donating ability and well-known photochemical properties.[11,12] In these studies, it was confirmed that singlet excited **2T** and **4T** can donate an electron to both T and C. Furthermore, the excess electron injection from **2T** to A was confirmed, indicating that EET through consecutive As could be examined.[12] For the study of the EET in DNA with various sequence, a new donor with an electron donor ability higher than **2T** and **4T** should be employed.

In the present study, as a photosensitizing electron donor, the author used dimer and trimer (**2E** and **3E**, respectively) of 3,4-ethylenedioxythiophene (EDOT)[13] and terthiophene (**3T**) as a reference (Figure 1-1). Because of strongly electron donating nature of the ether substituent, EDOT-based oligomers are expected to reduce various nucleobases efficiently. The redox and spectroscopic properties of EDOT-based oligothiophenes are compared with those of oligothiophenes in Table 1-1. To clarify dynamics of excess electron injection process, the dyad molecules of oligothiophene and nucleotide (Figure 1-1) were examined by femtosecond laser flash photolysis in this study. In all dyads, oligothiophenes were tethered to 3'-position of nucleobases. The present study revealed that the charge separation (CS) and charge recombination (CR) processes in these dyads can be analyzed by the Marcus theory and conformation of the dyad structure has an important role in the ET dynamics.

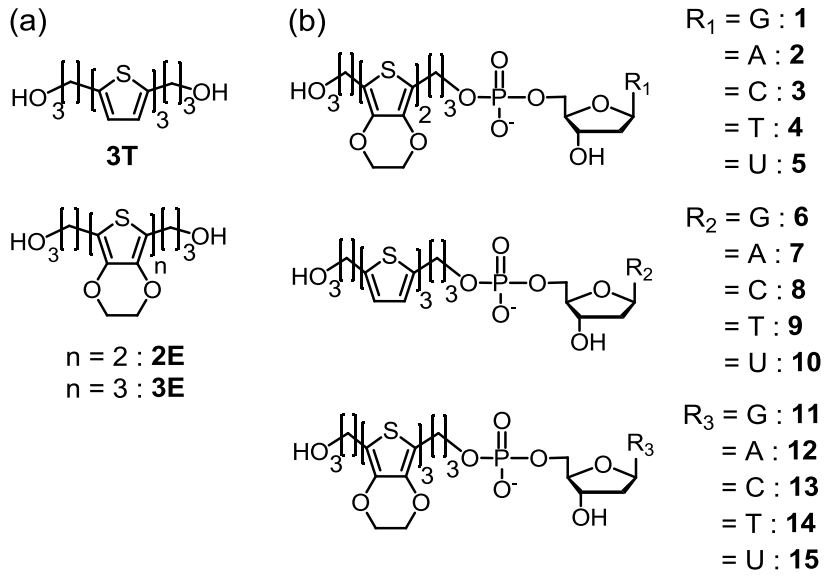

Figure 1-1. Structures of (a) **2E**, **3T**, and **3E**, and (b) dyads **1-15**.

Table 1-1. Oxidation potentials in the ground (E_{OX}) and singlet excited state (E_{OXS1}), singlet excitation energy (E_{S1}), and absorption peak positions in the singlet excited state (λ_{S1}) and radical cation state ($\lambda^{\bullet+}$) of oligothiophenes, **2T** and **3T**, and oligo(EDOT)s, **2E** and **3E**.

	E_{OX}[a] (V)	E_{S1}[b] (eV)	E_{OXS1}[a, c] (V)	λ_{S1} (nm)	$\lambda^{\bullet+}$ (nm)
2T[d]	1.28	3.53	−2.25	503	445
2E	0.65[e]	3.54	−2.89	530[f]	440[f]
3T	1.19[e]	3.08	−1.89	605[f]	585[f]
3E	0.41[e]	3.02	−2.61	620[f]	536[f]

[a] Units: V versus NHE. [b] Estimated from the cross-point of the absorption and fluorescence spectra. [c] $E_{OXS1} = E_{OX} - E_{S1}$. [d] From ref. 12 and 14 [e] From ref. 13. [f] This study.

Experimental Section

Synthesis of 2E

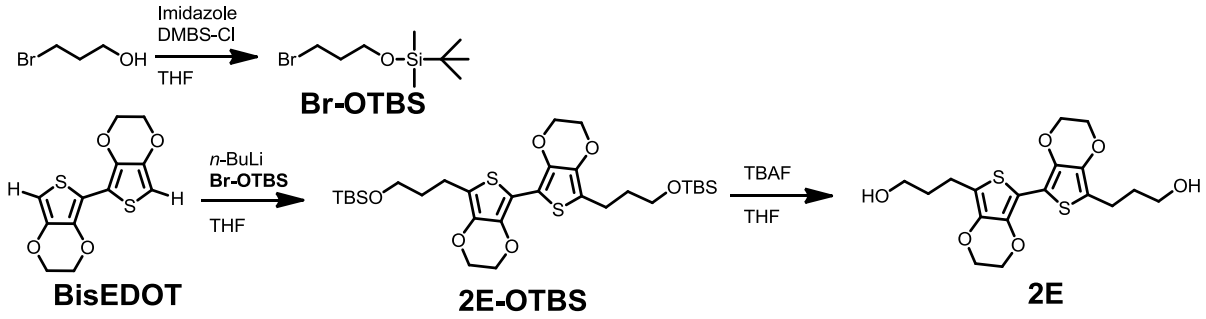

Scheme 1-1. Synthesis of **2E**.

2E was synthesized according to the procedure in the reference paper[13] using **BisEDOT**[15] and **Br-OTBS**[16] as starting materials (Scheme 1-1). Yield of two-step reaction was 40%. Due to the very poor solubility of **2E**, the corresponding ^{13}C NMR spectrum was not determined: mp 184-186 °C; ^{1}H NMR (400 MHz, $CDCl_3$) δ 1.85 (m, 4H), 2.77 (t, J = 7.2 Hz, 4H), 3.66 (q, J = 5.6 Hz, 4H), 4.31−4.22 (m, 8H) ppm; FAB-HRMS calcd for $C_{18}H_{22}O_6S_2$ 398.09, found 398.08.

Synthesis of 3E

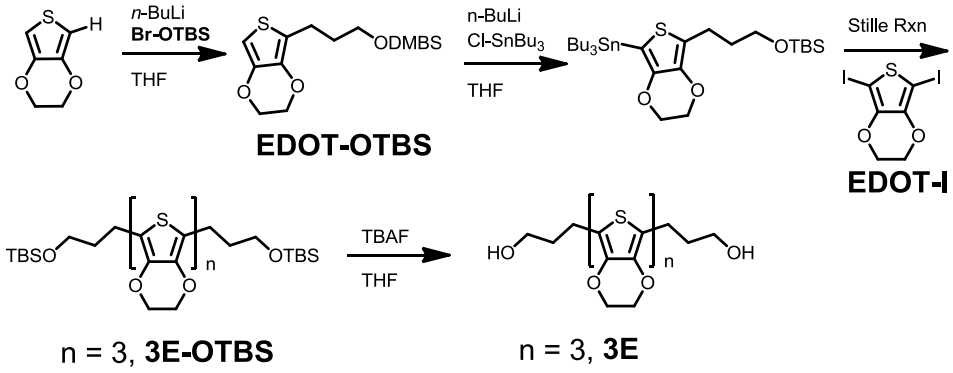

Scheme 1-2. Synthesis of **3E**

The synthesis of **EDOT-OTBS** is similar to the one of **2E-OTBS** (Scheme 1-2). Yield: 15%; Colorless oil; ^{1}H NMR (400 MHz, $CDCl_3$) δ 0.05 (m, 6H), 0.90 (s, 9H), 1.84 (m, 4H), 2.71 (t, J = 7.2 Hz, 2H), 3.65 (t, J = 5.2 Hz, 2H), 4.17 (m, 4H), 6.11 (s, 1H) ppm; ^{13}C NMR (100 MHz, $CDCl_3$) δ −5.33, 18.30, 22.25, 25.92, 33.26, 62.16, 64.49, 64.65, 95.14, 117.62, 137.55, 141.45 ppm; FAB-HRMS calcd for $C_{15}H_{26}O_3SSi$ 314.14, found 315.15 ([M+H$^+$]).

3E-OTBS was synthesized according to the reported procedure (Scheme 1-2).[13] Yield: 35%; mp 238-240 °C; ^{1}H NMR (400 MHz, $CDCl_3$) δ 0.05 (m, 12H), 0.90 (s, 18H), 1.84 (m, 4H), 2.71 (t, J = 7.2 Hz, 4H), 3.66 (t, J = 6.4 Hz, 4H), 4.36−4.20 (m, 12H). ^{13}C NMR (100 MHz, $CDCl_3$) δ −5.27, 18.35, 22.20, 25.98, 33.32, 62.28, 64.51, 64.94, 65.13, 106.06, 107.81, 115.65, 136.00, 136.59, 137.24; FAB-HRMS calcd for $C_{36}H_{54}O_8S_3Si_2$ 766.25, found 766.25.

The synthetic procedure of **3E** form **3E-OTBS** was the same as the one of **2E** (Scheme 1-2). Yield: 90%. Due to the very poor solubility of **2E**, the corresponding ^{13}C NMR spectrum was not determined: mp 192-194 °C; ^{1}H NMR (400 MHz, $CDCl_3$) δ 1.85 (m, 4H), 2.77 (t, J = 7.2 Hz, 4H), 3.66 (m, 4H), 4.31−4.22 (m, 12H); FAB-HRMS calcd for $C_{24}H_{26}O_8S_3$ 538.08, found 538.08.

Synthesis of 3T

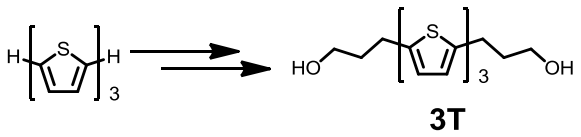

3T

Scheme 1-3. Synthesis of **3T**.

3T was synthesized according to the reported procedure (Scheme 1-3) and the ^{1}H NMR spectrum was the same as the literature data.[17]

DNA Synthesis. The sensitizers, **2E**, **3T**, and **3E**, were converted to corresponding phosphoramidite derivatives by similar procedures as previously reported.[17,18] All reagents were purchased from Glen Research (USA). All dyad molecules were synthesized on an Applied Biosystems 3400 DNA synthesizer with standard solid-phase techniques and purified on a JASCO HPLC with a reversed-phase C-18 column with an acetonitrile/ammonium formate (50 mm) gradient. The dyad compounds were characterized by MALDI-TOF mass spectroscopy (Table 1-2).

Table 1-2. MALDI-TOF MS of DNA dyads.

	Calculated	Found		Calculated	Found		Calculated	Found
1	727.143	726.494	**6**	693.598	694.431	**11**	867.132	866.301
2	711.148	710.486	**7**	677.603	678.069	**12**	851.137	851.071
3	687.137	686.760	**8**	653.592	653.910	**13**	827.126	826.998
4	702.136	701.208	**9**	668.591	668.114	**14**	842.125	841.881
5	688.121	687.559	**10**	654.576	654.210	**15**	828.110	827.469

Apparatus. Steady-state absorption and fluorescence spectra were measured using a Shimadzu UV-3100PC and Horiba FluoroMax-4P, respectively. The subpicosecond transient absorption spectra were measured by the pump and probe method using a regeneratively amplified Ti:sapphire laser (Spectra Physics, Spitfire Pro F, 1 kHz) pumped by a Nd:YLF laser (Spectra Physics, Empower 15). The seed pulse was generated by the Ti:sapphire laser (Spectra Physics, MaiTai VFSJ-W). Samples were excited using 345, 370, or 400 nm laser pulse. The 345 and 370 nm laser pulses were generated by an optical parametric amplifier,[19] while the 400 nm lase pulse was the second harmonic generation of output of the amplifier. A white continuum pulse, which was generated by focusing the residual of the fundamental light to a sapphire plate after a computer controlled optical delay, was divided into two parts and used as the probe and the reference lights, of which the latter was used to compensate the laser fluctuation. The both probe and reference lights were directed to a rotating sample cell with 1.0 mm of optical path and were detected with a charge-coupled device detector equipped with a polychromator (Solar, MS3504).

Results and Discussion

Steady-state absorption spectra of **1**−**15** are shown in Figures 1-2. Absorption bands due to **2E**, **3T**, and **3E** appeared in the wavelength region longer than 300 nm for all dyads, while absorption bands around 275 nm are attributable to nucleobases. Fluorescence from the oligothiophene of the dyads was observed by selective excitation of oligothiophene as shown in Figures 1-2. It is clear that fluorescence intensity largely depends on the nucleobase, while peak position depends on oligothiophenes. To understand variations in the fluorescence intensity, driving forces for CS and CR ($-\Delta G_{CS}$ and $-\Delta G_{CR}$, respectively) were calculated using eq. (1-1) and (1-2),[3,20]

$$-\Delta G_{CS} = -(E_{OXS1} - E_{RED} + C) \quad (1\text{-}1)$$

$$-\Delta G_{CR} = -(E_{RED} - E_{OX} + C) \quad (1\text{-}2)$$

where E_{RED} and E_{OX} are the reduction potential of the nucleobases and oxidation potential of oligothiophenes (Table 1-1) reported in literature.[3] C is the Coulombic term, which was estimated to be −0.1 eV.[20] From Table 1-3, it was confirmed that the extent of fluorescence quenching increased as an increase in the $-\Delta G_{CS}$ value, indicating contribution of photoinduced CS in deactivation pathway of the singlet excited oligothiophenes. Notably, dyad **1** also showed fluorescence with reduced intensity, indicating a possibility that G acts as an electron acceptor by using **2E** as a donor. Similar fluorescence quenching was observed with dyads with **3E** and **3T** except for the cases of **6**, **7**, and **11**, as expected from the highly negative $-\Delta G_{CS}$ values, supporting the CS from the excited **3E** and **3T**. Because of the delay fluorescence, which is caused by the CR process, quantitative correlation between fluorescence intensity and the CS rate constant was not discussed.

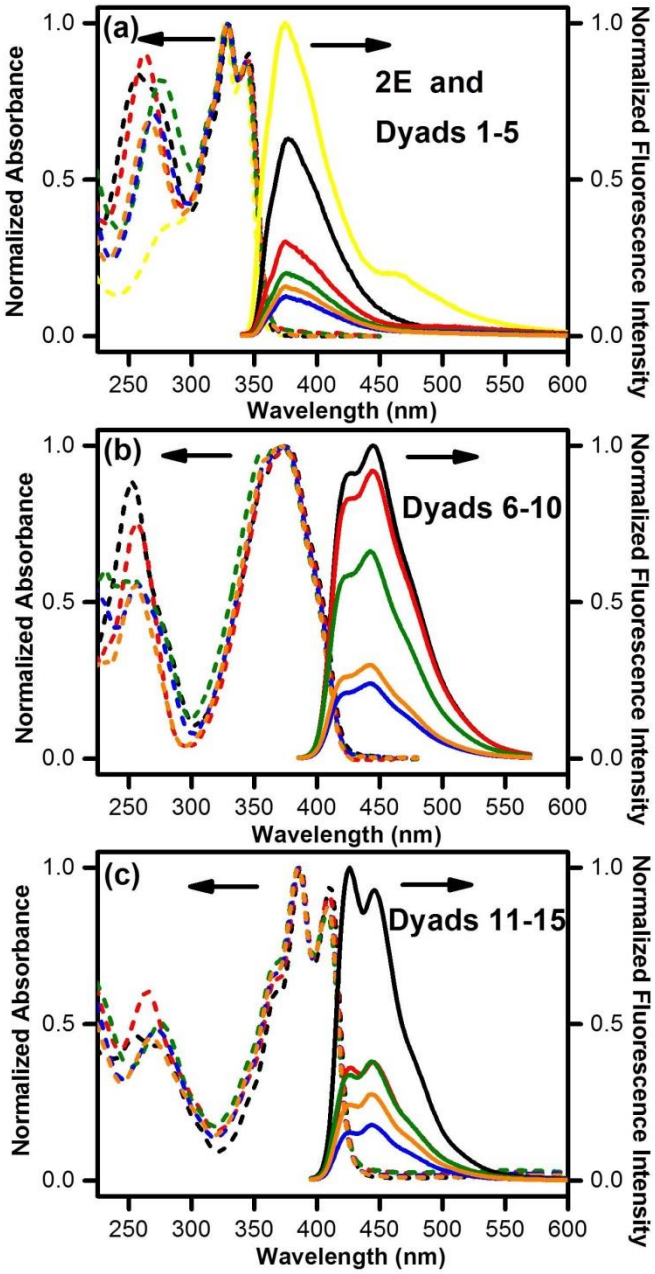

Figure 1-2. Normalized absorption (dashed lines) and fluorescence (solid lines) spectra of (a) **2E** (yellow) and **1** (black), **2** (red), **3** (green), **4** (blue), and **5** (orange), (b) dyads **6** (black), **7** (red), **8** (green), **9** (blue), and **10** (orange), and (c) dyads **11** (black), **12** (red), **13** (green), **14** (blue), and **15** (orange) in NaCl (0.1 M) and sodium phosphate (10 mM, pH 7.0).

Table 1-2. Driving forces ($-\Delta G_{CS}$ and $-\Delta G_{CR}$) and rate constants (k_{CS} and k_{CR}) of CS and CR in dyads **1-15**.

Dyad	$-\Delta G_{CS}$[a] (eV)	k_{CS}[b] (s^{-1})	$-\Delta G_{CR}$[a] (eV)	k_{CR}[c] (s^{-1})
1	0.01	6.4×10^{11}	3.63	1.1×10^{11}
2	0.32	1.0×10^{12}	3.32	6.7×10^{10}
3	0.54	7.7×10^{11}	3.10	2.9×10^{11}
4	0.63	1.0×10^{12}	3.01	3.8×10^{11}
5	0.73	2.5×10^{12}	2.91	3.4×10^{11}
6	−0.75	--[d]	3.93	--[d]
7	−0.44	--[d]	3.62	--[d]
8	−0.22	3.5×10^{10}	3.40	6.5×10^{9}
9	−0.13	5.8×10^{10}	3.31	6.5×10^{9}
10	−0.03	8.7×10^{10}	3.21	7.3×10^{9}
11	−0.27	--[d]	3.39	--[d]
12	0.04	1.1×10^{11}	3.08	8.3×10^{10}[e]
13	0.26	1.1×10^{12}	2.86	2.8×10^{11}[e]
14	0.35	1.8×10^{12}	2.77	3.7×10^{11}[e]
15	0.45	2.0×10^{12}	2.67	3.7×10^{11}[e]

[a] $-\Delta G_{CS}$ and $-\Delta G_{CR}$ were calculated using eq. (1-1) and (1-2), respectively. [b] Estimated error is less than 20%. [c] Estimated error is less than 10%. [d] Not observed. [e] Rate constant of the fast component.

CS dynamics of the oligothiophene-nucleotide dyads were investigated by transient absorption measurements. The femtosecond laser flash photolysis studies were carried out by selective excitation of photosensitizers, **2E**, **3T**, and **3E**. As a representative case, the transient absorption spectra and a kinetic trace of ΔO.D. of **12** are shown in Figures 1-3a and 1-3b, respectively. In Figure 1-3a, **12** showed an absorption band at 620 nm immediately after the excitation, which is attributed to ^{1}**3E*** generated by the laser pulse. With the decay of the absorption band at 620 nm within 10 ps approximately, an absorption band at 536 nm appeared concomitantly. Because the 536 nm band is similar to the absorption band of **3T**$^{\bullet+}$ in position, this band is attributed to **3E**$^{\bullet+}$, indicating the electron injection from ^{1}**3E*** to A in accordance with the positive $-\Delta G_{CS}$ value. The CS states were deactivated by CR to generate

the ground state mainly. Spectra observed at longer delay time (longer than hundreds picoseconds) can be attributed to solvated electron, which did not participate in reduction of nucleobase. Figure 1-3b shows its kinetic trace and a fitted curve assuming 1.1×10^{11} s^{-1} of a rising component as well as a decay discussed later. Similar CS processes were confirmed with all dyads except for **6**, **7**, and **11**, which exhibited only absorption band of the singlet excited state of photosensitizing electron donors, indicating the absence of CS due to highly negative $-\Delta G_{CS}$ values. The transient absorption spectra of **2E** and **1**−**15** are shown in Figures 1-5, 1-6, and 1-7.

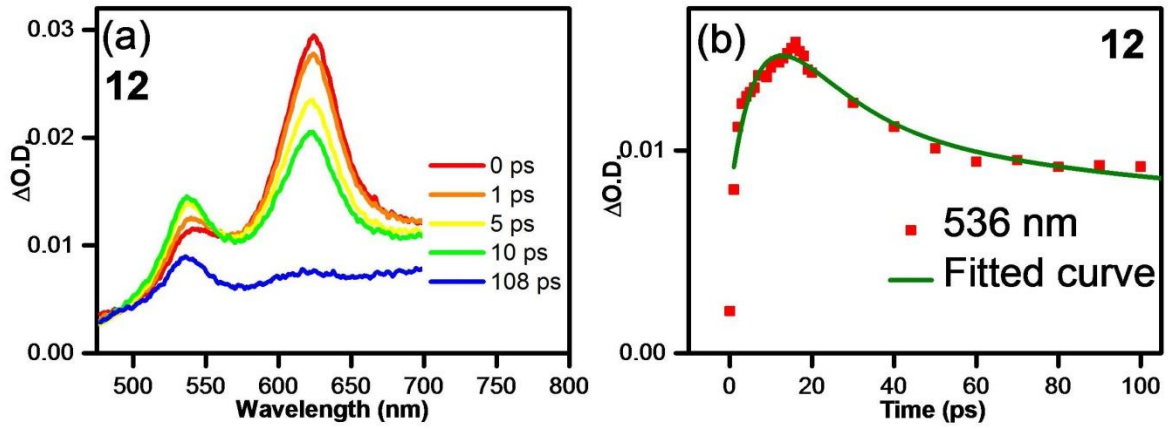

Figure 1-3. (a) Transient absorption spectra of **12** during laser flash photolysis using 400 nm femtosecond laser pulse as the excitation pulse. (b) The kinetic trace of ΔO.D. at 536 nm of **12** (red square) and fitted curve (green line).

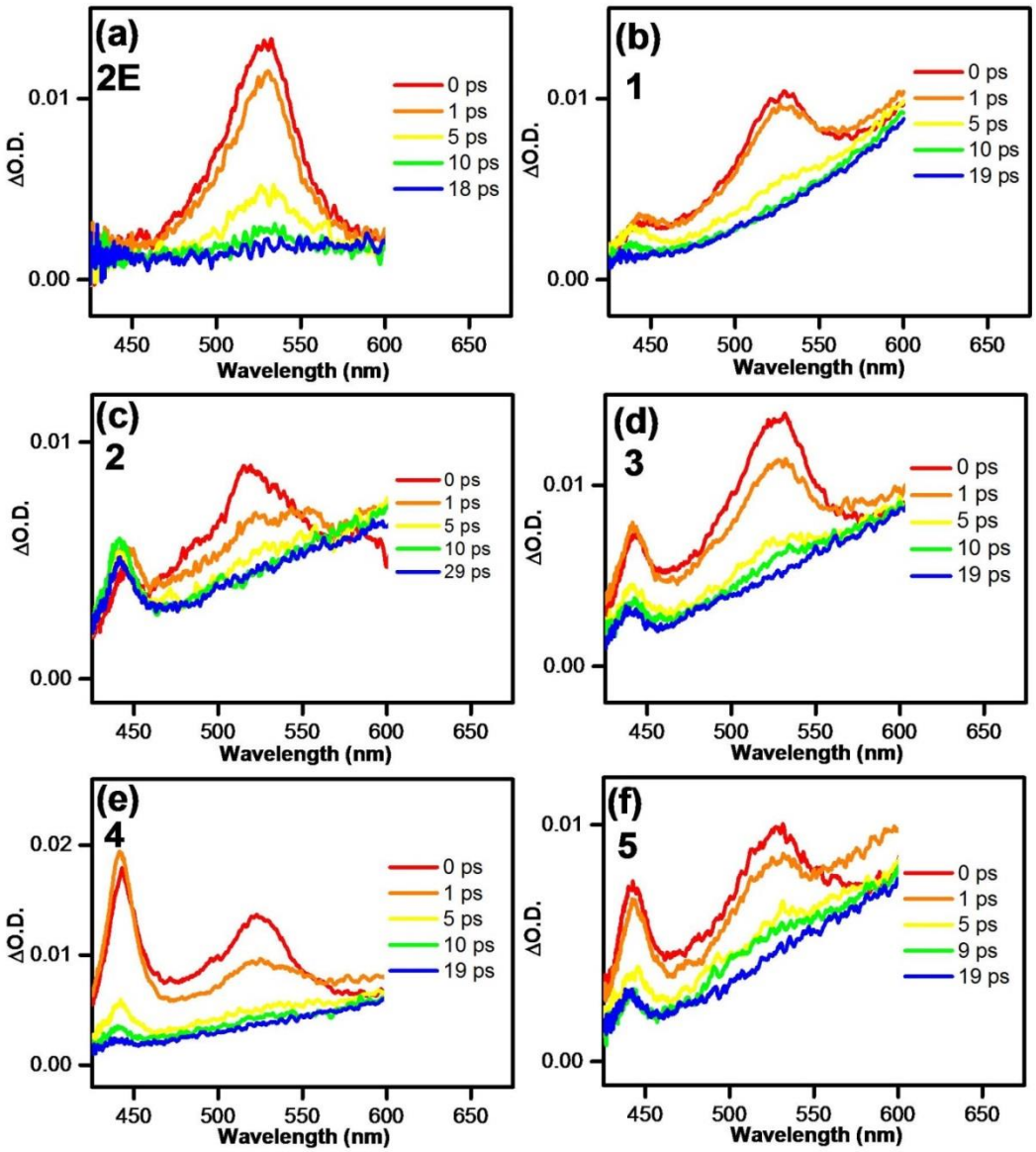

Figure 1-4. Transient absorption spectra during the laser flash photolysis of **2E** and dyad **1**–**5** upon excitation with 345-nm femtosecond laser pulse.

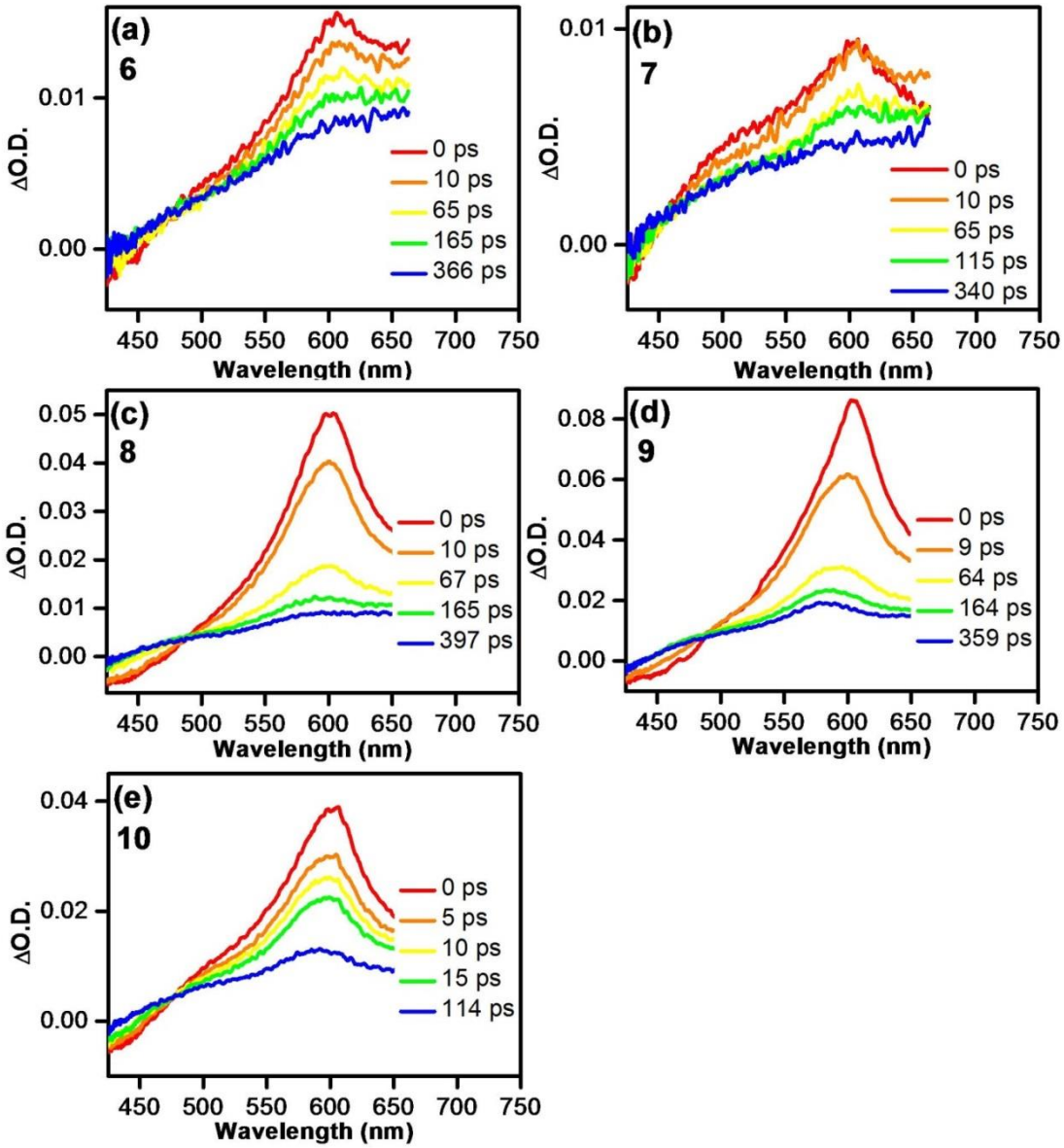

Figure 1-5. Transient absorption spectra during the laser flash photolysis of dyads **6**–**10** upon excitation with 370-nm femtosecond laser pulse.

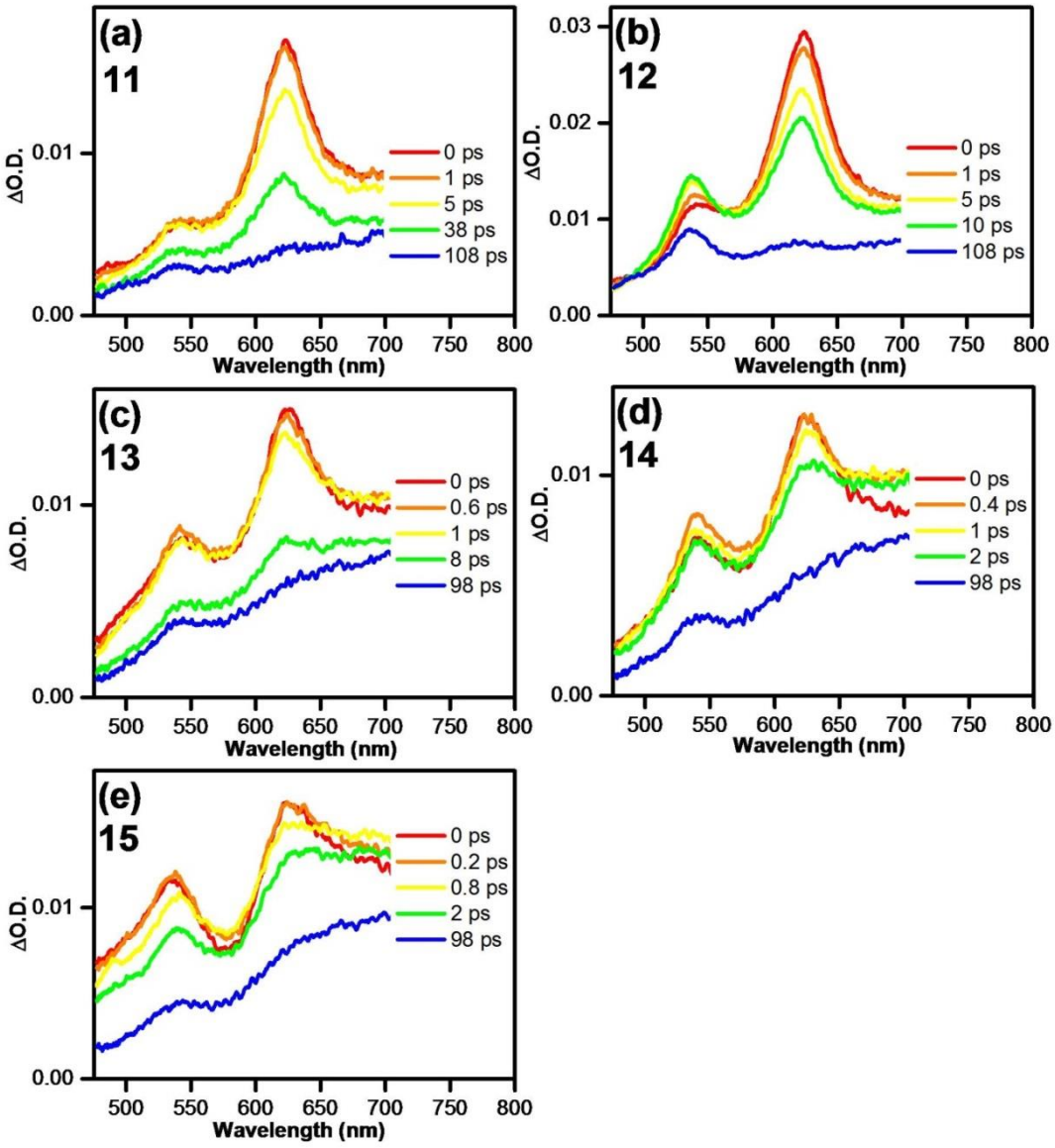

Figure 1-6. Transient absorption spectra during the laser flash photolysis of dyads **11**–**15** upon excitation with 400-nm femtosecond laser pulse.

The rate constants of CS (k_{CS}) of all dyads were obtained by applying a single exponential function to the rising kinetic profile of oligothiophene radical cation and by applying a single exponential function to the decaying kinetic profile of singlet excited oligothiophene. The rate constants for CR (k_{CR}) were obtained by applying single exponential function to the decaying kinetic profile of oligothiophene radical cation. For dyads **12**–**15**, dual exponential function has to be applied to realize an adequate fit. The estimated rate constants are summarized in Table 1-2 along with the driving force ($-\Delta G$) values. Notably, CS was confirmed even when G was used as the electron acceptor, despite G is known as a hole carrier in DNA.[1,2] In addition, the CS process in dyad with A as the electron acceptor was accelerated by using stronger electron donating photosensitizer (**2E** and **3E**) compared to our previous report.[12] Thus, these results indicate that all natural nucleobases act as an acceptor of an excess electron by using EDOT oligomers as electron donors.

As indicated in the above section, **12**–**15** decayed according to the dual exponential function (Table 1-3). Like dinucleobases dyads, the donor-acceptor dyads are expected to exist in various conformations in solution, which can be classified to stacked and unstacked forms as shown in Figure 1-7. The conformational changes have large effects on various kinetics in dinucleobases dyads and donor-acceptor dyads as indicated by both experimental[21-29] and theoretical studies.[26,30-32] The author assumed that the fast and slow rate constants are due to the stacked and the unstacked forms, respectively, because faster CS and CR will be possible with shorter donor-acceptor distance in the stacked form (Figure 1-7). Because time scale for the stacking/unstacking conformational change is reported to be on the order of 10 ns,[32] conformational change will not compete with the CS and CR processes. If the author assume identical extinction coefficients for oligothiophene radical cations in the stacked and unstacked forms, the ratio of the pre-exponential factor, F_s, will represent ratio of the stacked and unstacked forms. From this assumption, it is indicated that 15-40% of dyads are in the unstacked form, while 60-85% are in the stacked form (Table 1-3). Notably, major contribution of the stacked form was also indicated by the theoretical calculation for ground state of dinucleobases dyads and dimers.[31,32] In the case of CS processes of **12**–**15**, contributions of the stacked and unstacked forms are also expected, while they are hard to be distinguished because of fast kinetics. From the F_s values in Table 1-3 and results of theoretical works, the stacked form is expected to contribute to the kinetics mainly. For dyads expect for **12**–**15**, stacked forms can be taken into account.

Table 1-3. Rate constants (k_{CR} and $k_{CR'}$) and pre-exponential factors (A and A') of CR in dyad **12-15**.

Dyad	k_{CR}[a] (10^{10} s^{-1})	$A \times 10^3$ [a]	$k_{CR'}$[a] (10^{10} s^{-1})	$A' \times 10^3$ [a]	F_s[b]
12	8.3	34	1.1	5.8	0.85
13	28	2.7	0.47	1.6	0.63
14	37	2.1	1.1	1.4	0.60
15	37	3.4	0.81	1.8	0.65

[a] Estimated error is less than 10%. [b] $F_s = A/(A + A')$, which was estimated as the fraction of stacked form of dyads in solution.

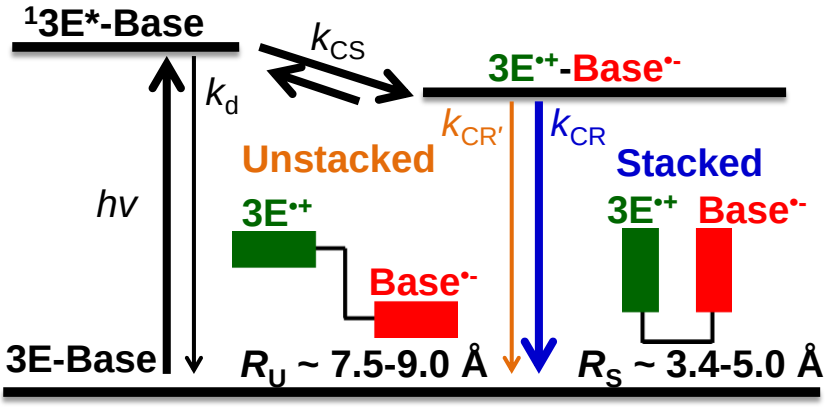

Figure 1-7. Proposed schematic energy diagram of CS and CR of **3E** dyads (**12-15**). R_U and R_S are the distance between **3E** and nucleobase (A, C, T, and U) in the stacked[30-33] and unstacked forms[30,34], respectively. k_{CR} and $k_{CR'}$ are the CR rate constants in the stacked and unstacked forms, respectively.

It is evident from the estimated rate constants, the k_{CS} value became larger with an increase in the $-\Delta G_{CS}$ value and the k_{CR} value became smaller with an increase in the $-\Delta G_{CR}$ value, thereby indicating that both CS and CR processes in **1**–**15** comply with the Marcus theory.[35,36] This relationship became clear when the observed rate constants were plotted against the $-\Delta G$ ($-\Delta G_{CS}$ and $-\Delta G_{CR}$) values (Figure 1-8). It is noted that for **12**−**15**, only k_{CR} values of the stacked form were included in Figure 1-8. According to the Marcus theory, the electron-transfer rate (k_{ET}) can be expressed using eq. (1-3).[36]

$$k_{ET} = \sqrt{\frac{\pi}{\hbar^2 \lambda_S k_B T}} |V|^2 \sum_m \left(e^{-S} \left(\frac{S^m}{m!} \right) \right) \exp\left(- \frac{(\lambda_S + \Delta G + m\hbar\langle\omega\rangle)^2}{4\lambda_S k_B T} \right) \quad (1\text{-}3)$$

$$S = \frac{\lambda_V}{\hbar\langle\omega\rangle} \quad (1\text{-}4)$$

In eq. (1-3), λ_S is the solvent reorganization energy, V is the electronic coupling, S is the electron-vibration coupling constant given by eq (1-4), and $\langle\omega\rangle$ is the averaged angular frequency. In eq. (1-4), λ_V is the internal reorganization energy. Along with our previous report,[12] the rate constants of CS and CR processes were well-reproduced by the Marcus theory with the parameters similar to the ones of hole injection and recombination processes.[37] For CS and CR processes in photosensitizer-nucleotide dyads, this result yields valuable insights that the dynamics of oxidation and reduction of nucleobases by photosensitizers show driving force dependence similar to each other at room temperature. Slightly larger electronic coupling for electron injection (0.050 eV) than hole injection (0.043 eV) is also interesting because it suggests slightly larger interaction between LUMOs of donor and acceptors.

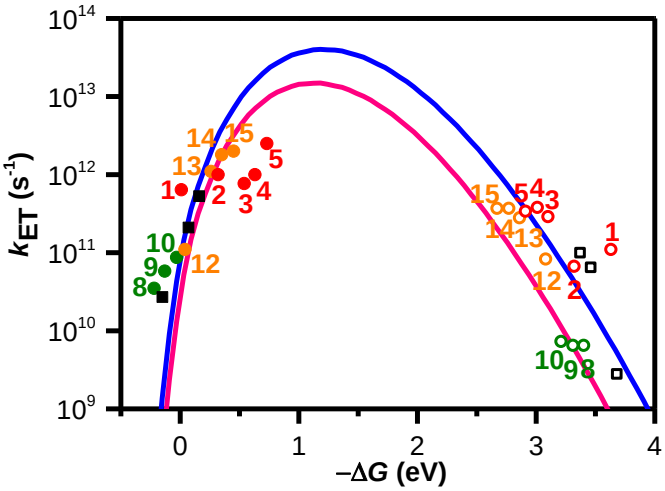

Figure 1-5. ΔG (ΔG_{CS} and ΔG_{CR}) dependence of k_{ET} (k_{CS} ● and k_{CR} ○). Numbers close to the marks indicate compounds. The solid and hollow black squares are the **2T** dyads.[12] The solid and hollow red circles are the dyads **1**–**5**. The solid and hollow green circles are corresponded to the dyads **8**–**10**. The solid and hollow orange circles are corresponded to the dyads **12-15**. The solid blue line was calculated by eqs. (3) and (4) using λ_S, λ_V, V, and $\hbar<\omega>$ of 0.20, 1.10, 0.050, and 0.19 eV, respectively.[12] The solid pink line was calculated using λ_S, λ_V, V, and $\hbar<\omega>$ of 0.23, 0.99, 0.043, and 0.19 eV, respectively.[37]

Conclusion

By using strongly electron-donating oligothiophenes as electron donors, a panoramic survey of CS and CR processes in dyads with all natural nucleobases as electron acceptors was accomplished on the basis of the Marcus theory. In addition, the conformation effect on CR was found.

References

(1) Wagenknecht, H.-A. *Nat. Prod. Rep.* **2006**, *23*, 973.

(2) Fujitsuka, M.; Majima, T. *Phys. Chem. Chem. Phys.* **2012**, *14*, 11234.

(3) Seidel, C. A. M.; Schulz, A.; Sauer, M. H. M. *J. Phys. Chem.* **1996**, *100*, 5541.

(4) Lewis, F. D.; Liu, X.; Wu, Y.; Miller, S. E.; Wasielewski, M. R.; Letsinger, R. L.; Sanishvili, R.; Joachimiak, A.; Tereshko, V.; Egli, M. *J. Am. Chem. Soc.* **1999**, *121*, 9905.

(5) Lewis, F. D.; Liu, X.; Miller, S. E.; Hayes R. T.; Wasielewski, M. R. *J. Am. Chem. Soc.* **2002**, *124*, 11280.

(6) Daublain, P.; Thazhathveetil, A. K.; Wang, Q.; Trifonov, A.; Fiebig, T.; Lewis, F. D. *J. Am. Chem. Soc.* **2009**, *131*, 16790.

(7) Daublain, P.; Thazhathveetil, A. K.; Shafirovich, V.; Wang, Q.; Trifonov, A.; Fiebig, T.; Lewis, F. D. *J. Phys. Chem. B* **2010**, *114*, 14265.

(8) Tainaka, K.; Fujitsuka, M.; Takada, T.; Kawai, K.; Majima, T. *J. Phys. Chem. B* **2010**, *114*, 14657.

(9) Park, M. J.; Fujitsuka, M.; Nishitera, H.; Kawai, K.; Majima, T. *Chem. Commun.* **2012**, *48*, 11008.

(10) Wagner, C.; Wagenknecht, H.-A. *Chem. Eur. J.* **2005**, *11*, 1871.

(11) Park, M. J.; Fujitsuka, M. Kawai, K.; Majima, T. *J. Am. Chem. Soc.* **2011**, *133*, 15320.

(12) Park, M. J.; Fujitsuka, M. Kawai, K.; Majima, T. *Chem. Eur. J.* **2012**, *18*, 2056.

(13) Turbiez, M.; Frère, P.; Roncali, J. *J. Org. Chem.* **2003**, *68*, 5357.

(14) Dietrich, M.; Heinze, J. *J. Am. Chem. Soc.* **1990**, *112*, 5142.

(15) Zhao, X.; Pinto, M. R.; Hardison, L. M.; Mwaura, J.; Muller, J.; Jiang, H.; Witker, D.; Kleiman, V. D.; Reynolds, J. R., Schanze, K. S. *Macromolecules* **2006**, *39*, 6355.

(16) Maeda, Y.; Saito, K.; Akamatsu, N.; Chiba, Y.; Ohno, S.; Okui, Y.; Yamada, M.; Hasegawa, T.; Kako, M.; Akasaka, T. *J. Am. Chem. Soc.* **2012**, *134*, 18101.

(17) Ng, P. S.; Laing, B. M.; Balasundarum, G.; Pingle, M.; Friedman, A. Bergstrom, D. E. *Bioconjugate Chem*. **2010**, *21*, 1545.

(18) Lewis, F. D.; Liu, X.; Miller, S. E.; Hayes R. T.; Wasielewski, M. R. *J. Am. Chem. Soc.*, **2002**, *124*, 14020.

(19) Fujitsuka, M.; Cho, D. W.; Tojo, S.; Inoue, A.; Shiragami, T.; Yasuda, M.; Majima, T. *J. Phys. Chem. A*, **2007**, *111*, 10574.

(20) Weller, A. *Zeit. Phys. Chem. Neue Folge* **1982**, *133*, 93.

(21) Su, C.; Middleton, C. T.; Kohler, B. *J. Phys. Chem. B* **2012**, *116*, 10266.

(22) Keane, P. M.; Wojdyla, M.; Doorley, G. W.; Kelly, J. M.; Clark, I. P.; Parker, A. W.; Greetham, G. M.; Magno, L. M.; Quinn, S. J. *Phys. Chem. Chem. Phys.* **2012**, *14*, 6307.

(23) Doorley, G. W.; Wojdyla, M.; Watson, G. W.; Towrie, M.; A.; Parker, A. W.; Kelly, J. M.; Quinn, S. J. *J. Phys. Chem. Lett.* **2013**, *4*, 2739.

(24) Fiebig, T.; Wan, C.; and Zewail, A. H. *ChemPhysChem* **2002**, 3, 781.

(25) Carmieli, R.; Smeigh, A. L.; Mickley Conron, S. M.; Thazhathveetil, A. K.; Fuki, M.; Kobori, Y.; Lewis, F. D.; Wasielewski, M. R. *J. Am. Chem. Soc.* **2012**, *134*, 11251.

(26) Merz, T.; Wenninger, M.; Weinberger, M.; Riedle,E.; Wagenknecht, H. -A.; Schütz, M. *Phys. Chem. Chem. Phys.* **2013**, *15*, 18607.

(27) Chen, J.; Kohler, B. *J. Am. Chem. Soc.* **2014**, *136*, 6362.

(28) Schreier, W. J.; Schrader, T. E.; Koller, F. O.; Gilch, P.; Crespo-Hernandez, C. E.; Swaminathan, V. N.; Carell, T.; Zinth, W.; Kohler, B. *Science*, **2007**, *315*, 625.

(29) Kneuttinger, C. A.; Kashiwazaki, G.; Prill, S.; Heil, K.; Müller, M.; Carell, T. *Photochem. Photobiol.* **2014**, *90*, 1.

(30) Norberg, J.; Nilsson, L. *J. Am. Chem. Soc.* **1995**,*117*, 10832.

(31) Norberg, J.; Nilsson, L. *Biophys. J.* **1995**, *69*, 2277.

(32) Jafilan, S.; Klein, L.; Hyun, C.; Florián, J. *J. Phys. Chem. B* **2012**, *116*, 3613.

(33) Lewis, F. D.; Wu, T.; Zhang, Y.; Letsinger, R. L.; Greenfield, S. R.; Wasielewski, M. R. *Science* **1997**, *277*, 673.

(34) Liu, Q.; Scaringe, W. A.; Sommer, S. S. *Nucleic Acids Res.* **2000**, *28*, 940.

(35) Marcus, R. A. *J. Chem. Phys.* **1956**, *24*, 966.

(36) Bixon, M.; Jortner, M. *Adv. Chem. Phys.* **1999**, *106*, 35.

(37) Lewis, F. D.; Kalgutkar, R. S.; Wu, Y.; Liu, X.; Liu, J.; Hayes, R. T.; Miller, S. E.; Wasielewski, M. R. *J. Am. Chem. Soc.* **2000**, *122*, 12346.

Chapter 2. Sequence Dependence of Excess-Electron Transfer in DNA:

Chapter 2-1. How Does Guanine−Cytosine Base Pair Affect Excess-Electron Transfer in DNA?

Abstract

Charge transfer and proton transfer in DNA have attracted wide attention due to their relevance in biological processes and so on. Especially, excess-electron transfer (EET) in DNA has strong relation to DNA repair. However, our understanding on EET in DNA still remains limited. Herein, by using a strongly electron-donating photosensitizer, trimer of 3,4-ethylenedioxythiophene (**3E**), and an electron acceptor, diphenylacetylene (**DPA**), two series of functionalized DNA oligomers were synthesized for investigation of EET dynamics in DNA. The transient absorption measurements during femtosecond laser flash photolysis showed that guanine:cytosine (G:C) base pair affects EET dynamics in DNA by two possible mechanisms: the excess-electron quenching by proton transfer with the complementary G after formation of $C^{\bullet-}$ and the EET hindrance by inserting a G:C base pair as a potential barrier in consecutive thymines (Ts). In the present paper, the author provided useful information based on the direct kinetic measurements, which allowed us to discuss EET through oligonucleotides for the investigation of DNA damage/repair.

Introduction

The mechanisms and dynamics of charge transfer (CT) over long distances in DNA, which possesses well-ordered continuously π-π stacking nucleobases, have attracted the attention of scientists for decades.[1,2] From a mechanistic viewpoint, CT can be classified as hole transfer (HT), an oxidative process, and excess electron transfer (EET), a reductive process. Both oxidation and reduction of DNA are essential also from a biological viewpoint. It is well-known that the oxidation of DNA promotes oxidative damage.[3-6] In contrast, the reduction of DNA can repair DNA lesions such as cyclobutane thymine–thymine (T−T) dimers.[7] Thus, thorough investigation of CT in DNA will provide important biological insights.

Recently, numerous reviews have provided detailed summaries of the sequence-dependent dynamics of HT through guanine (G) and adenine (A), which exhibit relatively low oxidation potentials.[1,2,8-9] In contrast, only limited data are available on EET, in which thymine (T) and cytosine (C) act as charge carriers, due to their relatively high reduction potentials.[9] To study the dynamics of EET in DNA, researchers have employed excess electron injection by electrochemical methods[1,10] and radiolysis.[11-13] Photochemical methods based on photo-induced electron transfer (PET) are also commonly used in biochemical studies *in vitro*. Several research groups have performed photochemical product analyses of EET and have elucidated the hopping mechanism.[1,2,14-23]

These results indicate that EET is a sequence-dependent process. It has been also noted that pH affects the dynamics of EET in DNA. Because the protonated C radical anion, which can be generated by proton transfer from the complementary base, G, or from surrounding water molecules, will limit or terminate EET.[19,21,24-26] Thus, T is considered to be a primary excess electron carrier. Steenken and co-workers[27-29] proposed a proton-transfer reaction pathway for the G:C base pair radical anion (G:C$^{\bullet-}$ base pair) as shown in Scheme 2-1-1, which is a thermodynamically favorable process and has been supported by various experimental[30,31] and theoretical studies.[32-34]

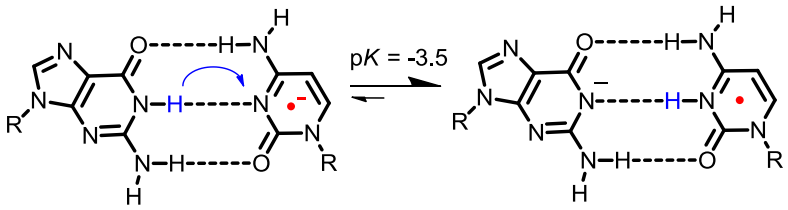

Scheme 2-1-1. Proposed proton-transfer reaction pathway for G:C$^{\bullet-}$ base pair.[27]

Although the rate constant of proton transfer in G:C$^{\bullet-}$ base pairs (k_{PT}) was theoretically calculated to be 10^{11} s^{-1},[35] it has not been determined directly. Furthermore, limited information is available on the effect of G:C base pairs on EET dynamics. To clarify the dynamics of EET in DNA, a femtosecond laser flash photolysis study of a donor-DNA-acceptor system is necessary. One of the key steps in the study of EET in DNA by photochemical techniques is injection of excess electrons to DNA from a photo-sensitizing electron donor. For the transient absorption measurements, generation of the donor radical cation with a strong absorption band is preferable. The injected excess electrons are expected to migrate through the DNA by hopping mechanism, and then are trapped by an electron acceptor attached to the DNA. To date, various photo-sensitizing electron donors have been used for the excess electron injection to DNA, such as stilbenediether,[36-37] pyrene and its derivatives,[22-23,38-39] phenothiazine,[21] and oligothiophenes[40-42]. In our previous report, our lab used a bithiophene derivative as a photo-sensitizing electron donor, and the author expected the excess electron hopping rate among consecutive Cs to be 10^{9}–10^{10} s^{-1}, which is slower than the excess electron hopping rate among Ts.[41] However, the sequence dependence of EET in DNA has not been clarified because of insufficient donor ability of a bithiophene derivative. In addition, EET through G:C pair has been discussed by experiments based on the product analysis, which hardly provided kinetic information.[19,21] In the present paper, the author synthesized DNA oligomers containing **3E**, a trimer of 3,4-ethylenedioxythiophene (EDOT), as a photo-sensitizing electron donor with sufficient donor-ability and diphenylacetylene (**DPA**) as an electron acceptor (Figure 2-1-1), and examined them by femtosecond laser flash photolysis. This study clarifies the role of G:C base pairs in the dynamics of EET in DNA. In addition, dynamics in G:C$^{\bullet-}$ base pairs is estimated experimentally to clarify its role in EET in DNA.

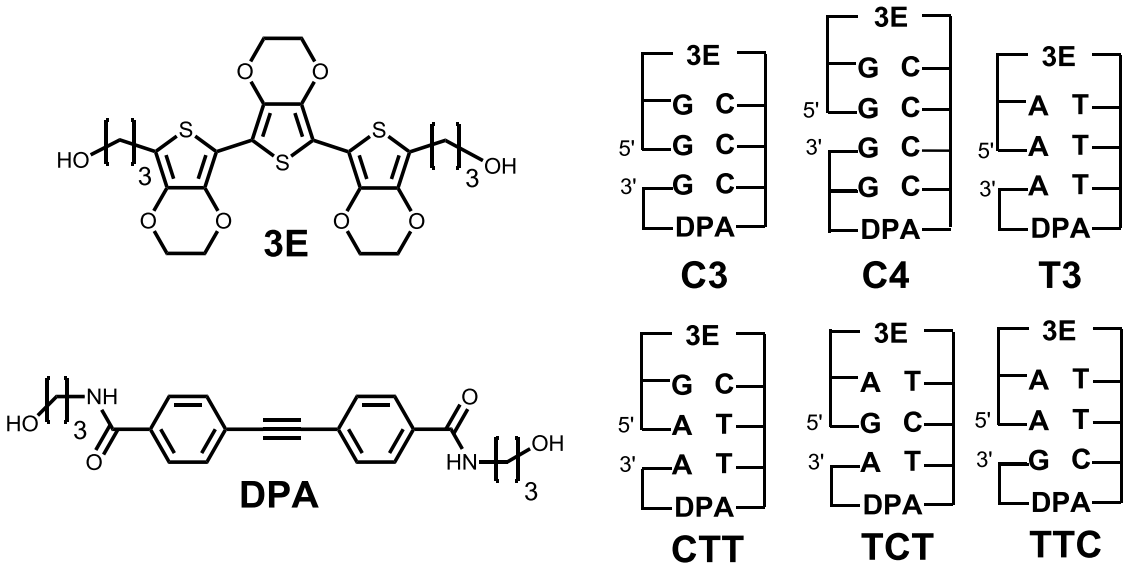

Figure 2-1-1. Structures of **3E**, **DPA**, and DNA oligomers (**C3**, **C4**, **T3**, **CTT**, **TCT**, and **TTC**). The gap between the 5' and 3' indicates a missing phosphate linker between two nucleobases in nicked dumbbell structure.

Experimental Section

DNA synthesis. 3E and **DPA** were prepared and converted to their phosphoramidite derivatives by a procedure previously reported.[40,42-44] All reagents were purchased from Glen Research (USA). All DNA oligomers were synthesized on an Applied Biosystems 3400 DNA synthesizer with standard solid-phase techniques and purified on a JASCO HPLC with a reversed-phase C-18 column with an acetonitrile/ammonium formate (50 mm) gradient. The DNA dyads were characterized by MALDI-TOF mass spectroscopy (Table 2-1-1).

Table 2-1-1. MALDI-TOF MS and melting temperature (T_m) [a] of the DNA oligomers.

DNA	MALDI-TOF MS		T_m,	DNA	MALDI-TOF MS		T_m,
	Calculated	Found	℃		Calculated	Found	℃
C3	2833.50	2832.54	42	**CTT**	2833.47	2835.20	41
C4	3451.60	3452.85	47	**TCT**	2833.47	2835.21	40
T3	2831.48	2833.06	36	**TTC**	2833.47	2835.85	40

[a] Measured in buffer solution (0.1 M NaCl and 10 mM sodium phosphate, pH 7.0 ± 0.1) at a heating rate of 0.5 ℃/min.

Apparatus. Steady-state absorption, fluorescence, circular dichroism (CD) spectra, and melting temperature profiles were measured using a Shimadzu UV3100PC, Horiba FluoroMax-4P, JASCO CDJ720, and Shimadzu UV2700, respectively. The subpicosecond transient absorption spectra were measured by the pump and probe method using a regeneratively amplified Ti:sapphire laser (Spectra Physics, Spitfire Pro F, 1 kHz) pumped by a Nd:YLF laser (Spectra Physics, Empower 15).[45] The seed pulse was generated by the Ti:sapphire laser (Spectra Physics, MaiTai VFSJ-W). Samples were excited using the 400 nm laser pulse, which was the second harmonic generation of the output of the amplifier. The supercontinuum was generated by focusing output of the amplifier on a sapphire plate. The chirp was corrected by a home-made program based on the optical Kerr effect cross correlation method.[46] The time resolution of the present system is ~300 fs.

Results and Discussion

All DNA oligomers were synthesized as indicated in the experimental section. Steady-state absorption spectra are shown in Figures 2-1-2a. A clear peak at approximately 260 nm corresponds to the nucleobases. Absorption bands indicating **DPA** were observed at approximately 300–350 nm, [38-40,43] whereas absorption bands at approximately 350–430 nm are attributable to **3E**.[42,44] The circular dichroism (CD) spectra of DNA oligomers are shown in Figures 2-1-2b. In this region (< 300 nm), the CD spectra of all DNA oligomers are similar to those of DNA with a B-type duplex structure.[40,47] The unclear spectra in the 225-300 nm region for **TCT** and **TTC** might be due to the slight difference from complete B-form structure. However, in the 350–430 nm region, a negatively induced CD indicating a **3E** chromophore was confirmed for all DNA oligomers.[48] Thus, the author assumed that these sequences are almost B-form structures in all cases based on these reasons.

Fluorescence from the **3E** of the DNA oligomers was observed by selective excitation of **3E** at 385 nm, as shown in Figures 2-1-2c. It is clear that fluorescence intensity largely depends on the neighboring nucleobase. A similar phenomenon was reported in our previous paper, which confirmed that the rate constant for charge separation (CS) between the singlet excited **3E** and the neighboring nucleobase strongly depends on the driving force for CS.[42] Notably, the fluorescence intensity of the DNA oligomer was weaker than that of the dyad of **3E** and the corresponding nucleobase. This finding indicates that in the nicked dumbbell DNA **3E** is held in close proximity to the nucleobase, while **3E** in the dyad is not always held at close to nucleobase resulting in incomplete fluorescence quenching in the dyad. In the

present study, quantitative analysis of CS rate on the basis of the fluorescence quantum yield was not carried out, because the delayed fluorescence, which is caused by the charge recombination (CR) process, is included in the steady state measurements.[42,49] Thermal dissociation profiles are shown in Figure 2-1-2d. The melting temperatures of DNA oligomers are shown in Table 2-1-1.

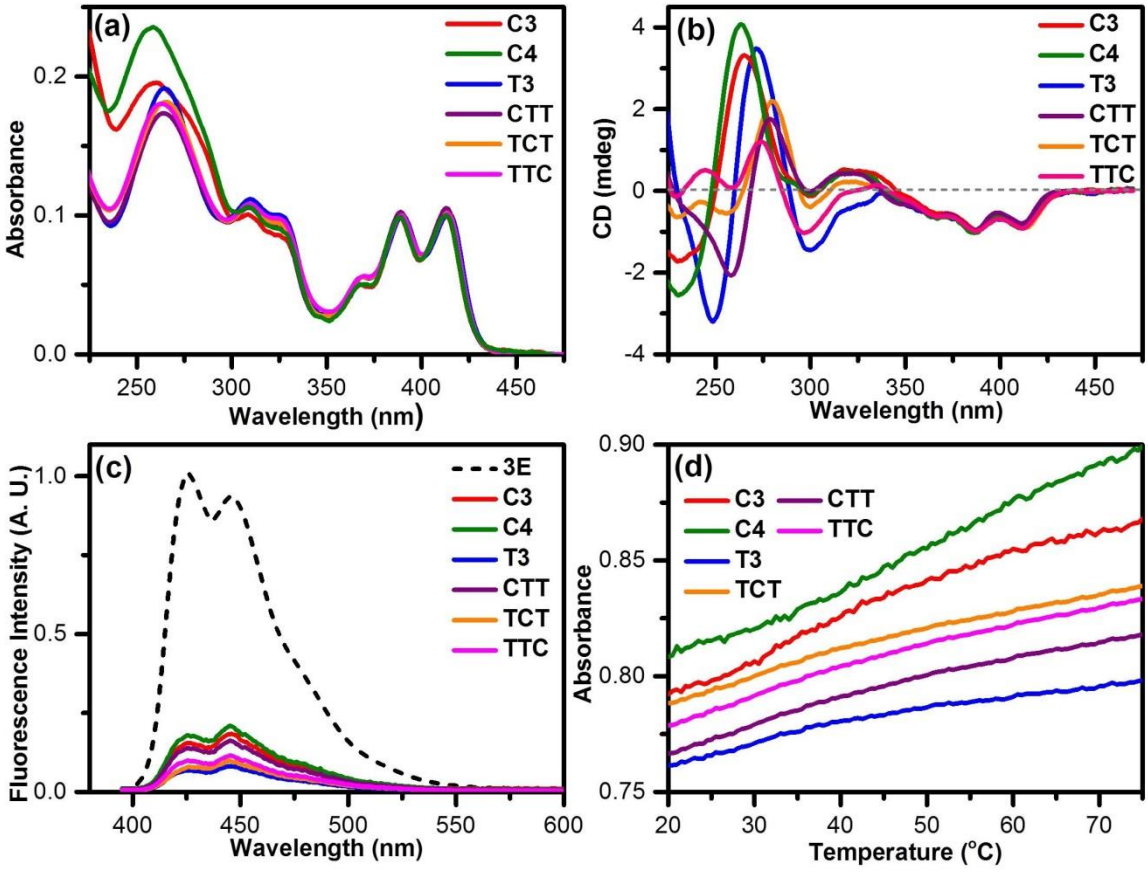

Figure 2-1-2. (a) Absorption, (b) circular dichroism, (c) fluorescence spectra (λ_{ex} = 385 nm), and (d) thermal dissociation profiles of DNA oligomers (~10^{-5} M) **C3** (red), **C4** (green), **T3** (blue), **CTT** (purple), **TCT** (orange), and **TTC** (pink) in buffer solution (0.1 M NaCl and 10 mM sodium phosphate, pH 7.0 ± 0.1) at 298 K. Fluorescence spectra of **3E** (black dash line). Absorbance of the sample was matched at λ_{ex}.

The dynamics of EET in the DNA oligomers were investigated by transient absorption measurements during femtosecond laser flash photolysis, using a 400-nm laser pulse, which selectively excites **3E**, the electron-donating photosensitizer in the DNA oligomers. The transient absorption spectra from the laser flash photolysis of **C3** and **C4** are shown in Figure 2-1-3.

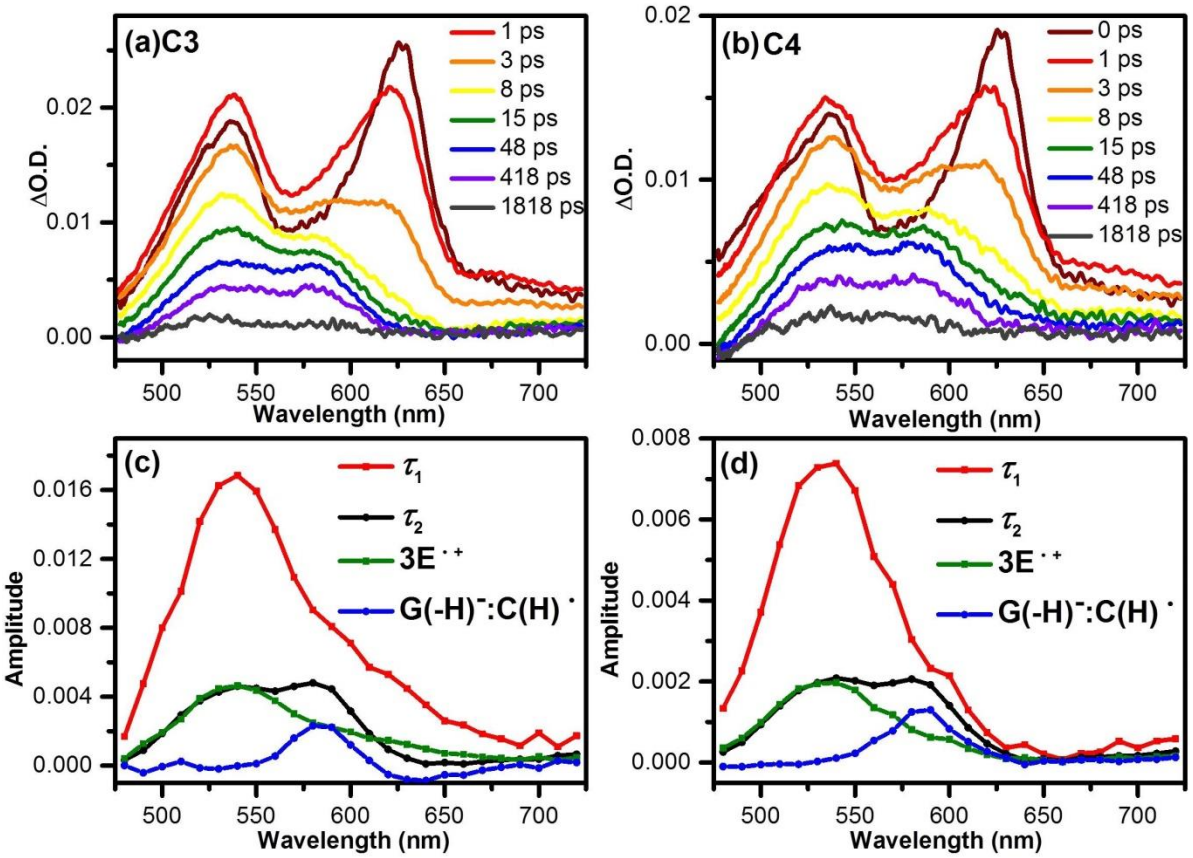

Figure 2-1-3. Transient absorption spectra during the laser flash photolysis of (a) **C3** and (b) **C4** upon excitation with 400-nm femtosecond laser pulse. (b) Species-associated spectra obtained by global fitting using a double exponential function for (c) **C3** and (d) **C4** (red: τ_1 (**3E**$^{\bullet+}$−G:C$^{\bullet-}$), black: τ_2 (**3E**$^{\bullet+}$−G(−H)$^{-}$:C(H)$^{\bullet}$) and normalized by intensity at 540 nm (green: **3E**$^{\bullet+}$, blue: G(−H)$^{-}$:C(H)$^{\bullet}$).

The dynamics of EET in the DNA oligomers were investigated by transient absorption measurements during femtosecond laser flash photolysis, using a 400-nm laser pulse, which selectively excites **3E**, the electron-donating photosensitizer in the DNA oligomers. The transient absorption spectra from the laser flash photolysis of **C3** shown in Figure 2-1-3a, will be discussed as a representative example. Immediately following excitation, **C3** showed an absorption band at 620 nm, which can be attributed to the singlet excited **3E** generated by the laser pulse.[42] An absorption band at 540 nm caused by **3E** radical cation (**3E**$^{\bullet+}$) appeared within 1 ps after excitation, indicating rapid excess electron injection from the singlet excited **3E** to C.[42] It should be noted that the singlet excited **3E** would be quenched by only C in **C3** and **C4** according to our previous paper.[42] Thus, the author excluded the possibility of G$^{\bullet-}$:C

formation. With a delay after the excitation pulse, an absorption band at 580 nm was observed. Based on the theoretical study of one-electron-reduced G:C base pairs, the absorption band at 580 nm can be attributed to $G(-H)^{-}:C(H)^{\bullet}$, the product of proton-transfer reaction of $G:C^{\bullet-}$ base pair.[50] Transient absorption spectra at 10 ps – 2 ns after excitation in 460 – 740 nm region were analyzed by global analysis assuming generation and decay of two-components (Figure 2-1-3c). In Figure 2-1-3c, the species-associated spectrum for the faster component (τ_1) is attributed to $\mathbf{3E}^{\bullet+}$–$G:C^{\bullet-}$, and that for the slower component (τ_2) is attributed to $\mathbf{3E}^{\bullet+}$–$G(-H)^{-}:C(H)^{\bullet}$. The absorption band due to $G(-H)^{-}:C(H)^{\bullet}$ (blue line in Figure 2-1-3c) was obtained by subtracting the absorption band of $\mathbf{3E}^{\bullet+}$ (green line) from the spectra of τ_2 component. Although contributions of $\mathbf{3E}^{\bullet+}$ and $G(-H)^{-}:C(H)^{\bullet}$ were confirmed in Figure 2-1-3c, $\mathbf{DPA}^{\bullet-}$, which causes an absorption band at 500 nm,[38-40,51] was not observed. It indicated that the excess electrons did not reach **DPA,** as shown in Figure 2-1-4, due to the stability of the proton transfer product. Similar results were confirmed in **C4**.

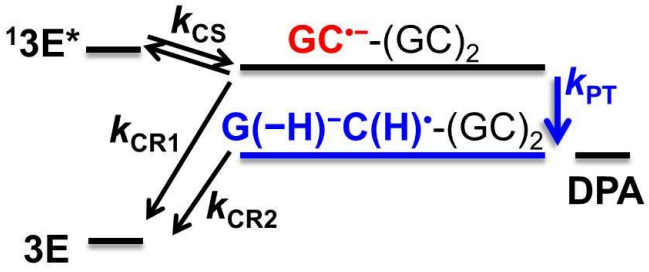

Figure 2-1-4. Proposed schematic energy diagram for CS from the singlet excited **3E** to C followed by proton transfer and CR processes. k_{CS} is the rate constants for CS from the singlet excited **3E** to C. k_{CR1} is the initial CR between C radical anion and $\mathbf{3E}^{\bullet+}$. k_{PT} is proton transfer. k_{CR2} is CR process between $\mathbf{3E}^{\bullet+}$ and the proton transfer product. The energy difference between $G:C^{\bullet-}$ and $G(-H)^{-}:C(H)^{\bullet}$ is ~0.21 eV,[27] which is similar to that between $G:C^{\bullet-}$ and **DPA** ($E_{red\text{-}C} - E_{red\text{-}\mathbf{DPA}} = 0.23$ eV). [9,40]

The rate constants for CS (k_{CS}) was evaluated from decay of **3E*** and formation of $\mathbf{3E}^{\bullet+}$. The initial CR between the nucleobase radical anion and $\mathbf{3E}^{\bullet+}$ (k_{CR1}), proton transfer (k_{PT}), and recombination between $\mathbf{3E}^{\bullet+}$ and the proton transfer product (k_{CR2}) were determined by global analysis and estimated yield of the products, and are listed in Table 2-1-2.

Table 2-1-2. Rate constants of CS from the singlet excited **3E** (k_{CS}), initial charge recombination of **3E**$^{\bullet+}$–C$^{\bullet-}$ (k_{CR1}), proton transfer in G:C$^{\bullet-}$ base pair (k_{PT}), and CR of G(−H)$^{-}$:C(H)$^{\bullet}$ (k_{CR2}).

DNA	k_{CS}[a] (s^{-1})	k_{CR1}[a] (s^{-1})	k_{PT}[a] (s^{-1})	k_{CR2}[a] (s^{-1})
C3	1.1×10^{12}	1.1×10^{11}	2.7×10^{10}	3.3×10^{9}
C4	1.1×10^{12}	1.0×10^{11}	2.5×10^{10}	2.5×10^{9}

[a] Estimated error is less than 10%.

Both k_{CS} and k_{CR1} are almost identical to the values for DNA dyads reported in our previous paper.[42] Since k_{CR1} is on the order of 10^{11} s^{-1} while PT is on the 10^{10} s^{-1}, CR is the major competing process of proton transfer in G:C$^{\bullet-}$ base pair (Figure 2-1-4) in consecutive Cs, **C3** and **C4**. Both experimental[27-31] and theoretical[32-34] studies have suggested that proton transfer is thermodynamically favorable in G:C$^{\bullet-}$ base pair. The reaction pathway for the CR of G(−H)$^{-}$:C(H)$^{\bullet}$ was proposed by Steenken et al., as shown in Scheme 2-1-2.[27] Compared to neutral G or any other nucleobases, deprotonated G is expected to be oxidized easily. Thus, CR with **3E**$^{\bullet+}$ to generate a radical pair may be possible. On the basis of the p*K* data,[27] the proton transfer in G(−H)$^{-}$:C(H)$^{\bullet}$ generating G:C$^{\bullet-}$ base pair will take 10 ns, which is not in accordance with k_{CR2}, supporting the reaction pathway shown in Scheme 2-1-2. To the best of our knowledge, this is the first direct measurement of the dynamics of proton transfer in G:C$^{\bullet-}$ base pair. The estimated k_{PT} value was concordant with the theoretical predictions.[35,50] It should be noted that neither fast k_{PT} nor k_{CR1} resulted in **DPA**$^{\bullet-}$ generation.

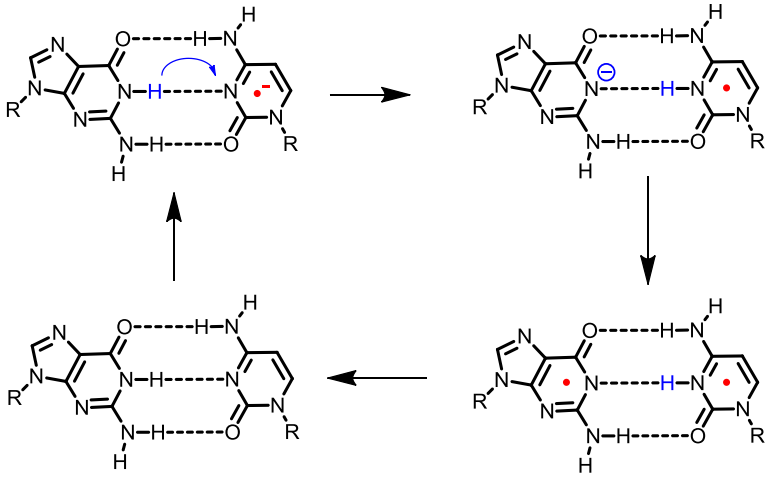

Scheme 2-1-2. Proposed reaction pathway for the CR of G(−H)$^{-}$:C(H)$^{\bullet}$.[27]

The effect of G:C pairs in EET was further examined using DNA oligomers that incorporated both A:T and G:C pairs. The transient absorption spectra observed during the laser flash photolysis of **TCT**, **T3**, **CTT**, and **TTC** using a 400-nm femtosecond laser pulse are shown in Figure 2-1-5. Here, the transient absorption spectra of **TCT** will be discussed as an representative case. Generation of $\mathbf{3E}^{\bullet+}$ within 1 ps was confirmed (Figures 2-1-5a). An additional absorption band was confirmed at approximately 500 nm, which indicates generation of $\mathbf{DPA}^{\bullet-}$. Due to the overlap of absorption band of $\mathbf{3E}^{\bullet+}$ and $\mathbf{DPA}^{\bullet-}$, the author used global fitting assuming two species. The species-associated spectrum (Figure 2-1-5b) for the faster component (τ_1) is attributed to $\mathbf{3E}^{\bullet+}$−DNA$^{\bullet-}$−**DPA**, and that for the slower component (τ_2) is attributed to $\mathbf{3E}^{\bullet+}$−DNA−$\mathbf{DPA}^{\bullet-}$, whereas contribution of the proton transfer products was not observed. In the present case, the rate of the fast component can be attributed to the sum of initial CR between $\mathbf{3E}^{\bullet+}$ and T$^{\bullet-}$ (k_{CR1}) and k_{ET} (Table 2-1-3). The k_{CR1} and k_{ET} were determined on the basis of the generation yields. The slower decay component in the DNA oligomers can be attributed to the rate of CR of $\mathbf{3E}^{\bullet+}$ and $\mathbf{DPA}^{\bullet-}$ (k_{BET}). Similar results were observed in **T3**, **CTT**, and **TTC,** as shown in Figures 2-1-5c−h.

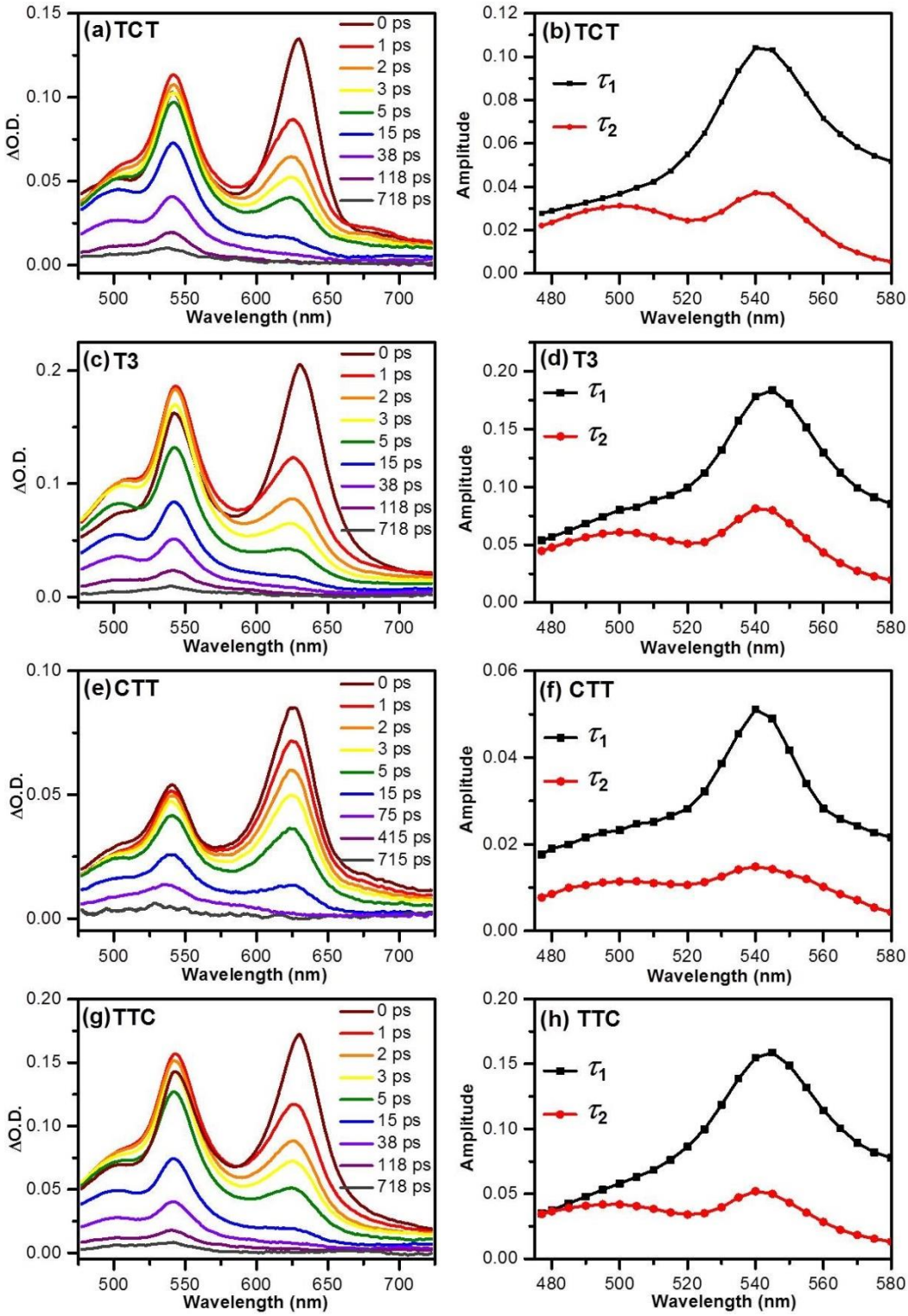

Figure 2-1-5. Transient absorption spectra during the laser flash photolysis of (a) **TCT** (c) **T3**, (e) **CTT,** and (g) **TTC** upon excitation with 400-nm femtosecond laser pulse. Species-associated spectra obtained by global fitting using a double exponential function for (b) **TCT** (d) **T3**, (f) **CTT,** and (h) **TTC**. (black: τ_1 (**3E**$^{\bullet+}$−DNA$^{\bullet-}$−**DPA**) and red: τ_2 (**3E**$^{\bullet+}$−DNA−**DPA**$^{\bullet-}$))

Table 2-1-3. Rate constants for CS from the singlet excited **3E** (k_{CS}), initial CR between **3E**$^{\bullet+}$−DNA$^{\bullet-}$ (k_{CR1}), **DPA**$^{\bullet-}$ generation (k_{ET}), CR of **3E**$^{\bullet+}$−DNA−**DPA**$^{\bullet-}$ (k_{BET}), and quantum yield of excess-electron transfer.

DNA	k_{CS}[a] (s^{-1})	k_{CR1}[a] (s^{-1})	k_{ET}[a] (s^{-1})	k_{BET}[b] (s^{-1})	Φ_{EET}[c]
T3	1.5×10^{12}	9.9×10^{10}	4.9×10^{10}	2.0×10^{10}	0.33
CTT	1.2×10^{12}	7.8×10^{10}	2.2×10^{10}	1.4×10^{10}	0.22
TCT	1.4×10^{12}	7.6×10^{10}	2.4×10^{10}	1.5×10^{10}	0.24
TTC	1.5×10^{12}	7.5×10^{10}	2.5×10^{10}	1.5×10^{10}	0.25

[a] Estimated error is less than 10%. [b] Estimation error is less than 5%. [c] $\Phi_{EET} = k_{ET}/(k_{ET} + k_{CR1})$, which was estimated as the quantum yield of excess-electron transfer in DNA oligomers. The estimation error is less than 10%.

From Table 2-1-3, it is clear that k_{CS} and k_{CR1} were similar to the values reported for the dyads.[42] From the k_{ET} value of **T3**, the excess electron hopping rate in consecutive Ts ($k_{intra\text{-}T}$) is estimated to be 22×10^{10} s^{-1} on the basis of the random walk model as shown in Eq (2-1-1),[52,53]

$$\tau(N) = (1/2k_{hop})N^2 \quad (2\text{-}1\text{-}1)$$

where $\tau(N)$ is the time required for N hopping steps, i.e, k_{ET}^{-1} and k_{hop} is the rate constant for a single hopping between neighboring Ts. The $k_{T\text{-}HOP}$ reported here is higher than that reported previously,[39,40] because the slightly larger driving force required for electron injection from the singlet excited **3E** will cause structural fluctuations which would assist the hopping process and enhance k_{ET}.[54] Notably, an intervening G:C base pair in the consecutive Ts slowed down the k_{ET} value to ~50%, regardless of the position of the G:C base pair in the DNA oligomers. In addition, the yield of formation of **DPA**$^{\bullet-}$ with respect to the initial **3E**$^{\bullet+}$ generation showed a decrease of ~30% in **CTT**, **TCT**, and **TTC**.

In Figure 2-1-6, two possible energetic diagrams for EET in **TCT** are shown: Mechanism in Figure 2-1-6a is based on the facts that the reduction potential of C is more negative than that of T by 0.09 V and the generation of G(−H)$^{-}$:C(H)$^{\bullet}$ was negligible in the transient absorption spectra during the laser flash photolysis. Thus, C is assumed to be an electron carrier in Figure 2-1-6a. On the other hand, mechanism in Figure 2-1-6b assumes that C acts as a spacer or a barrier for electron tunneling. In the case of mechanism shown in Figure 2-1-6a, the electron transfer from G:C$^{\bullet-}$ base pair to T (k_{EET2}) should be slightly faster than the

proton transfer in G:C$^{\bullet-}$ base pair (k_{PT} ~10^{10} s^{-1}), to explain the reduced quantum yield for generation of **DPA**$^{\bullet-}$. As shown in Figure 2-1-6a, k_{EET2} is expected to be faster than k_{EET1}, although a large difference is not expected, due to the smaller difference in the reduction potentials of C and T. These conditions are possible when taking the fast $k_{T\text{-}HOP}$ value observed in **T3** into account (10^{11} s^{-1}), which is faster than the proton transfer in G:C$^{\bullet-}$ base pair (k_{PT} ~10^{10} s^{-1}). Due to the smaller difference in the reduction potentials of C and T, k_{EET1} and k_{EET2} should be similar to $k_{T\text{-}HOP}$ and is expected on the order of 10^{11} s^{-1} (From eq. (1), $k_{intra\text{-}C} = k_{EET1} \approx k_{EET2} = (3^2/2) \times k_{ET} = 1 \times 10^{11}$ s^{-1}). Thus, the absence of PT can be explained by the slightly faster $k_{intra\text{-}C}$ than k_{PT}, while multiple Cs can completely trap an excess electron as seen in **C3** and **C4**. Therefore, the quenching ability of a single G:C pair in consecutive Ts is insufficient to terminate EET completely.

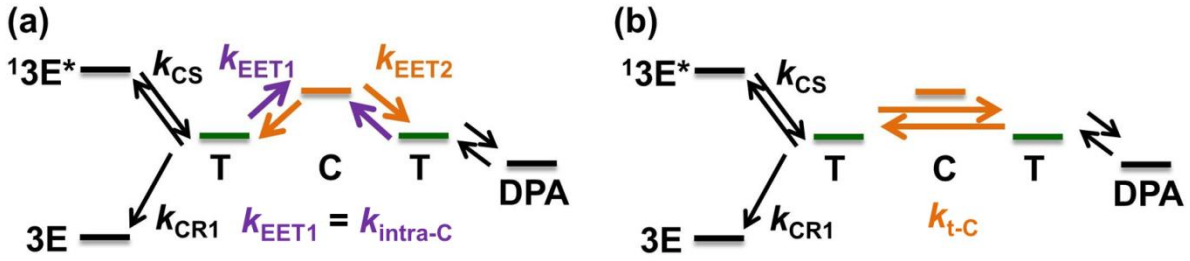

Figure 2-1-6. Proposed schematic energy diagrams of EET in **TCT** where C acts as (a) a carrier or (b) a spacer. Other processes are also indicated. k_{CS} is the rate constants for CS from the singlet excited **3E** to C. k_{CR1} is the initial CR between the nucleobase radical anion and **3E**$^{\bullet+}$. k_{EET1} is ET process from T radical anion to C. k_{EET2} is ET process from C radical anion to T. $k_{t\text{-}C}$ is ET process between Ts with inserting a G:C base pair.

Another mechanism, in which the G:C base pair acts as a spacer for tunneling (Figure 2-1-6b), is also plausible. Based on the one-dimensional random walk model,[52,53] the excess electron hopping rate in both **T3** ($k_{intra\text{-}T} = 22 \times 10^{10}$ s^{-1}) and **TCT** ($k_{t\text{-}C} = 4.9 \times 10^{10}$ s^{-1}, where two T act as hopping stones) can be estimated; thus, $k_{intra\text{-}T} = 4.5 \times k_{t\text{-}C}$. Previously, our lab reported HT in DNA with consecutive Gs through an intervening A:T base pair and found that the presence of an intervening A:T base pair slowed the rate of HT by a factor of ~100.[8,55] In contrast, the author found that in **TCT,** an intervening G:C base pair where two T act as hopping stones slowed EET rate by only a factor of 4.5. The smaller effect of C in consecutive Ts for EET can be explained on the basis of the barrier height to be overcomed.[56,57] A spacer A provides an energy barrier with a height of ~0.5 eV for HT in

consecutive Gs, whereas the energy barrier formed by C in consecutive Ts is ~0.1 eV.[9] Moreover, according to the electron-transfer theory, the electron transfer rate (k_{et}) depends on the donor–acceptor distance (R_{DA}), as shown in Eq. (2-1-2),[58-60]

$$k_{et} = k_0 \times \exp(-\beta R_{DA}) \quad (2\text{-}1\text{-}2)$$

where β is the damping factor and R_{DA} is the distance between two Ts in the present discussion. Thus, the minor distance dependence of EET in DNA oligomers can be explained by the small damping factor, calculated to be 0.43 $Å^{-1}$, which was similar to the value reported in our previous paper.[41]

Conclusion

The author studied the role of a G:C base pair in dynamics of EET in DNA using a femtosecond laser flash photolysis technique and successfully observed sequence-dependent EET through oligonucleobases including G:C pair. First, the dynamics of the proton-transfer reaction of $G:C^{\bullet-}$ base pair were confirmed for the first time. The k_{PT} was determined to be on the order of 10^{10} s^{-1}, which suggests that the rapid excess-electron trapping by proton transfer in $G:C^{\bullet-}$ base pair limits the participation of C in EET in DNA. This finding indicates that T plays a major role as an excess-electron carrier. Second, the author found that the rate of EET in DNA oligomers is affected by the involvement of a G:C base pair: one G:C pair in consecutive Ts decreased the rate of EET to ~50%. Thus, it is clear that EET by hopping is sequence-dependent and occurs faster in consecutive Ts than Cs. Deeper studies are currently in progress with direct measurement of EET rates in various DNA sequences to improve our understanding in mechanisms for EET in DNA.

References

(1) Genereux, J. C.; Barton, J. K. *Chem. Rev.* **2010**, *110*, 1642.

(2) Wagenknecht, H.-A. *Nat. Prod. Rep.* **2006**, *23*, 973.

(3) Burrows, C. J.; Muller, J. G. *Chem. Rev.* **1998**, *98*, 1109.

(4) Armitage, B. *Chem. Rev.* **1998**, *98*, 1171.

(5) Kanvah, S.; Joseph, J.; Schuster, G. B.; Barnett, R. N.; Cleveland, C. L.; Landman, U. *Acc. Chem. Res.* **2010**, *43*, 280.

(6) Barnett, R. N.; Joseph, J.; Landman, U. Schuster, G. B. *J. Am. Chem. Soc.* **2013**, *135*, 3904.

(7) Carell, T. *Angew. Chem. Int. Ed.* **1995**, *34*, 2491.

(8) Kawai, K.; Majima, T. *Acc. Chem. Res.* **2013**, *46*, 2616.

(9) Seidel, C. A. M.; Schulz, A.; Sauer, M. H. M. *J. Phys. Chem.* **1996**, *100*, 5541.

(10) Paleček, E.; Bartošík, M. *Chem. Rev.* **2012**, *112*, 3427.

(11) Messer, A.; Carpenter, K.; Forzley, K.; Buchanan, J.; Yang, S.; Razskazovskii, Y.; Cai, Z.; Sevilla, M. D. *J. Phys. Chem. B* **2000**, *104*, 1128.

(12) Cai, Z.; Gu, Z.; Sevilla, M. D. *J. Phys. Chem. B* **2000**, *104*, 10406.

(13) Kawai, K.; Kimura, T.; Kawabata, K.; Tojo, S.; Majima, T. *J. Phys. Chem. B* **2003**, *107*, 12838.

(14) Henderson, P. T.; Jones, D.; Hampikian, G.; Kan, Y.; Schuster, G. B. *Proc. Natl. Acad. Sci. USA* **1999**, *96*, 8353.

(15) Behrens, C.; Burgdorf, L. T.; Schwögler, A.; Carell, T. *Angew. Chem. Int. Ed.* **2002**, *41*, 1763.

(16) Ito, T.; Rokita, S. E. *J. Am. Chem. Soc.* **2003**, *125*, 11480.

(17) Behrens, C.; Ober, M.; Carell, T. *Eur. J. Org. Chem.* **2002**, *19*, 3281.

(18) Behrens, C.; Carell, T. *Chem. Commun.* **2003**, 14, 1632.

(19) Ito, T.; Rokita, S. E. *Angew. Chem. Int. Ed.* **2004**, *43*, 1839.

(20) Wagenknecht, H.-A. *Angew. Chem. Int. Ed.* **2003**, *42*, 2454.

(21) Wagner, C.; Wagenknecht, H.-A. *Chem.— Eur. J.* **2005**, *11*, 1871.

(22) Daublain, P.; Thazhathveetil, A. K.; Wang, Q.; Trifonov, A.; Fiebig, T.; Lewis, F. D. *J. Am. Chem. Soc.* **2009**, *131*, 16790.

(23) Daublain, P.; Thazhathveetil, A. K.; Shafirovich, V.; Wang, Q.; Trifonov, A.; Fiebig, T.; Lewis, F. D. *J. Phys. Chem. B* **2010**, *114*, 14265.

(24) Huber, R.; Fiebig, T.; Wagenknecht, H.-A. *Chem. Commun.* **2003**, *15*, 1878.

(25) Raytchev, M.; Mayer, E.; Amann, N.; Wagenknecht, H.-A.; Fiebig, T. *ChemPhysChem* **2004**, *5*, 706.

(26) Cai, Z.; Li, X.; Sevilla, M. D. *J. Phys. Chem. B* **2002**, *106*, 2755.

(27) Steenken, S.; Telo, J. P.; Novais, H. M.; Candeias, L. P. *J. Am. Chem. Soc.* **1992**, *114*, 4701.

(28) Steenken, S. *Chem. Rev.* **1989**, *89*, 503.

(29) Steenken, S. *Biol. Chem.* **1997**, *378*, 1293.

(30) Yamagami, R.; Kobayashi, K.; Tagawa, S. *J. Am. Chem. Soc.* **2008**, *130*, 14772.

(31) Szyperska, A.; Rak, J.; Leszczynski, J.; Li, X.; Ko, Y. J.; Wang, H.; Bowen, K. H. *ChemPhysChem* **2010**, *11*, 880.

(32) Li, X.; Cai, Z.; Sevilla, M. D. *J. Phys. Chem. B* **2001**, *105*, 10115.

(33) Richardson, N. A.; Wesolowski, S. S.; Schaefer, H. F. *J. Am. Chem. Soc.* **2002**, *124*, 10163.

(34) Gupta, A.; Jaeger, H. M.; Compaan, K. R.; Schaefer, H. F. *J. Phys. Chem. B* **2012**, *116*, 5579.

(35) Chen, H.-Y.; Kao, C.-L.; Hsu, S. C. N. *J. Am. Chem. Soc.* **2009**, *131*, 15930.

(36) Lewis, F. D.; Liu, X.; Wu, Y.; Miller, S. E.; Wasielewski, M. R.; Letsinger, R. L.; Sanishvili, R.; Joachimiak, A.; Tereshko, V.; Egli, M. *J. Am. Chem. Soc.* **1999**, *121*, 9905.

(37) Lewis, F. D.; Liu, X.; Miller, S. E.; Hayes, R. T.; Wasielewski, M. R. *J. Am. Chem. Soc.* **2002**, *124*, 11280.

(38) Tainaka, K.; Fujitsuka, M.; Takada, T.; Kawai, K.; Majima, T. *J. Phys. Chem. B* **2010**, *114*, 14657.

(39) Park, M. J.; Fujitsuka, M.; Nishitera, H.; Kawai, K.; Majima, T. *Chem. Commun.* **2012**, *48*, 11008.

(40) Park, M. J.; Fujitsuka, M.; Kawai, K.; Majima, T. *J. Am. Chem. Soc.* **2011**, *133*, 15320.

(41) Park, M. J.; Fujitsuka, M.; Kawai, K.; Majima, T. *Chem. —Eur. J.* **2012**, *18*, 2056.

(42) Lin, S.-H.; Fujitsuka, M.; Ishikawa, M.; Majima, T. *J. Phys. Chem. B* **2014**, *118*, 12186.

(43) Lewis, F. D.; Liu, X.; Miller, S. E.; Hayes, R. T.; Wasielewski, M. R. *J. Am. Chem. Soc.* **2002**, *124*, 14020.

(44) Turbiez, M.; Frère, P.; Roncali, J. *J. Org. Chem.* **2003**, *68*, 5357.

(45) Fujitsuka, M.; Cho, D. W.; Tojo, S.; Inoue, A.; Shiragami, T.; Yasuda, M.; Majima, T. *J. Phys. Chem. A* **2007**, *111*, 10574.

(46) Yamaguchi, S.; Hamaguchi, H. *Appl. Spectrosc.* **1995**, *49*, 1513.

(47) Vura-Weis, J.; Wasielewski, M. R.; Thazhathveetil, A. K.; Lewis, F. D. *J. Am. Chem. Soc.* **2009**, *131*, 9722.

(48) Joy, J.; Cheriya, R. T.; Nagarajan, K.; Shaji, A.; Hariharan, M. *J. Phys. Chem. C* **2013**, *117*, 17927.

(49) Gorczak, N.; Fujii, T.; Mishra, A. K.; Houtepen, A. J.; Grozema, F. C.; Lewis, F. D. *J. Phys. Chem. B* **2015**, *119*, 7673.

(50) Hsu, S. C. N.; Wang, T.-P.; Kao, C.-L.; Chen, H.-F.; Yang, P.-Y.; Chen, H.-Y. *J. Phys. Chem. B* **2013**, *117*, 2096.

(51) Lewis, F. D.; Liu, X.; Miller, S. E.; Wasielewski, M. R. *J. Am. Chem. Soc.* **1999**, *121*, 9746.

(52) Conron, S. M. M.; Thazhathveetil, A. K.; Wasielewski, M. R.; Burin, A. L.; Lewis, F. D. *J. Am. Chem. Soc.* **2010**, *132*, 14388.

(53) Bar-Haim, A.; Klafter, J. *J. Chem. Phys.* **1998**, *109*, 5187.

(54) Grozema, F. C.; Tonzani, S.; Berlin, Y. A.; Schatz, G. C.; Siebbeles, L. D. A.; Ratner, M. A. *J. Am. Chem. Soc.* **2008**, *130*, 5157.

(55) Takada, T.; Kawai, K.; Fujitsuka, M.; Majima, T. *Chem. —Eur. J.* **2005**, *11*, 3835.

(56) Lewis, F. D.; Liu, J.; Weigel, W.; Rettig, W.; Kurnikov, I. V.; Beratan, I. V. *Proc. Natl. Acad. Sci. U.S.A.* **2002**, *99*, 12536.

(57) Liu, C. -S.; Schuster, G. B. *J. Am. Chem. Soc.*, **2003**, *125*, 6098.

(58) Marcus, R. A. *Angew. Chem. Int. Ed.* **1993**, *32*, 1111.

(59) Jortner, J.; Bixon, M.; Langenbacher, T.; Michel-Beyerle, M. E. *Proc. Natl. Acad. Sci. U.S.A.* **1998,** *95*, 12759.

(60) Meggers, E,; Maria E. Michel-Beyerle, M. E. M.-B; Giese, B. *J. Am. Chem. Soc.*, **1998**, *120*, 12950.

Chapter 2-2. Dynamics of Excess-Electron Transfer via Alternating Adenine:Thymine Sequences in DNA

Abstract

In this study, the author present the results of our investigation into the sequence-dependent excess-electron transfer (EET) dynamics in DNA, which plays an important role in DNA damage/repair. There are many published studies on EET in consecutive adenine:thymine (A:T) sequences (**Tn**), but those in alternating A:T sequences (**ATn**) remain limited. Here, two series of functionalized DNA oligomers, **Tn** and **ATn**, were synthesized with a strongly electron-donating photosensitizer, a trimer of ethylenedioxythiophene (**3E**), and an electron acceptor, diphenylacetylene (**DPA**). Laser flash photolysis experiments showed that the EET rate constant of **AT3** is 2 times lower than that of **T3** due to the lack of π-stacking of Ts in **AT3**. Thus, it was indicated that excess-electron hopping is affected by the interaction between LUMOs of nucleotides.

Introduction

The dynamics of charge transfer in DNA by either oxidative hole transfer (HT) or reductive excess-electron transfer (EET) have attracted the attention of scientists for decades because of their relevance to DNA damage/repair, which is important for all living organisms.[1-4] Positive charges, holes, are mainly at guanine (G) or adenine (A) nucleotides and thus migrate through the HOMOs in DNA. On the other hand, negative charges, excess electrons, migrate through the LUMOs of cytosine (C) or thymine (T) in DNA.[4,5] To date, numerous papers employing photochemical product analysis have provided information about the dynamics of EET through intrastrand T and C due to their relatively high reduction potentials in DNA.[2,4,5] According to these results, it has been indicated that EET is a sequence-dependent process. It was confirmed that the protonated C radical anion, which can be generated by proton transfer from the complementary base, G, or from surrounding water molecules, will limit or terminate EET.[6-11] Thus, T is considered to be a primary excess electron carrier. Several groups including us reported the dynamics of intrastrand EET in DNA through adenine:thymine (A:T) sequences,[2-4,8-21] however, investigations on interstrand EET in alternating A:T sequences in DNA, in which interaction between the LUMOs of Ts does not exist, are still limited. For example, Carell and co-workers reported an interstrand EET in PNA:DNA double strands based on product analysis.[22] Their qualitative results showed that an interstrand EET can efficiently proceed in PNA:DNA double strands, indicating EET in PNA:DNA is somewhat influenced by the precise stacking situation. On the other hand, for interstrand HT in DNA, Lewis's group reported that the efficiency of interstrand HT in DNA is lower than that of intrastrand HT by a factor of 4 due to the lack of interaction between the HOMOs of As, based on laser flash photolysis studies.[23] Our Lab reported similar results in our previous report.[24] Thus, direct measurement of the dynamics of EET in DNA by laser flash photolysis is essential for a quantitative understanding of interstrand EET.

In the present study, the author used femtosecond laser flash photolysis technique to examine intrastrand and interstrand EET dynamics in DNA oligomers, **Tn** and **ATn**, which possess consecutive and alternating A:T sequences, respectively. One of the key steps in the study of EET in DNA by laser flash photolysis technique is injection of excess electrons to DNA from a photosensitizing electron donor. For the transient absorption measurements, generation of the donor radical cation with a strong absorption band is preferable. The injected excess electrons are expected to migrate through the DNA by hopping mechanism,

and then are trapped by an electron acceptor attached to the DNA. As a photosensitizing electron donor and an electron acceptor for end-cap modified DNAs, a trimer of ethylenedioxythiophene (**3E**) and diphenylacetylene (**DPA**) were used, respectively (Figure 2-2-1), because **3E** and **DPA** were found to accomplish efficient excess electron injection and trapping, respectively.[11,25-27] In this study, the author clarifies the role of LUMO interaction in the dynamics of EET in DNA.

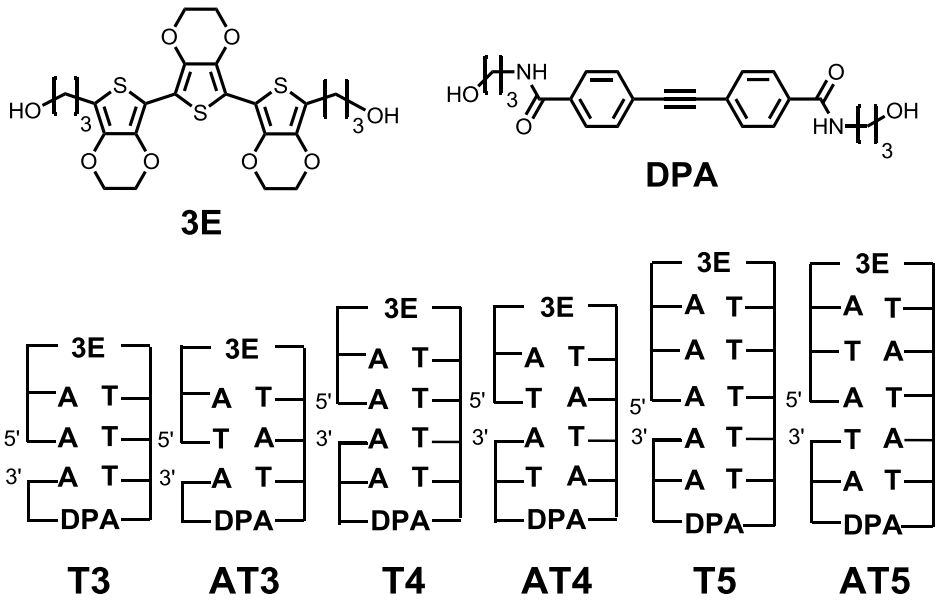

Figure 2-2-1. Structures of **3E**, **DPA**, and DNA oligomers. The gap between the 5' and 3' indicates a missing phosphate linker between two nucleotides in nicked dumbbell structure.

Experimental Section

DNA synthesis. 3E and **DPA** were prepared and converted to their phosphoramidite derivatives by the similar procedures as previously reported.[11,25-27] All reagents were purchased from Glen Research (USA). All DNA oligomers were synthesized on an Applied Biosystems 3400 DNA synthesizer with standard solid-phase techniques and purified on a JASCO HPLC with a reversed-phase C-18 column with an acetonitrile/ammonium formate (50 mm) gradient. The DNA oligomers were characterized by MALDI-TOF mass spectroscopy (Table 2-2-1).

Table 2-2-1. MALDI-TOF MS and melting temperature (T_m) of the DNA oligomers.

DNA	MALDI-TOF MS		T_m,	DNA	MALDI-TOF MS		T_m,
	Calculated	Found	℃		Calculated	Found	℃
T3	2831.48	2833.06	36	**AT3**	2831.48	2833.01	40
T4	3448.57	3453.07	45	**AT4**	3448.57	3450.22	43
T5	4065.66	4068.36	48	**AT5**	4065.66	4069.03	48

[a] Measured in buffer solution (0.1 M NaCl and 10 mM sodium phosphate, pH 7.0 ± 0.1) at a heating rate of 0.5 ℃/min.

Apparatus. Steady-state absorption, fluorescence, circular dichroism (CD) spectra, and melting temperature profiles were measured using a Shimadzu UV3100PC, Horiba FluoroMax-4P, JASCO CDJ720, and Shimadzu UV2700, respectively. The subpicosecond transient absorption spectra were measured by the pump and probe method using a regeneratively amplified Ti:sapphire laser (Spectra Physics, Spitfire Pro F, 1 kHz) pumped by a Nd:YLF laser (Spectra Physics, Empower 15).[28] The seed pulse was generated by the Ti:sapphire laser (Spectra Physics, MaiTai VFSJ-W). Samples were excited using the 400-nm laser pulse, which was the second harmonic generation of the output of the amplifier. The supercontinuum was generated by focusing output of the amplifier on a sapphire plate. The chirp was corrected by a home-made program based on the optical Kerr effect cross correlation method.[29] The time resolution of the present system is ~300 fs.

Results and Discussion

The DNA oligomers were synthesized as indicated in the experimental section, and characterizations of the DNA oligomers by HPLC and MALDI-TOF MS. Steady-state absorption spectra are shown in Figure 2-2-2a. A clear peak at approximately 260 nm corresponds to the nucleotides. Similar to our previous results, absorption bands indicating **DPA** were observed at approximately 300–350 nm, whereas absorption bands at approximately 350–430 nm are attributable to **3E**.[11,25-27,30] CD spectra of the DNA oligomers are shown in Figure 2-2-2b. In the region shorter than 300 nm, the CD spectra of all DNA oligomers are similar to those of DNA with a B-type duplex structure.[11,31-33] The unclear spectra in the 225-300 nm region for **T4** and **AT4** might be due to the slight difference from complete B-form structure. However, in the 350–430 nm region, a negatively induced CD

indicating a **3E** chromophore was confirmed for all DNA oligomers, including **T4** and **AT4**.[11,34] These findings indicate that the DNA oligomers are almost B-form structures. Fluorescence from the **3E** of the DNA oligomers was observed by selective excitation of **3E** at 385 nm, as shown in Figure 2-2-2c.

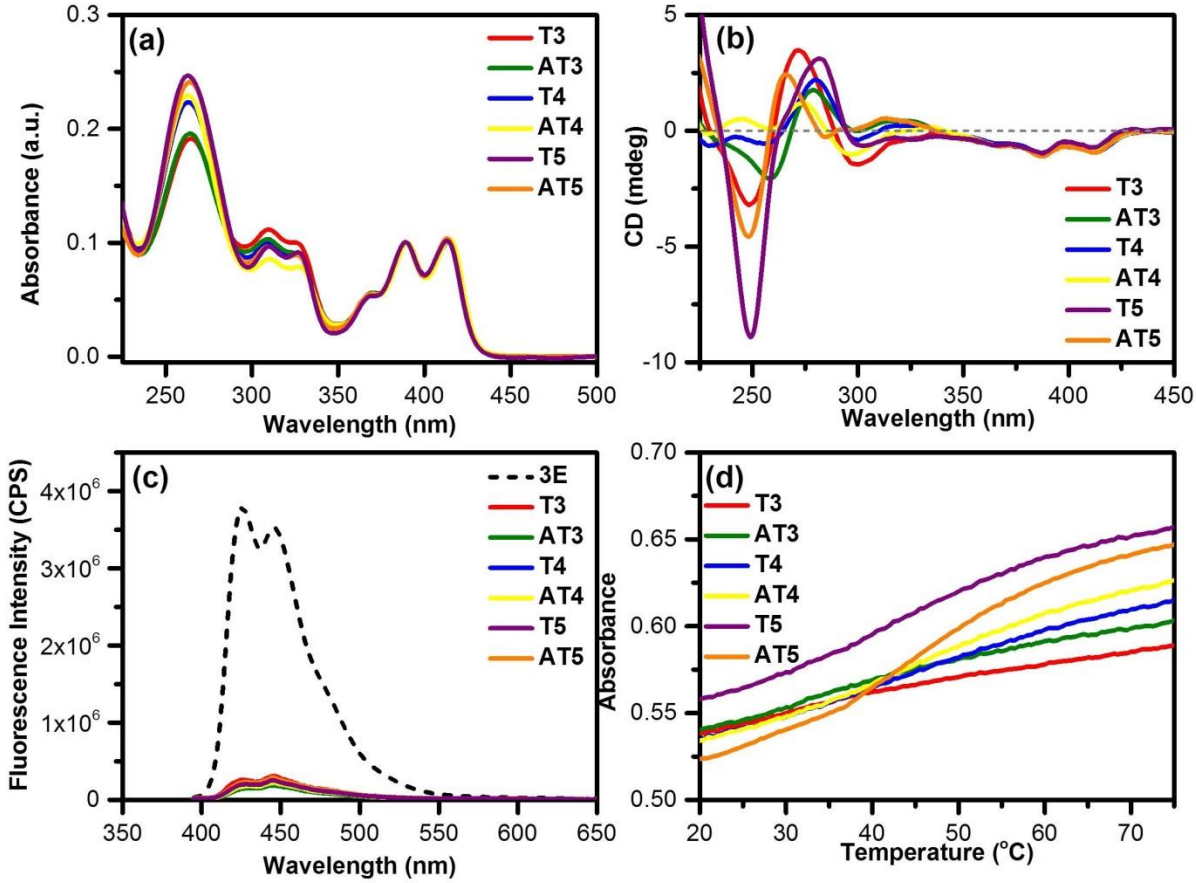

Figure 2-2-2. (a) Absorption, (b) circular dichroism, (c) fluorescence spectra (λ_{ex} = 385 nm), and (d) thermal dissociation profiles of DNA oligomers (~10^{-5} M) **T3** (red), **AT3** (green), **T4** (blue), **AT4** (yellow), **T5** (purple), and **AT6** (orange) in buffer solution (0.1 M NaCl and 10 mM sodium phosphate, pH 7.0 ± 0.1) at 298 K. Fluorescence spectra of **3E** (black dash line). Absorbance of the sample was matched at λ_{ex}.

The fluorescence quenching caused by charge separation (CS) between **3E** in excited singlet state (^{1}**3E***) and the neighboring nucleotide T, the primary quencher, was confirmed. Notably, the fluorescence intensity of the DNA oligomer was weaker than that of the dyad of **3E** and the corresponding nucleotide, indicating that in the DNA oligomers, **3E** was close to the nucleotide, whereas in the dyads the position of **3E** with respect to the nucleotide was flexible.[27] The correlation between fluorescence quantum yield and the CS rate constant was

not discussed due to the delayed fluorescence, which was caused by the charge recombination (CR) process.[11,18,27] Thermal dissociation profiles for the DNA oligomers (Figure 2-2-2d) indicate that with increasing the number of base pair in DNA the T_m becomes higher.

The dynamics of EET in the DNA oligomers were investigated by transient absorption measurements during femtosecond laser flash photolysis using a 400-nm laser pulse, which selectively excites **3E** in the DNA oligomers. The transient absorption spectra of **AT3**, **AT4**, and **AT5** are shown in Figure 2-2-3. On the other hand, the transient absorption spectra of **T3**, **T4**, and **T5** are shown in Figure 2-2-4. Immediately following the excitation, **AT3** showed an absorption band at 620 nm, which can be attributed to ^{1}**3E*** generated by the laser pulse. [11,27] An absorption band at 540 nm caused by **3E**$^{\bullet+}$ appeared within 1 ps after excitation, indicating rapid excess electron injection from ^{1}**3E*** to T.[11,27] An additional absorption band was confirmed at around 500 nm, which indicates generation of **DPA**$^{\bullet-}$.[25,26] Due to the overlap of the absorption bands of **3E**$^{\bullet+}$ and **DPA**$^{\bullet-}$, global fitting was applied to the spectra at 1 ps − 1 ns after excitation assuming two species. The species-associated spectrum (Figure 2-2-3b) for the faster component (τ_1) is attributed to **3E**$^{\bullet+}$−DNA$^{\bullet-}$−**DPA**, and the slower component (τ_2) is attributed to **3E**$^{\bullet+}$−DNA−**DPA**$^{\bullet-}$. However, **DPA**$^{\bullet-}$ generation was not observed in **AT4** and **AT5** as shown in Figure 2-2-3c, d, e and f. Thus, the species-associated spectrum for the faster component (τ_1) of **AT4** (Figure 2-2-3d) is attributed to **3E**$^{\bullet+}$−(T$^{\bullet-}$)T$_3$ in **AT4**, and the slower component (τ_2) is attributed to **3E**$^{\bullet+}$−T$_3$(T$^{\bullet-}$) in **AT4** (Figure 2-2-5a). Similar results were found in **AT5** (Figure 2-2-5b). In the present case, τ_1 can be attributed to the sum of the initial charge recombination (CR) between **3E**$^{\bullet+}$ and the neighboring T$^{\bullet-}$ (k_{CR}) and EET in DNA (k_{ET}) (Table 2-2-2). k_{CR} and k_{ET} were determined from the τ_1 value and the generation yield of **3E**$^{\bullet+}$−DNA−**DPA**$^{\bullet-}$. τ_2 can be attributed to k_{BET}, i.e., the CR rate constant of **3E**$^{\bullet+}$−DNA−**DPA**$^{\bullet-}$ for **AT3,** and **3E**$^{\bullet+}$−T$_3$(T$^{\bullet-}$) for **AT4**. The estimated rate constants are summarized in Table 2-2-2.

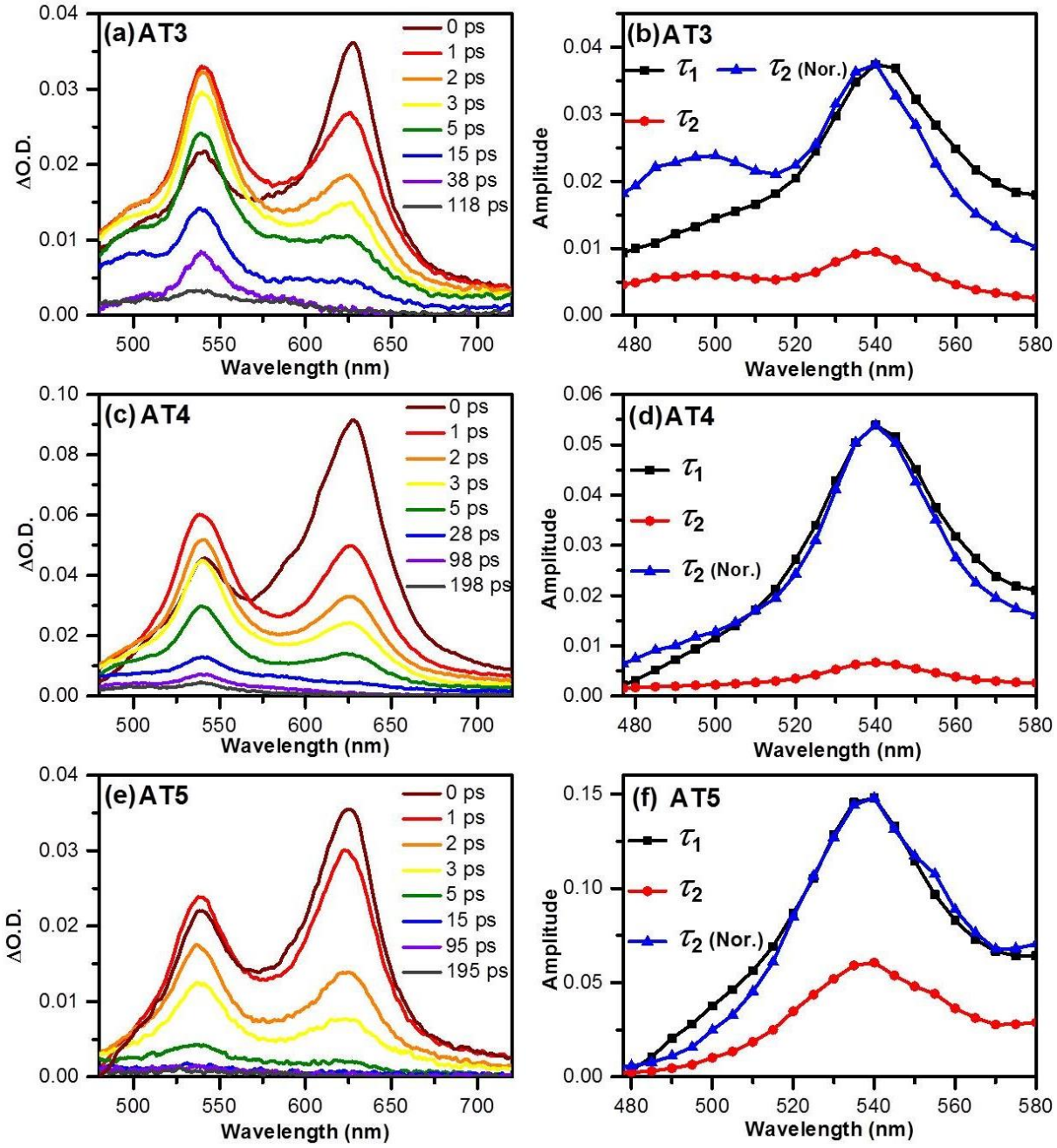

Figure 2-2-3. Transient absorption spectra during the laser flash photolysis of (a) **AT3**, (c) **AT4**, and (e) **AT5** upon excitation with 400-nm femtosecond laser pulse. Species-associated spectra obtained by global fitting using a double exponential function for (b) **AT3**, (d) **AT4**, and (f) **AT5** (black: τ_1, red: τ_2, and blue: normalized spectra of τ_2. τ_1 and τ_2 correspond to $(k_{CR} + k_{ET})^{-1}$ and k_{BET}^{-1}, respectively).

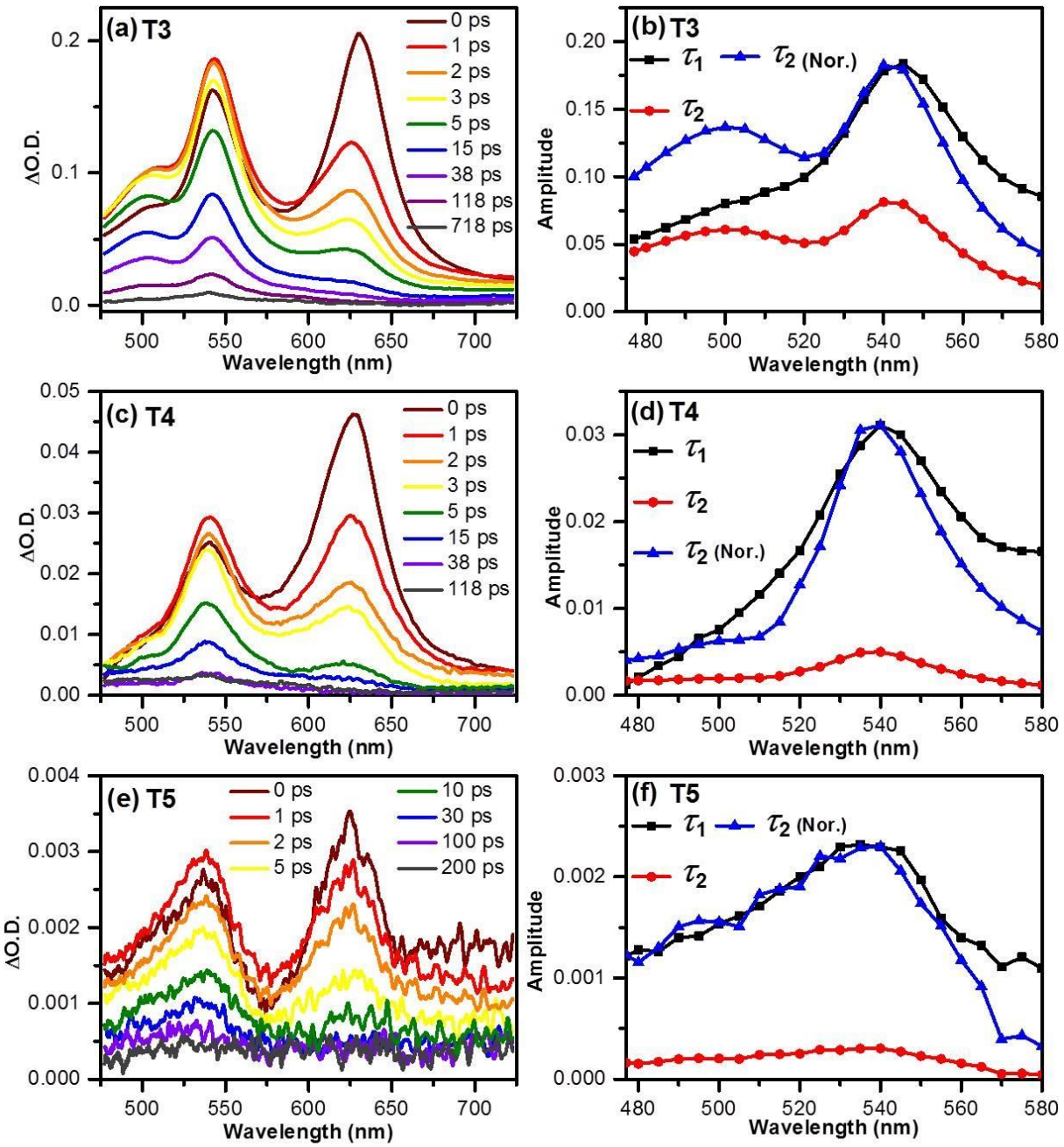

Figure 2-2-4. Transient absorption spectra during the laser flash photolysis of (a) **T3**, (c) **T4**, and (e) **T5** upon excitation with a 400-nm femtosecond laser pulse. Species-associated spectra obtained by global fitting using a double exponential function for (b) **T3**, (d) **T4**, and (f) **T5** (black: τ_1, red: τ_2, and blue: normalized spectra of τ_2. τ_1 and τ_2 correspond to $(k_{CR} + k_{ET})^{-1}$ and k_{BET}^{-1}, respectively).

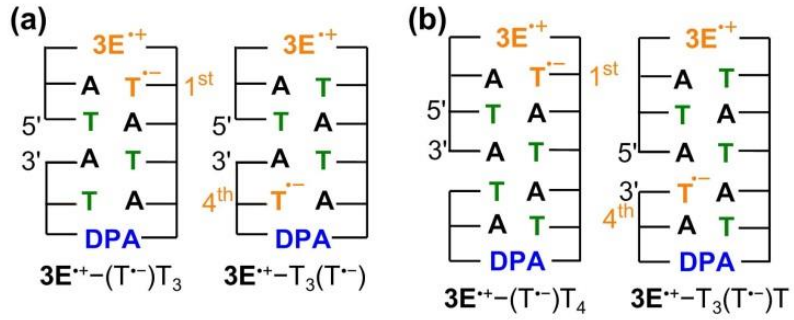

Figure 2-2-5. EET products in (a) **AT4** and (b) **AT5** by laser flash photolysis.

Table 2-2-2. Rate Constants (k_{CS}, k_{ET}, k_{CR}, and k_{BET}) in DNA Oligomers.

DNA	$k_{CS}{}^{a}$ (s^{-1})	$k_{CR}{}^{a}$ (s^{-1})	$k_{ET}{}^{a}$ (s^{-1})	$k_{BET}{}^{b}$ (s^{-1})
T3[c]	1.5×10^{12}	9.9×10^{10}	4.9×10^{10}	2.0×10^{10}
AT3	1.5×10^{12}	9.4×10^{10}	2.4×10^{10}	8.8×10^{9}
T4	1.4×10^{12}	2.0×10^{11}	3.0×10^{10}	3.0×10^{10}
AT4	1.4×10^{12}	2.0×10^{11}	1.4×10^{10}	1.4×10^{10}
T5	1.6×10^{12}	2.0×10^{11}	2.9×10^{10}	3.2×10^{10}
AT5	1.5×10^{12}	3.6×10^{11}	1.5×10^{10}	1.6×10^{10}

[a] Estimated error is less than 10%. [b] Estimated error is less than 5%. [c] Reference 11. [d] Not observed.

It is clear that the k_{CS} values were similar to the reported ones, which indicate that ^{1}**3E*** was quenched by CS to generate **3E**$^{\bullet+}$ and T$^{\bullet-}$.[11, 27] **DPA**$^{\bullet-}$ generation in **AT4** and **AT5** was negligible because CR between **3E**$^{\bullet+}$ and DNA$^{\bullet-}$ was faster than the EET process through the Ts. Similar results were observed in **T4**, and **T5** (Figure 2-2-4). Therefore, the CR process limits the quantum efficiency of EET through both consecutive and alternating A:T sequences when the DNA length was longer than 17.0 Å (4-base pairs intervening between **3E** and **DPA**). In **T3** and **AT3**, **3E**$^{\bullet+}$–T_3–**DPA**$^{\bullet-}$ was observed, indicating that excess electrons did reach **DPA**, as indicated in Figure 2-2-6. Although an excess electron did not reach **DPA**, excess electron seems to reach the 4th T from **3E** (Figure 2-2-5) because of the similarity in the k_{BET} values of **AT4** and **AT5**. For **T4** and **T5**, the similarities in the k_{ET} and k_{BET} values were also confirmed, indicating the formation of **3E**$^{\bullet+}$–T_3(T$^{\bullet-}$) in **T4** and **3E**$^{\bullet+}$–T_3(T$^{\bullet-}$)T in **T5**. These results support our hypothesis that the range for excess-electron transfer for both interstrand and interstrand in **3E**–DNA–**DPA** can be up to 13.6 Å but not longer than 17.0 Å

when using **3E** as the photosensitizer, i.e. the k_{BET} rate limits the extent of EET. In addition, it was suggested that EET in DNA is more efficient in Ts with continuous π-stacking than in Ts without stacking, because the k_{BET} values of **T4** and **T5** are larger than those of **AT4** and **AT5**, respectively.

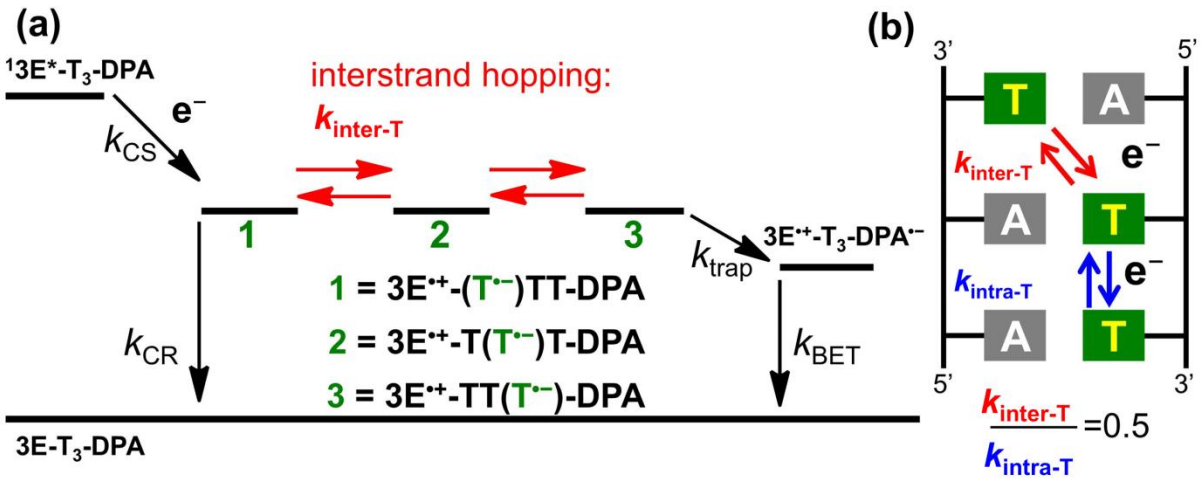

Figure 2-2-6. (a) Proposed schematic energy diagram of EET by T-hopping in **AT3**. (b) Illustration of excess-electron hopping in DNA through alternating and consecutive A:T sequences.

The excess electron hopping rate in both consecutive and alternating Ts can be estimated on the basis of the random work model (eq 2-2-1), [35, 36]

$$\tau(N) = (1/2k_{hop})N^2 \qquad (2\text{-}2\text{-}1)$$

where $\tau(N)$ is the time required for N hopping steps, i.e., k_{ET}^{-1}, and k_{hop} is the rate constant for a single hopping between neighboring nucleotides for intrastrand ($k_{intra\text{-}T}$) or interstrand ($k_{inter\text{-}T}$) EET. The excess electron hopping rates in **AT3** ($k_{inter\text{-}T}$) and **T3** ($k_{intra\text{-}T}$)[11] were estimated to be 1.1×10^{11} s^{-1} and 2.2×10^{11} s^{-1}, respectively. Hence, $k_{inter\text{-}T} = 0.5 \times k_{intra\text{-}T}$ (Figure 2-2-6b). These results indicate that interstrand EET in DNA is limited by insufficient interaction between the LUMOs of Ts. Thus, with increasing DNA length, the excess-electron hopping process is more easily terminated in alternating A:T sequences than in consecutive T sequences.

As mentioned previously, it is reported that the quantum efficiency of HT through 3 base pairs of alternating A:T is 4 times smaller than that of consecutive As.[23] In **AT3**, on the other hand, the quantum efficiency of EET is 0.20, which is smaller than **T3** (0.33)[11] by a factor of 1.6. Thus, EET in DNA is less affected by the alternating sequence of nucleotides than HT in

DNA, probably due to efficient interactions of LUMOs in the case of EET. These results indicate the relatively small difference in efficiency of interstrand and intrastrand EET in DNA, which is consistent with strand cleavage studies.[22]

Conclusion

To the best of our knowledge, the present paper provides the first investigation of interstrand EET dynamics in alternating A:T sequences in DNA oligomers by laser flash photolysis. These results showed that both rate constant and efficiency of interstrand EET are almost 2 times lower than those of intrastrand EET due to the lack of π-stacking of Ts. Thus, it is clear that EET by stepwise hopping is a sequence-dependent process. However, the relatively small difference between interstrand and intrastrand EET indicates that EET through LUMOs of nucleotides is more efficient than HT through HOMOs of nucleotides in DNA.

References

(1) Henderson, P. T.; Jones, D.; Hampikian, G.; Kan, Y.; Schuster, G. B. *Proc. Natl. Acad. Sci. USA* **1999**, *96*, 8353.

(2) Wagenknecht, H.-A. *Nat. Prod. Rep.* **2006**, *23*, 973.

(3) Genereux, J. C.; Barton, J. K. *Chem. Rev.* **2010**, *110*, 1642.

(4) Fujitsuka, M.; Majima, T. *Phys. Chem. Chem. Phys.* **2012**, *14*, 11234.

(5) Seidel, C. A. M.; Schulz, A.; Sauer, M. H. M. *J. Phys. Chem.* **1996**, *100*, 5541.

(6) Huber, R.; Fiebig, T.; Wagenknecht, H.-A. *Chem. Commun.* **2003**, *15*, 1878.

(7) Raytchev, M.; Mayer, E.; Amann, N.; Wagenknecht, H.-A.; Fiebig, T. *ChemPhysChem* **2004**, *5*, 706.

(8) Ito, T.; Rokita, S. E. *Angew. Chem. Int. Ed.* **2004**, *43*, 1839.

(9) Wagner, C.; Wagenknecht, H.-A. *Chem. —Eur. J.* **2005**, *11*, 1871.

(10) Cai, Z.; Li, X.; Sevilla, M. D. *J. Phys. Chem. B* **2002**, *106*, 2755.

(11) Lin, S. -H.; Fujitsuka, M.; Majima, T. *J. Phys. Chem. B* **2015**, *119*, 7994.

(12) Behrens, C.; Burgdorf, L. T.; Schwögler, A.; Carell, T. *Angew. Chem. Int. Ed.* **2002**, *41*, 1763.

(13) Behrens, C.; Carell, T. *Chem. Commun.* **2003**, 14, 1632.

(14) Wagenknecht, H.-A. *Angew. Chem. Int. Ed.* **2003**, *42*, 2454.

(15) Lewis, F. D.; Liu, X.; Wu, Y.; Miller, S. E.; Wasielewski, M. R.; Letsinger, R. L.; Sanishvili, R.; Joachimiak, A.; Tereshko, V.; Egli, M. *J. Am. Chem. Soc.* **1999**, *121*, 9905.

(16) Daublain, P.; Thazhathveetil, A. K.; Wang, Q.; Trifonov, A.; Fiebig, T.; Lewis, F. D. *J. Am. Chem. Soc.* **2009**, *131*, 16790.

(17) Daublain, P.; Thazhathveetil, A. K.; Shafirovich, V.; Wang, Q.; Trifonov, A.; Fiebig, T.; Lewis, F. D. *J. Phys. Chem. B* **2010**, *114*, 14265.

(18) Gorczak, N.; Fujii, T.; Mishra, A. K.; Houtepen, A. J.; Grozema, F. C.; Lewis, F. D. *J. Phys. Chem. B* **2015**, *119*, 7673-7680.

(19) Tainaka, K.; Fujitsuka, M.; Takada, T.; Kawai, K.; Majima, T. *J. Phys. Chem. B* **2010**, *114*, 14657.

(20) Park, M. J.; Fujitsuka, M.; Kawai, K.; Majima, T. *J. Am. Chem. Soc.* **2011**, *133*, 15320.

(21) Park, M. J.; Fujitsuka, M.; Nishitera, H.; Kawai, K.; Majima, T. *Chem. Commun.* **2012**, *48*, 11008.

(22) Cichon, M. K.; Haas, H. C.; Grolle, F.; Mees, A.; Carell, T. *J. Am. Chem. Soc.* **2002**, *124*, 13984.

(23) Lewis, F. D.; Daublain, P.; Cohen, B.; Vura-Weis, J.; Shafirovich,V.; Wasielewski, M. R. *J. Am. Chem. Soc.* **2007**, *129*, 15130.

(24) Takada, T.; Kawai, K.; Cai, X.; Sugimoto, A.; Fujitsuka, M.; Majima, T. *J. Am. Chem. Soc.* **2004**, *126*, 1125.

(25) Lewis, F. D.; Liu, X.; Miller, S. E.; Wasielewski, M. R. *J. Am. Chem. Soc.* **1999**, *121*, 9746.

(26) Lewis, F. D.; Liu, X.; Miller, S. E.; Hayes, R. T.; Wasielewski, M. R. *J. Am. Chem. Soc.* **2002**, *124*, 14020.

(27) Lin, S. -H.; Fujitsuka, M.; Ishikawa, M.; Majima, T. *J. Phys. Chem. B* **2014,** *118*, 12186.

(28) Fujitsuka, M.; Cho, D. W.; Tojo, S.; Inoue, A.; Shiragami, T.; Yasuda, M.; Majima, T. *J. Phys. Chem. A* **2007**, *111*, 10574.

(29) Yamaguchi, S.; Hamaguchi, H. *Appl. Spectrosc.* **1995**, *49*, 1513.

(30) Turbiez, M.; Frère, P.; Roncali, J. *J. Org. Chem.* **2003**, *68*, 5357.

(31) Lewis, F. D.; Zhang, L.; Liu, X.; Zuo, X.; Tiede, D. M.; Long, H.; Schatz, G. C. *J. Am. Chem. Soc.* **2005**, *127*, 14445.

(32) Vura-Weis, J.; Wasielewski, M. R.; Thazhathveetil, A. K.; Lewis, F. D. *J. Am. Chem. Soc.* **2009**, *131*, 9722.

(33) Patwardhan, S.; Tonzani, S.; Lewis, F. D.; Siebbeles, L. D. A.; Schatz, G. C.; Grozema, F. C. *J. Phys. Chem. B* **2012**, *116*, 11447.

(34) Joy, J.; Cheriya, R. T.; Nagarajan, K.; Shaji, A.; Hariharan, M. *J. Phys. Chem. C* **2013**, *117*, 17927.

(35) Bar-Haim, A.; Klafter, J. *J. Chem. Phys.* **1998**, *109*, 5187.

(36) Conron, S. M. M.; Thazhathveetil, A. K.; Wasielewski, M. R.; Burin, A. L.; Lewis, F. D. *J. Am. Chem. Soc.* **2010**, *132*, 14388.

Chapter 2-3. Sequence-Dependent Photocurrent Generation through Long-Distance Excess-Electron Transfer in DNA

Abstract

Due to the well-ordered continuously π stacking of nucleobases, DNA is considered as a biomaterial for charge transfer in biosensors and so on. For cathodic photocurrent generations caused by hole transfer in DNA, it has been confirmed to be sensitive to DNA structure and base pair stacking. However, such information has not been investigated for anodic photocurrent generations caused by excess-electron transfer in DNA. In the present study, the author used the photoelectrochemical technique to measure the anodic photocurrent generation of DNA films on Au electrode to clarify the dynamics of excess-electron transfer in DNA. Our results indicate that sequence dependence of photocurrent generation is caused by long-distance excess-electron transfer in DNA, which is dominated by the hopping mechanism.

Introduction

DNA has attracted much attention as a biomaterial for charge transfer (CT) since the first suggestion of DNA conductivity.[1-3] In recent years, due to the highly sensitive for DNA structure such as mismatches and lesions that perturb the π stacking between base pairs, several studies on DNA sensors assembled by DNA-modified electrodes for detection of DNA damage *in vitro* using electrochemical techniques have been reported.[2] On the other hand, due to the state of the arts of organic solar cells, based on photon-to-electron conversions in π stacking multicromophores, the photoelectrochemical technique has also showed wide applications on DNA sensors with new mode of signal transduction compared to conventional electrochemical techniques.[4] Moreover, DNA is expected to be a scaffold for building a one-dimension array with π stacking, which can conduct electrons efficiently.[5-8] In addition, understanding of oxidative CT, hole transfer (HT), is important to explaining biological phenomena such as DNA damages.[9,10] In contrast, reductive CT, excess-electron transfer (EET), can be considered as a key process that closely relates to the repair of damaged DNA such as T-T lesions.[11] Since the photoelectrochemical technique can be operated at a low applied potential to ensure the orientation of DNA films,[4,12] the photoelectochemical device shows its prospects as a platform for studying CT in DNA.

To date, several groups including us have been studied cathodic photocurrent generation of DNA films on electrode to realize sequence dependence of HT in DNA.[13-15] However, to our knowledge, such experiments have not been performed to study long-distance EET in DNA. For EET in DNA, thymine (T) and cytosine (C) are considered as electron carriers in the energetic aspects.[16] Although sequence dependence of EET in DNA has been clarified by employing donor−DNA−acceptor system with short sequence using laser flash photolysis,[17,18] it is still unclear for long-distance EET in DNA. Here, the author prepared three kinds of **3E**-modified DNA oligomers (**ATn**, **CT6** and **GT6**, Figure 2-3-1) to understand sequence dependence of photocurrent generation caused by long-distance EET in DNA.

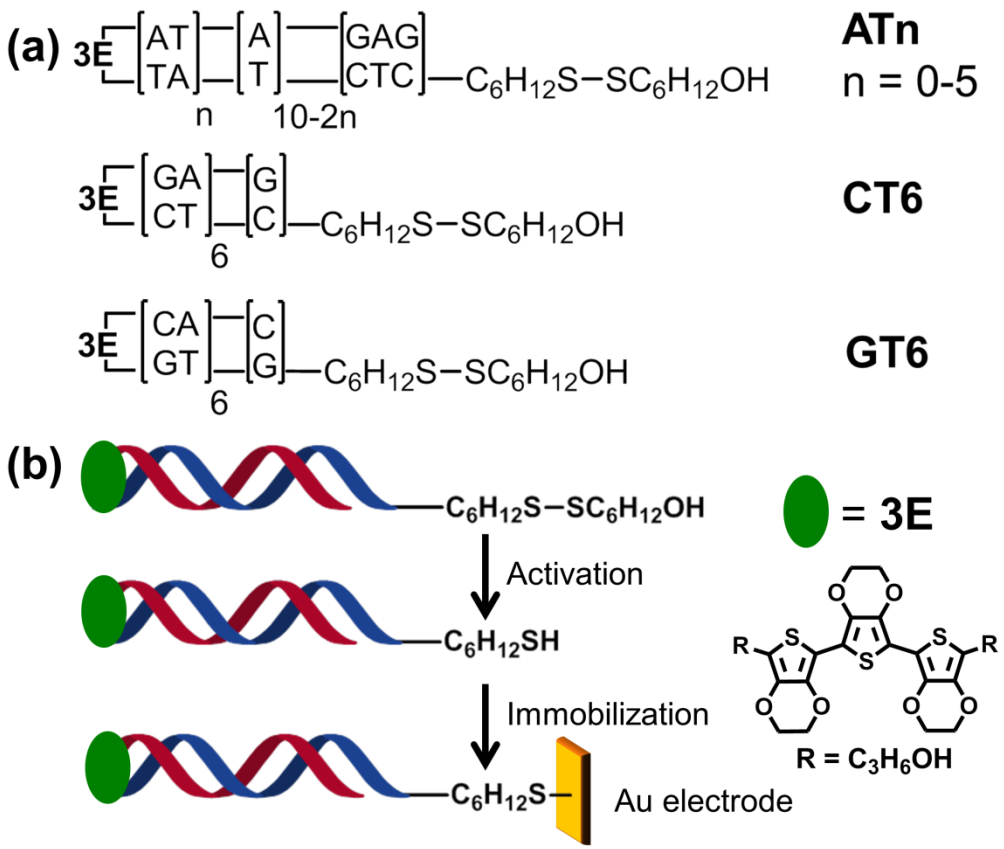

Figure 2-3-1. (a) DNA oligomers used in this study. (b) Preparation process of DNA films.

Experimental Section

Synthesis of DNA oligomers. The sensitizers, **3E**, was prepared and converted to its phosphoramidite derivatives by similar procedure as previously reported.[19,20] All reagents were purchased from Glen Research (USA). All DNA oligomers were synthesized on an Applied Biosystems 3400 DNA synthesizer with standard solid-phase techniques and characterized by MALDI-TOF mass spectroscopy (Table 2-3-1). The DNA oligomers were purified on a JASCO HPLC with a reversed-phase C-18 column with acetonitrile/50 mM ammonium formate gradient.

Preparation of DNA films on Au electrode. As shown in Figure Figure 2-3-1b, a DNA oligomer was activated by cleaving the disulfide linkage using 100 mM DDT (dithiothreitol), pH 8.5, at room temperature for 30 minutes. The crude activated DNA oligomers were purified using HPLC and then stored in solution A (20 mM Na phosphate buffer, 100 mM NaCl, and 10 mM TCEP (*tris*(2-carboxyethyl)phosphine), pH 7.0 ± 0.1)**.** Au electrodes (0.02 cm^2 in area) were successively polished and etched by similar procedure as previously reported.[21,22] The electrodes were then immersed by in 10 μM solutions of activated DNA in

buffer solution A for 12-18 hr at room temperature. Subsequently, the modified electrodes were washed with 10 mM Tris buffer (pH 7.6), backfilled with the 10 mM solution of 6-mercapto−1-hexanol (MCH) in buffer solution A for 30 min, and then washing with Tris buffer to obtain the DNA films on Au electrode. For determining the surface coverage of DNA films on electrode, the author employed the method established by Tarlov and coworkers by chronocoulometry using $[Ru\text{-}(NH_3)_6]^{3+}$ as a redox label.[21] The surface coverage of the DNA films are summarized in Table 2-3-1.

Table 2-3-1. MALDI-TOF MS and melting temperature (T_m) of the DNA oligomers and Surface coverage of the DNA films on Au electrode.

DNA	Calculated	Found	T_m,[a] (℃)	Coverage[b] (pmol cm^{-2})
AT0	8907.392	8905.462	76	2.70 ± 0.21
AT1	8907.392	8905.960	74	3.08 ± 0.24
AT2	8907.392	8903.467	72	2.97 ± 0.29
AT3	8912.372	8908.219	70	2.41 ± 0.21
AT4	8907.392	8905.416	70	2.73 ± 0.25
AT5	8907.392	8910.459	69	2.52 ± 0.22
CT6	8912.372	8910.167	83	3.64 ± 0.27
GT6	8909.384	8913.245	88	3.07 ± 0.25

[a] Measured in ~2 x 10^{-5} M solution (0.1 M NaCl and 10 mM sodium phosphate, pH 7.0 ± 0.1) at a heating rate of 0.5 ℃/min from 10 ℃ to 100 ℃) with the absorbance at 260 nm recorded in 60 s intervals. [b] Coverage of the DNA films on electrode was determined by Tarlov's method.[20]

Apparatus. All samples of DNA oligomers were prepared in buffer solution B (10 mM sodium phosphate and 100 mM NaCl, pH 7.0 ± 0.1). Steady-state absorption, circular dichroism (CD) spectra, and melting temperature profiles were measured using a Shimadzu UV3100PC, JASCO CDJ720, and Shimadzu UV2700, respectively. The CD spectra of DNA oligomers were average data from ten scans, collected from 400 nm to 225 nm with a scanning rate of 100 nm min^{-1}. A standard three-electrode configuration, consisting of a gold electrode, an Ag/AgCl (saturated KCl) reference electrode, and a platinum wire auxiliary electrode in an electrochemical cell, was used for all electrochemical measurements using electrochemical analyzer (ALS, model 660B). Differential pulse voltammetry (DPV)

experiments were carried out at room temperature in buffer solution. The photoelectrochemical measurements were performed in buffer solution B by a Compact xenon lamp 300W (HAL-320W, Asahi Spectra) equipped with a band-pass filter (λ > 400 ± 10 nm). Photocurrents were monitored upon the irradiation at a bias voltage of −0.2 V vs Ag/AgCl with 100 μM ascorbic acid.

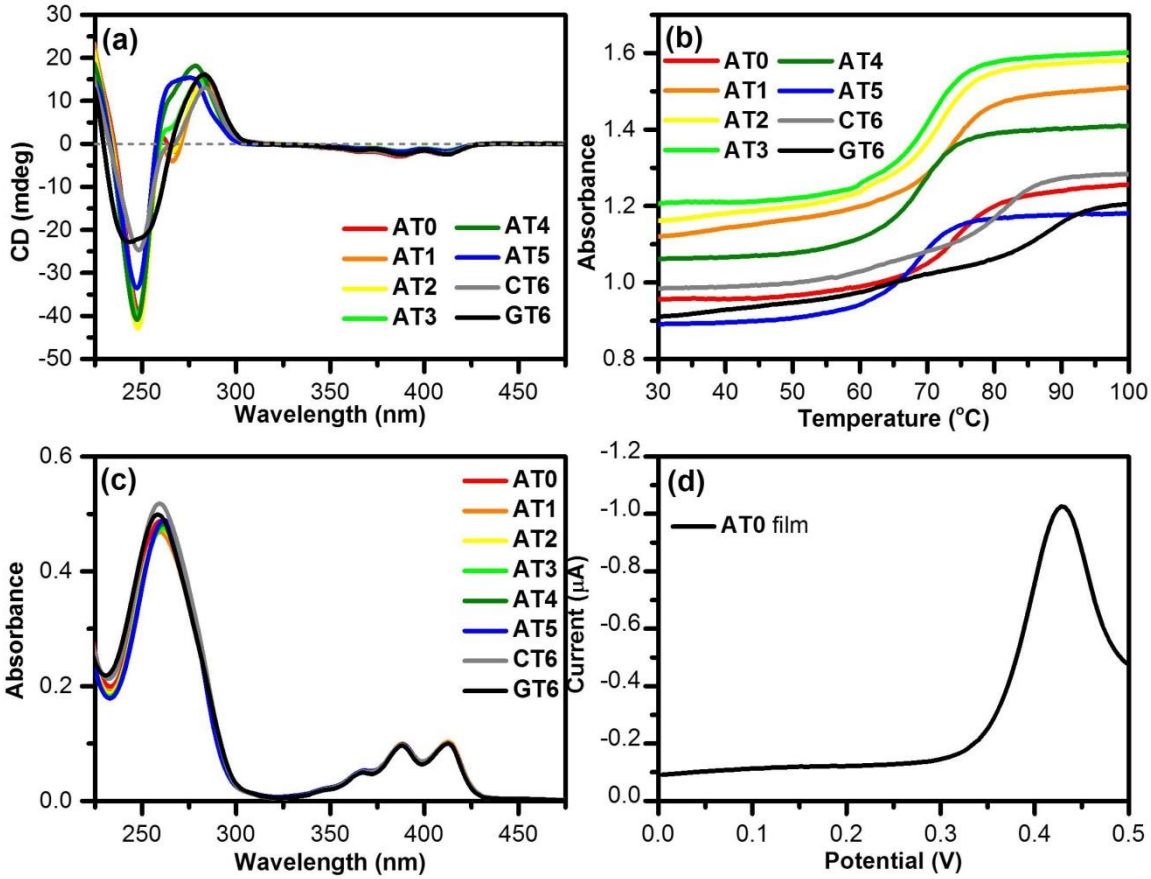

Figure 2-3-2. (a) Circular dichroism spectra, (d) thermal dissociation profiles, and (c) absorption spectra of DNA oligomers (~10^{-5} M) **AT0** (red), **AT1** (orange), **AT2** (yellow), **AT3** (green), **AT4** (olive), **AT5** (blue), **CT6** (gray), and **GT6** (black) in buffer solution B at 298 K. (d) DPV of electrodes modified with DNA oligomer **AT0** measured in buffer solution B.

For all DNA oligomers, formation of a B-type duplex structure under the experimental condition was indicated by circular dichroism (CD) and melting temperature (T_m) measurements (Figure 2-3-2a and b). Steady-state absorption spectra of all DNA oligomers (Figure 2-3-2c) show that all DNA oligomers exhibit absorption bands due to **3E** (390 and 410 nm) as well as that of nucleotides (around 260 nm).[17,18,20] Moreover, the DNA

modification on electrodes was confirmed by measurements of DPV (differential pulse voltammetry), showing that the oxidation at around 0.42 V generates a distinct radical cation of **3E**, $\mathbf{3E}^{\bullet+}$ (Figure 2-3-2d).[20]

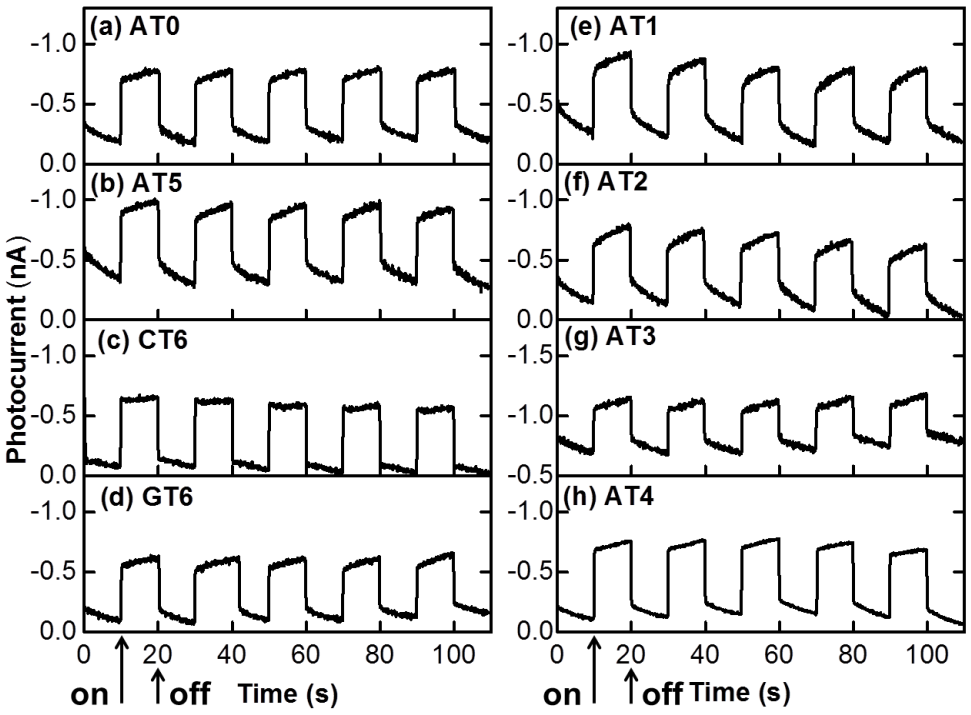

Figure 2-3-3. Photocurrent response of electrodes modified with DNA oligomers. Irradiation time: 10 s.

Photocurrent measurements of the DNA films on Au electrode were carried out using Compact xenon lamp 300W (HAL-320W, Asahi Spectra) equipped with a band-pass filter (λ > 400 ± 10 nm). Thus, only **3E** was excited according to absorption spectra of all DNA oligomers. To avoid the change of DNA film morphology, a potential of 200 mV versus Ag/AgCl was applied.[12] A stable anodic photocurrent appeared immediately upon irradiation of DNA films on Au electrode (Figure 2-3-3). Moreover, the author found the DNA films were stable during the photocurrent measurements for more than 100 s (Figure 2-3-3) under the experimental condition without morphology change.[12] A comparison of photocurrent generations of DNA films is shown in Figure 2-3-4.

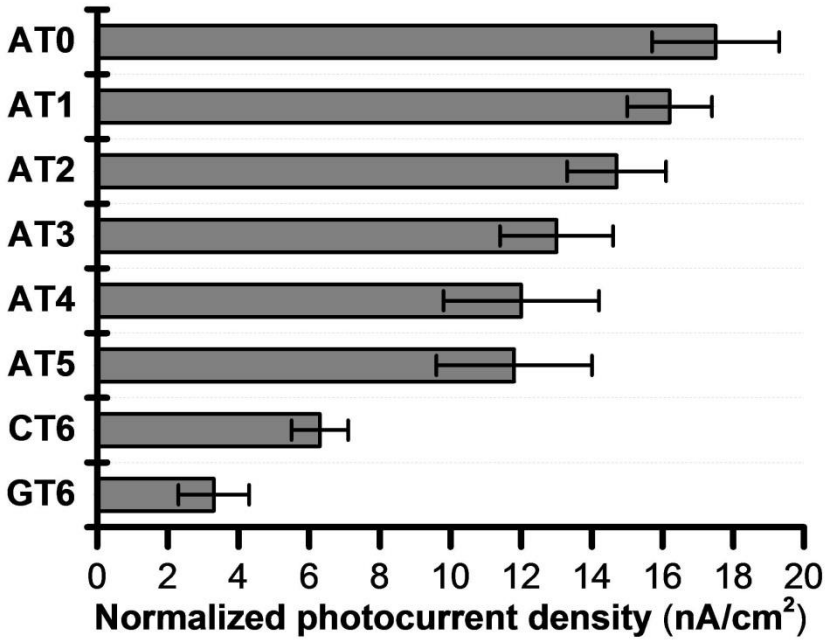

Figure 2-3-4. Normalized photocurrent density of DNA films. Error bars represent the standard deviation from five experiments.

It is clear that the normalized photocurrent density (I_P) results are strongly sequence-dependent. In **ATn**, the I_P decreases obviously as the number of alternating A:T base pair (n) increases. According to our previous paper,[18] this tendency can be originated by interstrand EET in DNA which is limited by insufficient interaction between the LUMOs of Ts. On the other hand, it showed a strong suppression in both **CT6** and **GT6**, indicating that the excess-electron hopping between T in both sequences are affected by a single G:C base pair, as mentioned in our previous paper.[17]

Energetic diagrams of the photocurrent generation of DNA films on Au electrode are shown in Figure 2-3-5. Photoexcitation of **3E** yields a charge separation state by excess-electron injection from the singlet excited **3E**, ^{1}**3E***, to T. The electron migrates through T then followed by hopping to the Au electrode to yield photocurrents. **3E**$^{\bullet+}$ is reduced in the presence of ascorbic acid, **AA**, as an electron-donating sacrifice, to regenerate **3E**. The redox levels of the components participate in the photocurrent generation are presented in Figure 3.[16,19,23] Notably, due to the strong sequence dependence of photocurrent generation and the energetic aspects showed in Figure 2-3-5, photocurrent generation of DNA films can be dominated by EET in DNA through T. Thus, from I_P, the author determined relative quantum yield of EET (Φ_{rel}) and the rate constant of EET (k_{ET}) of DNA films, summarized in Table 2-3-2.

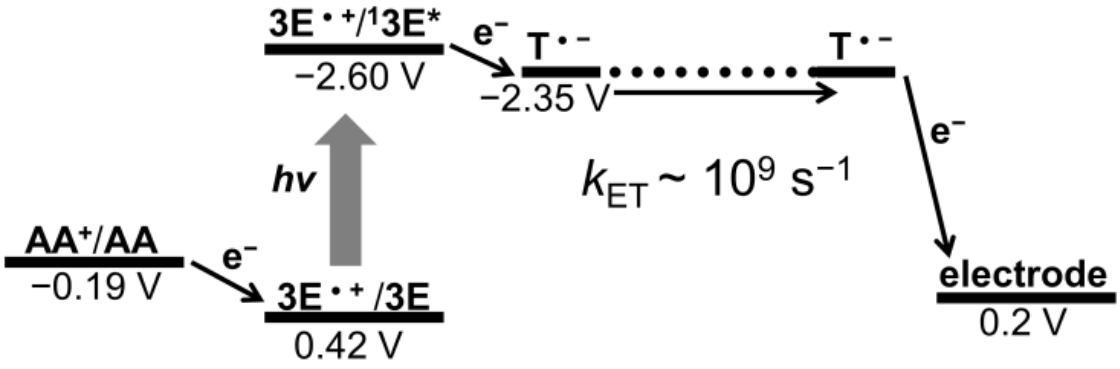

Figure 2-3-5. Energetic diagram of photocurrent generation of DNA film on Au electrode in the presence of ascorbic acid (**AA**). Potential versus Ag/AgCl.

Table 2-3-2. Normalized Photocurrent Density (I_P), Relative Quantum Yield of EET (Φ_{rel}), and the Rate Constant of EET (k_{ET}) of DNA Films.

DNA	I_P[a] (nA cm^{-2})	Φ_{rel}[b]	k_{ET} (s^{-1})
AT0	17.5 ± 1.8	1.00	3.1×10^{9} [c]
AT1	16.2 ± 1.2	0.93	2.9×10^{9} [d]
AT2	14.7 ± 1.4	0.84	2.6×10^{9} [c]
AT3	13.0 ± 1.6	0.74	2.3×10^{9} [d]
AT4	12.0 ± 2.2	0.69	2.1×10^{9} [d]
AT5	11.9 ± 2.2	0.68	2.1×10^{9} [d]
CT6	6.3 ± 0.8	0.36	1.1×10^{9} [d]
GT6	3.3 ± 1.0	0.19	5.8×10^{8} [d]

[a] Normalized by coverage of DNA films on electrode to be 1 pmolcm^{-2}. [b] Yields of the EET relative to that of **AT0** based on I_P. [c] Estimated on the basis of the random walk model and Φ_{rel}.

From the single-step excess-electron hopping rate ($k_{T\text{-}HOP} = 2.2 \times 10^{11}$ s^{-1}) of consecutive Ts (thymines) reported in our previous papers,[17,18] the rate of excess-electron transfer (k_{ET}) for **AT0** is estimated to be 3.1×10^{9} s^{-1} on the basis of the random work model as shown in Eq (2-3-1),[24,25]

$$\tau(N) = (1/2k_{hop})N^2 \quad (2\text{-}3\text{-}1)$$

where $\tau(N)$ is the time required for N hopping steps, i.e, k_{ET}^{-1} and $k_{T\text{-}HOP}$ is the rate constant for a single hopping between nucleobases (N = 12). On the other hand, the author employed

Φ_{rel} as the factor of k_{ET} for **AT1-5**, **CT6**, and **GT6**. Thus, in the case of **AT1**, k_{ET} for **AT1** can be estimated to be (k_{ET} for **AT0**) × (Φ_{rel} for **AT1**) = (3.1×10^9 s^{-1}) × (0.93) = 2.9×10^9 s^{-1}. From Table 1, it shows that the k_{ET} of **ATn** are influenced by the base pair stacking but similar to each other, indicating that the relatively small difference in efficiency of interstrand and intrastrand EET in DNA.[18] From **AT5**, the stepwise hopping rate (k_{hop}) can be estimated as 1.5×10^{11} s^{-1} on the basis of the random walk model (eq. 2-3-1).[24,25] This result is similar to our previous reported value (1.1×10^{11} s^{-1}) for interstrand EET in alternating A:T sequences. However, the k_{ET} of **CT6** and **GT6** are dramatically smaller than those of **ATn**, due to the insertion of single G:C base pair between consecutive Ts. To clarify this point, the author proposed two mechanisms for understanding sequence dependence of EET in **CT6** and **GT6**, respectively in Figure 2-3-6.

For **CT6** and **GT6**, two mechanisms for EET with kinetic constant of stepwise hopping ($k_{intra\text{-}C}$ and $k_{intra\text{-}G}$) and tunneling ($k_{t\text{-}C}$ and $k_{t\text{-}G}$) are shown in Figure 2-3-6a, b, c, and d, respectively. Although a large energetic difference is not expected between T and C (0.09 V),[16] the upward $k_{intra\text{-}C}$, which should be smaller than the downward ones, are discussed in the mechanism that C is assumed to be an electron carrier in **CT6** (Figure 2-3-6a). Thus, $k_{intra\text{-}C}$ can be determined as 8.0×10^{10} s^{-1}. It is clear that $k_{intra\text{-}C}$ is similar to previous reported value (1.0×10^{11} s^{-1}) obtained by laser flash photolysis.[17] Another mechanism, in which C is assumed to be a spacer (Figure 2-3-6b), $k_{t\text{-}C}$ can be determined as 2.0×10^{10} s^{-1} (From eq. 2-3-1, $k_{t\text{-}C} = (6^2/2) \times k_{ET} = 2.0 \times 10^{10}$ s^{-1}). However, $k_{t\text{-}C}$ reported here is smaller than previous reported value (4.9×10^{10} s^{-1}) by 2.5 times.[17] On the other hand, it is unlikely possible for the upward electron hopping in **GT6** due to a large energetic difference between T and G (0.62 V,[16] Figure 2-3-6c) when G is assumed to be an electron carrier. Another mechanism, in which G is assumed to be a spacer, $k_{t\text{-}G}$ can be determined as 1.0×10^{10} s^{-1} (Figure 2-3-6d). However, like intrastrand EET in **CT6**, interstrand EET in **GT6** should be expected when C acts as an electron carrier (Figure 2-3-6f and e). The author found $k_{inter\text{-}C}$ (4.2×10^{10} s^{-1}) is smaller than $k_{intra\text{-}C}$ by a factor of 0.5 due to the insufficient interaction between LUMOs of nucleobases, which is consistent to our previous results for interstrand and intrastrand EET through A:T sequence.[18] Thus, the author concludes the hopping mechanism plays an important role in sequence dependence of EET in DNA according to both the new results obtained by the photoelectrochemical technique and the previously reported values obtained by laser flash photolysis.

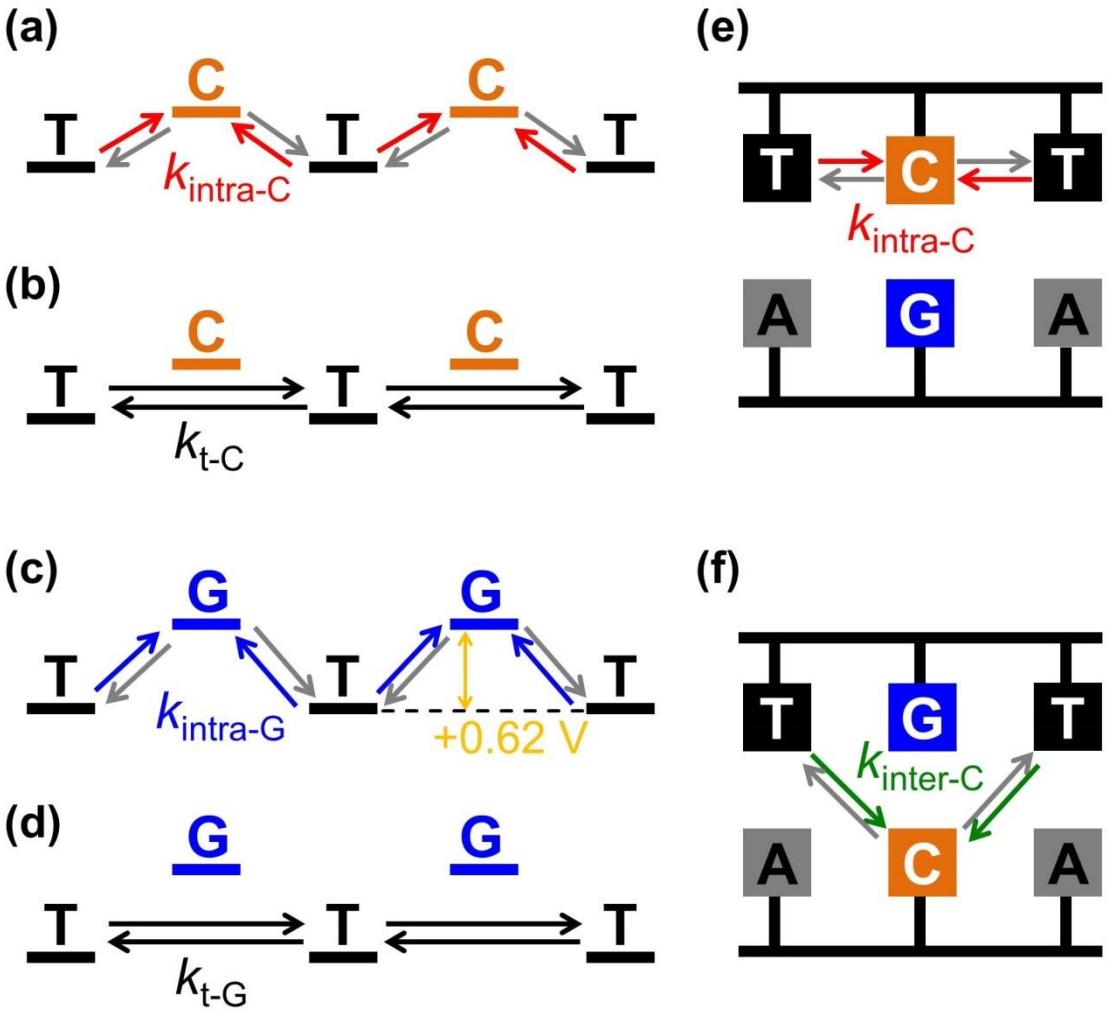

Figure 2-3-6. Proposed schematic energy diagram of EET in **CT6**, where C acts as (a) carrier or (b) a spacer, and in **GT6**, where G acts as (c) carrier or (d) a spacer. Illustration of EET in (e) **CT6** and (f) **GT6** by the hopping mechanism.

Notably, these result are not conflict to our previous results showed proton transfer of G:C$^{\bullet-}$ base pairs would terminate the EET in DNA when C acts as an electron carrier because the rate of proton transfer of G:C$^{\bullet-}$ base pair (k_{PT} = 2.6 × 10^{10} s^{-1})[17] is slightly smaller than both $k_{intra-C}$ and $k_{inter-C}$. In addition, the estimated stepwise hopping of approximately ~10^{10} s^{-1} can be used to calculate charge mobility (μ) as a value to be ~10^{-3} cm^2 V^{-1} s^{-1}, which is higher than that oh HT (~10^{-5} cm^2 V^{-1} s^{-1}).[26] Thus, with the respect to bioelectronics, EET in DNA is more promising for the applications than HT in DNA, which relates DNA damages.[9,10]

Conclusion

To the best of our knowledge, this is the first study that applying photoelectrochemical technique to study the dynamics of EET in DNA. Our results show sequence-dependent EET in DNA dominates photocurrent generation of DNA films on Au electrode. Although I_P of **CT6** and **GT6** were found to be smaller than those of **ATn**, however, due to the small difference in the reduction potential of C and T, C was found to be as an electron carrier when a single G:C base pair inserts in consecutive Ts regardless C is next to T or not. The author expects the photoelectrochemical technique will facilitate deeper investigations on dynamics of EET in DNA.

References

(1) Sontz, P. A.; Muren, N. B.; Barton, J. K. *Acc. Chem. Res.* **2012**, *45*, 1792.

(2) Paleček, E.; Bartošík, M. *Chem. Rev.* **2012**, *112*, 3427.

(3) Grodick, M. A.; Muren, N. B.; Barton, J. K. *Biochemistry* **2015**, *54*, 962.

(4) Zhao, W.-W.; Xu, J.-J.; Chen, H.-Y. *Chem. Rev.* **2014**, *114*, 7421.

(5) Willner, I.; Patolsky, F.; Wasserman, J. *Angew. Chem. Int. Ed.* **2001**, *40*, 1861.

(6) Bhosale, R.; Míšek, J.; Sakai, N.; Matile, S. *Chem. Soc. Rev.* **2010**, *39*, 138.

(7) Zhan, X.; Facchetti, A.; Barlow, S.; Marks, T. J.; Ratner, M. A.; Wasielewski, M. R.; Marder, S. R. *Adv. Mater.* **2011**, *23*, 268.

(8) Frischmann, P. D.; Mahata, K.; Würthner,F. *Chem. Soc. Rev.* **2013**, *42*, 1847.

(9) Wallace, S. S. *Free Radic. Biol. Med.* **2002**, *33*, 1.

(10) Kanvah, S.; Joseph, J.; Schuster, G. B.; Barnett, R. N.; Cleveland, C. L.; Landman, U. *Acc. Chem. Res.* **2010**, *43*, 280.

(11) Carell, T. *Angew. Chem. Int. Ed.* **1995**, *34*, 2491.

(12) Kelley, S. O.; Barton, J. K.; Jackson, N. M.; McPherson, L. D.; Potter, A. B.; Spain, E. M.; Allen, M. J.; Hill, M. G. *Langmuir* **1998**, *14*, 6781.

(13) Okamoto, A.; Kamei, T.; Tanaka, K.; Saito, I. *J. Am. Chem. Soc.* **2004**, *126*, 14732.

(14) Tanabe, K.; Iida, H.; Haruna, K.-i.; Kamei, T.; Okamoto, A.; Nishimoto, S.-i. *J. Am. Chem. Soc.* **2006**, *128*, 692.

(15) Takada, T.; Lin, C.; Majima, T. *Angew. Chem. Int. Ed.* **2007**, *46*, 6681.

(16) Seidel, C. A. M.; Schulz, A.; Sauer, M. H. M. *J. Phys. Chem.* **1996**, *100*, 5541.

(17) Lin, S.-H.; Fujitsuka, M.; Majima, T. *J. Phys. Chem. B* **2015**, *119*, 7994.

(18) Lin, S.-H.; Fujitsuka, M.; Majima, *Chem. —Eur. J.* **2015**, *21*, 16190.

(19) Lin, S.-H.; Fujitsuka, M.; Ishikawa, M.; Majima, T. *J. Phys. Chem. B* **2014**, *118*, 12186

(20) Turbiez, M.; Frère, P.; Roncali, J. *J. Org. Chem.* **2003**, *68*, 5357.

(21) Steel, A. B.; Herne, T. M.; Tarlov, M. J. *Anal. Chem.* **1998**, *70*, 4670.

(22) Fischer, L. M.; Tenje, M.; Heiskanen, A. R.; Masuda, N.; Castillo, J.; Bentien, A.; Émneus, J.; Jakobsen, M. H.; Boisen, A. *Microelectron. Eng.* **2009**, *86*, 1282.

(23) Matsui, T.; Kitagawa, Y.; Okumura, M.; Shigeta, Y. *J. Phys. Chem. A* **2015**, *119*, 369.

(24) Bar-Haim, A.; Klafter, J. *J. Chem. Phys.* **1998**, *109*, 5187.

(25) Conron, S. M. M.; Thazhathveetil, A. K.; Wasielewski, M. R.; Burin, A. L.; Lewis, F. D. *J. Am. Chem. Soc.* **2010**, *132*, 14388.

(26) Lewis, F. D.; Zhu, H.; Daublain, P.; Cohen, B.; Wasielewski, M. R. *Angew. Chem. Int. Ed.* **2006**, *45*, 7982.

Chapter 3. Fluctuation Effect on Excess-Electron Transfer in DNA: Excess-Electron Transfer in DNA by Fluctuation-Assisted Hopping Mechanism

Abstract

The dynamics of excess-electron transfer in DNA have attracted the attention of scientists from all kinds of research fields due to their importance in biological processes. To date, several studies on excess-electron transfer in consecutive adenine (A) :thymine (T) sequences in donor–DNA–acceptor systems have been published. However, the reported excess-electron transfer rate constants for consecutive Ts are in the range of 10^{10}–10^{11} s^{-1} depending on photosensitizing electron donors, which provided various driving forces for excess-electron injection to DNA. In this study, the author employed a strongly electron-donating photosensitizer, a dimer of 3,4-ethylenedioxythiophene (**2E**), and an electron acceptor, diphenylacetylene (**DPA**), to synthesize a series of modified DNA oligomers (**2-Tn**) to investigate excess-electron transfer dynamics in donor–DNA–acceptor by using femtosecond laser flash photolysis. The relation between free energy change for charge injection and excess-electron transfer rate among consecutive Ts was discussed based on the new results and the previously reported values. the author found that the intrinsic excess-electron hopping rate constant ($(3.8 \pm 1.5) \times 10^{10}$ s^{-1}) in DNA is consistent with the fluctuation frequency of the DNA sugar backbone and bases (3.3×10^{10} s^{-1}) and concluded that the structural fluctuation plays an important role in the dynamics of excess-electron transfer in DNA.

Introduction

Charge transfer in DNA with well-ordered nucleobases realizing continuously π-π stacking has attracted the attention of scientists for decades.[1-4] Numerous results from both theoretical and experimental studies suggest that electron-deficient intermediates generated by one-electron oxidation of DNA, i.e. the hole, can migrate among guanine (G) and adenine (A),[5-11] on the other hand, excess-electron transfer in DNA can occur through cytosine (C) and thymine (T) due to their relatively high reduction potentials.[12-14] Understanding of the mechanisms underlying oxidative and reductive charge transfers in DNA is critical to explain DNA damage/repair.[15-18] From this view point, several mechanisms based on various theoretical and experimental results have been proposed.[3]

To date, there are several studies on hole transfer in DNA. These studies employed systems such as donor–DNA–acceptor system and the results have revealed that both tunneling and hopping mechanisms are included in hole transfer in DNA. Usually, the rate of a single step electron/hole transfer through spacers by the tunneling mechanism can be expressed as an exponential function of the donor–acceptor distance (R_{DA}) as described by eq (3-1),[5,19,20]

$$k_{HT} = k_0 \times \exp(-\beta R_{DA}) \quad (3\text{-}1)$$

where β is the damping factor and k_0 is a temperature-dependent factor. For hole transfer by the tunneling mechanism, β has been determined as 0.3-1.0 $Å^{-1}$, and well reported values in previous studies are in the range of 0.7−0.8 $Å^{-1}$.[13,14,21] The variation in the reported values can be attributed to factors such as donor–acceptor energetics.[22] However, in some cases of hole transfer in DNA, β values as small as 0.1 $Å^{-1}$ have also been reported.[7,9,23] Such small values indicate that the multistep hopping mechanism is operative.[20,24,25] The hopping mechanism indicates the occurrence of multiple hole tunneling processes through DNA, and realizes long-range hole transfer over several hundreds of angstroms.[5,9] Thus, hole transfer in DNA via the hopping mechanism can be described by a single-step hopping rate. Our lab has determined the single-step hole hopping rate constant through a consecutive A sequence as 2×10^{10} s^{-1} in a donor–DNA–acceptor system by the nanosecond laser flash photolysis.[26] Lewis et al. also reported G-to-G and A-to-A hole hopping rate constants as 4.3×10^9 and 1.2×10^9 s^{-1}, respectively.[27] Thus, single-step hole hopping takes several tens to hundreds picoseconds.

In contrast to hole transfer, the nature of excess-electron transfer in DNA by the hopping mechanism is relatively less understood. Several research groups have determined the β value

of excess-electron transfer through Ts as 0.1–0.3 $Å^{-1}$ in accordance with the hopping mechanism.[28-35] Our research group has studied a series of modified DNAs to estimate single-step excess-electron hopping rates directly by using femtosecond laser flash photolysis techniques. For this purpose, various donor–DNA–acceptor systems have been synthesized.[36-40] As a photosensitizing electron donor, oligothiophenes (**2T**, **3T**, **4T**, **2E**, and **3E**) and aminopyrene derivative (**APy**) were employed, while diphenylacetylene (**DPA**) was used as an electron acceptor (Figure 3-1).[41-49] The redox and spectroscopic properties of photosensitizing electron donors are summarized in Table 3-1.

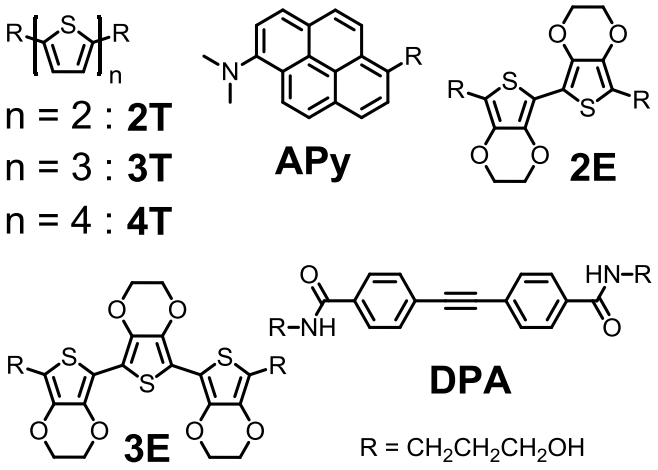

Figure 3-1. Structures of photosensitizing electron donors (**2T**, **3T**, **4T**, **APy**, **2E**, and **3E**) and electron acceptor (**DPA**).

Table 3-1. Driving forces for electron injection from the singlet excited electron donor to thymine ($-\Delta G_{CS}$) and **DPA** ($-\Delta G_{ET}$), and absorption peak positions in the singlet excited state (λ_{S1}) and radical cation state ($\lambda^{\bullet+}$) of **2T**, **3T**, **4T**, **APy**, **2T**, **2E**, and **3E**.

Donor	$-\Delta G_{CS}$[a] (eV)	$-\Delta G_{ET}$[a] (eV)	λ_{S1} (nm)	$\lambda^{\bullet+}$ (nm)
APy[b]	0.24	0.38	500–600	509
2T[c]	0.16	0.30	503	445
3T[c]	−0.13	0.01	605	585
4T[d]	0.09	0.23	>700	675
2E[e]	0.63	0.77	530	445
3E[c]	0.35	0.49	620	540

[a] Unit: V versus NHE. [b] From reference 46. [c] From reference 41. [d] From reference 43. [e] From reference 41.

From a series of the studies, the excess-electron hopping rate constant among consecutive Ts was determined to be in the order of 10^{10}–10^{11} s^{-1}.[43-46] These results indicate that the photosensitizing electron donor affects not only the excess-electron injection rate,[41,49,50] but also the hopping rate, although the factor governing this phenomenon is not clear.

In the present study, the author synthesized DNA oligomers (**2-Tn**) containing **2E** as a photosensitizing electron donor and **DPA** as an electron acceptor (Figure 3-2), and examined them by femtosecond laser flash photolysis, because **2E** realizes the largest driving force for excess-electron injection to DNA and is expected to cause a larger effect on excess-electron hopping than other electron donors. This study was aimed at the clarification of the energetic aspects of excess-electron transfer dynamics in donor–DNA–acceptor systems. The role of structural fluctuation in the excess-electron transfer in DNA is also discussed.

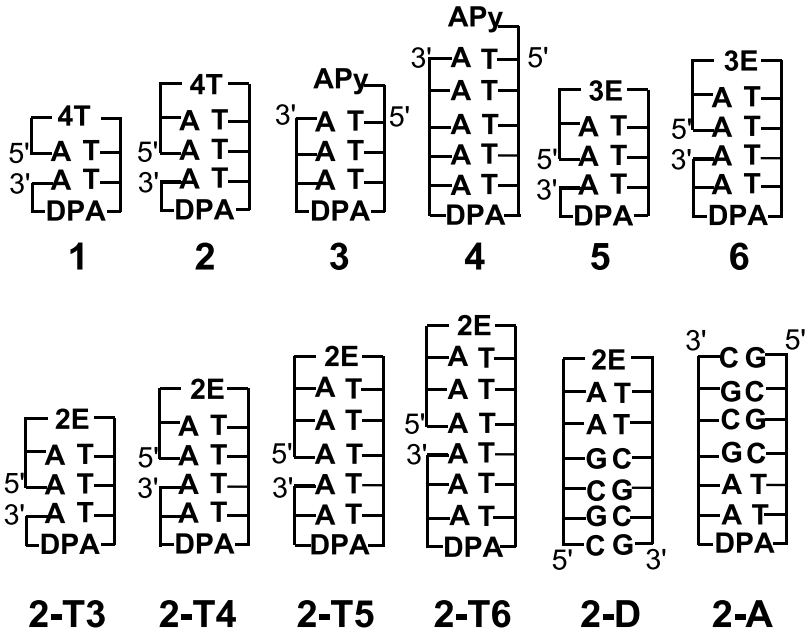

Figure 3-2. The DNA oligomers **1**–**6**, **2-Tn** (**2-T3**, **2-T4**, **2-T5**, and **2-T6**), **2-D**, and **2-A**. For **1**, **2**, **5**, **6**, and **2-Tn**, the gap between the 5' and 3' indicates a missing phosphate linker between two nucleobases in nicked-dumbbell structure.

Experimental Section

DNA synthesis. **2E** and **DPA** were prepared and converted to their phosphoramidite derivatives by a similar procedure as reported.[41,52] All the reagents were purchased from Glen Research (USA). All the DNA oligomers were synthesized on an Applied Biosystems 3400 DNA synthesizer with standard solid-phase techniques and were characterized using MALDI-

TOF mass spectroscopy (Table 3-2). The DNA oligomers were purified on a JASCO HPLC with a reversed-phase C-18 column with acetonitrile/50 mM ammonium formate gradient.

Table 3-2. MALDI-TOF MS and melting temperature (T_m) of the DNA oligomers.

DNA	MALDI-TOF MS		T_m, ℃	DNA	MALDI-TOF MS		T_m, ℃
	Calculated	Found			Calculated	Found	
2-T3	2692.508	2691.486	30	**2-T6**	4548.822	4542.762	50
2-T4	3310.674	3308.578	34	**2-D**	4106.013	4104.626	85
2-T5	3927.939	3925.670	48	**2-A**	4090.808	4086.706	88

[a] Measured in ~2 x 10^{-5} M solution (0.1 M NaCl and 10 mM sodium phosphate, pH 7.0 ± 0.1) at a heating rate of 0.5 ℃/min from 10 ℃ to 100 ℃) with the absorbance at 260 nm recorded in 60 s intervals.

Apparatus. All DNA oligomer samples were prepared in buffer solution (0.1 M NaCl and 10 mM sodium phosphate, pH 7.0 ± 0.1). Steady-state absorption, fluorescence, circular dichroism (CD) spectra, and melting temperature profiles were measured using a Shimadzu UV3100PC, Horiba FluoroMax-4P, JASCO CDJ720, and Shimadzu UV2700, respectively. The CD spectra of DNA oligomers were the average data from ten scans, collected from 400 nm to 225 nm with a scanning rate of 100 nm min^{-1}. The time-resolved transient absorption spectra of all DNA oligomers were measured by the pump and probe method using a regeneratively amplified Ti:sapphire laser (Spectra Physics, Spitfire Pro F, 1 kHz) pumped by a Nd:YLF laser (Spectra Physics, Empower 15).[53] The seed pulse was generated by the Ti:sapphire laser (Spectra Physics, MaiTai VFSJ-W). DNA oligomers were excited using the 350-nm laser pulse, which was generated by an optical parametric amplifier. The supercontinuum was generated by focusing the output of the amplifier on a sapphire plate. The chirp was corrected by a homemade program based on the optical Kerr effect cross correlation method.[54] The time resolution of the present system is ~300 fs.

Results and Discussion

In the steady-state absorption spectra shown in Figures 3-3a, a clear peak at around 260 nm for all the DNA oligomers is dominated by base pairs absorption. As the number of A:T base pairs increases, this peak increases in absorbance with a slightly blue shift for **2-Tn**. In

wavelengths longer than 300 nm, the absorption spectra of **2-Tn** are equivalent to the sum of those for **DPA**[52] and **2E**.[41,55] From the absorption spectra of **2-D** and **2-A**, it is clear that the only **2E** absorbs photons at 340–360 nm. Thus, transient absorption measurements were performed using an excitation pulse at 350 nm to excite **2E** without the interference of excited intermediates of **DPA**.

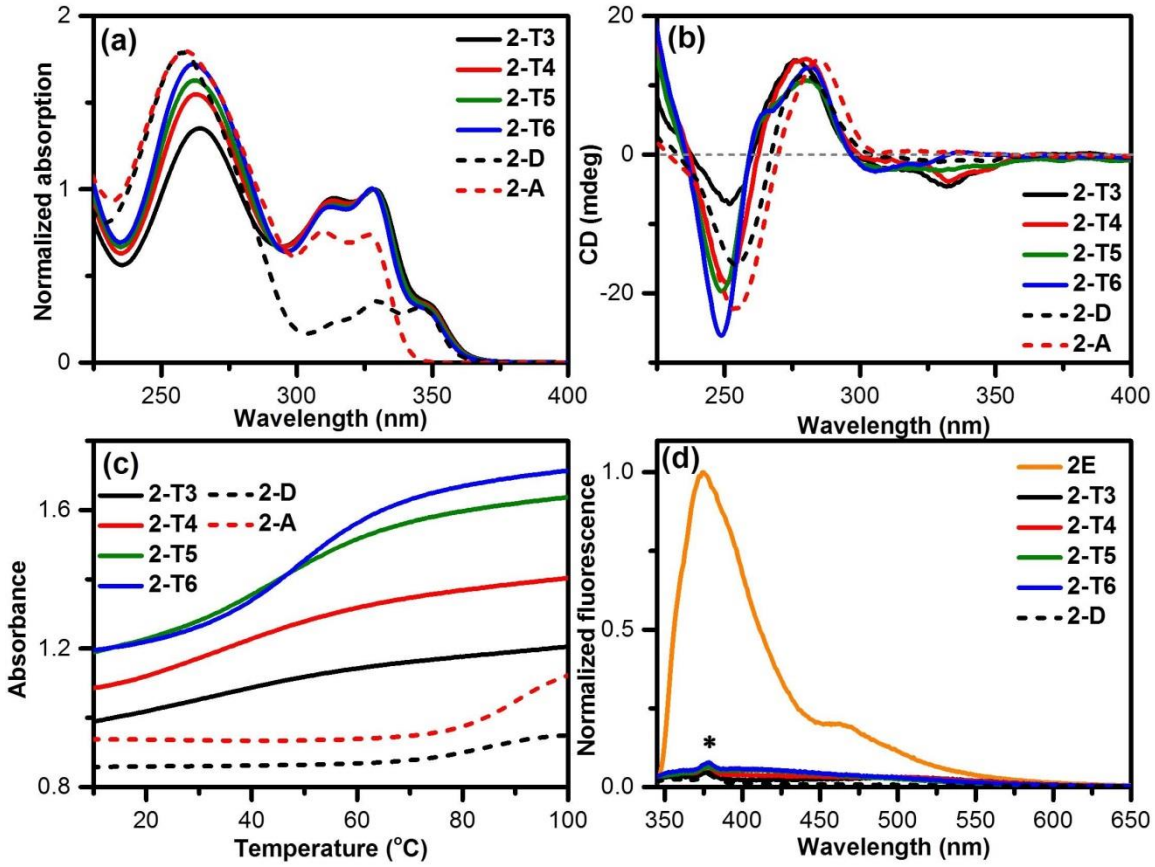

Figure 3-3. (a) Absorption, (b) circular dichroism spectra, (c) thermal dissociation profiles, and (d) fluorescence spectra (λ_{ex} = 340 nm) of DNA oligomers (~10^{-5} M) **2-T3** (black solid line), **2-T4** (red solid line), **2-T5** (green solid line), **2-T6** (blue solid line), **2-D** (black dash line), and **2-A** (red dash line) in buffer solution (0.1 M NaCl and 10 mM sodium phosphate, pH 7.0 ± 0.1) at 298 K. Fluorescence spectra of **2E** in Methanol (orange solid line). Absorbance of the sample was matched at λ_{ex}.

In the circular dichroism (CD) spectra of all DNA oligomers (Figure 3-3b), a positive band at around 280 nm and a negative band at around 250 nm were observed, indicating that all DNA oligomers possess a B-form structure.[43-47,56-58] Moreover, thermal dissociation profiles for the synthetic DNA oligomers (Figure 3-3c) indicate that with the increasing of number of

base pairs in DNA, the profile and T_m become clearer and higher, respectively. Thus, the author can point out that the B-form structure is responsible for the transient phenomena found with transient absorption measurements during femtosecond laser flash photolysis, which is consistent with previous reports. [43-47]

Fluorescence from **2E** of the DNA oligomers was measured by selective excitation of **2E** at 340 nm (Figure 3-3d). It is clear that the fluorescence intensities of **2-Tn** and **2-D** are lower than that of **2E**, regardless of the length of the DNA oligomers, which indicates that the fluorescence quenching is mainly due to excess-electron injection to adjacent T, and that the contribution of **DPA** is limited because of the distance between **2E** and **DPA**.

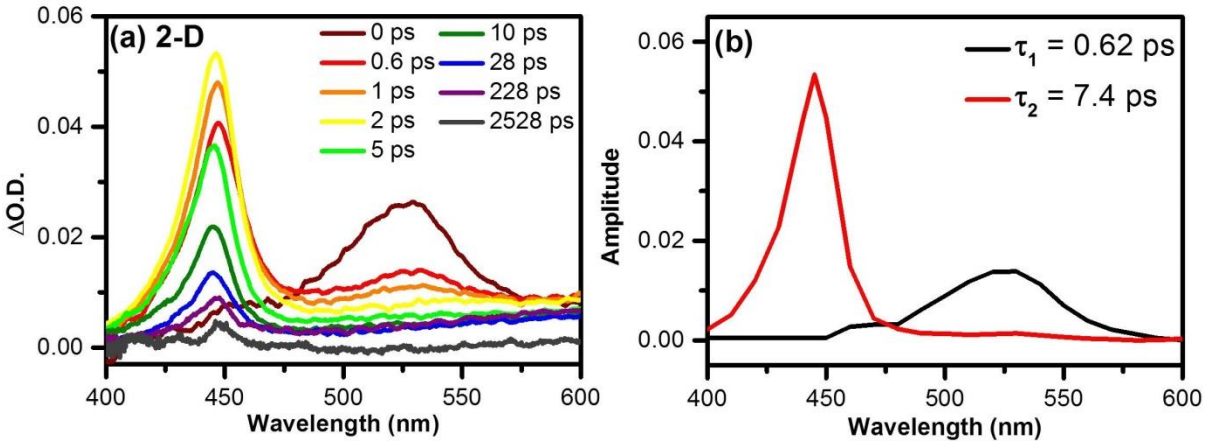

Figure 3-4. (a) Transient absorption spectra of **2-D** during the laser flash photolysis with 350-nm femtosecond laser pulse at 295 K. (b) Species-associated spectra obtained by global fitting using a double exponential function for **2-D** (black: τ_1 ($(k_{CS})^{-1}$, from ^{1}**2E***−DNA to **2E**$^{\bullet+}$−DNA$^{\bullet-}$), and red: τ_2 ($(k_{CR})^{-1}$, from **2E**$^{\bullet+}$−DNA to ground state **2E**−DNA).

The dynamics of excess-electron transfer in the DNA oligomers were investigated by transient absorption measurements during femtosecond laser flash photolysis by using a 350-nm laser pulse, which selectively excites **2E** (Figures 3-4). Immediately following excitation, the absorption band of ^{1}**2E*** was found at 530 nm for **2-D** (Figure 3-4a).[41] The decay of the 530 nm band and the rise of the 445 nm band attributable to the **2E** radical cation (**2E**$^{\bullet+}$) occurred within 1−2 ps, indicating rapid excess-electron injection to the adjacent T (charge separation, CS).[41] The k_{CS} and k_{CR} values of **2-D** were determined by global fitting assuming two species, i.e., ^{1}**2E***−DNA and **2E**$^{\bullet+}$−DNA$^{\bullet-}$ (Figure 3-4b).

On the other hand, **2-Tn** showed an additional absorption band at around 510 nm after decay of ^{1}**2E***, suggesting the generation of **DPA**$^{\bullet-}$ by excess-electron transfer (ET) (Figure 3-5).[43-49]

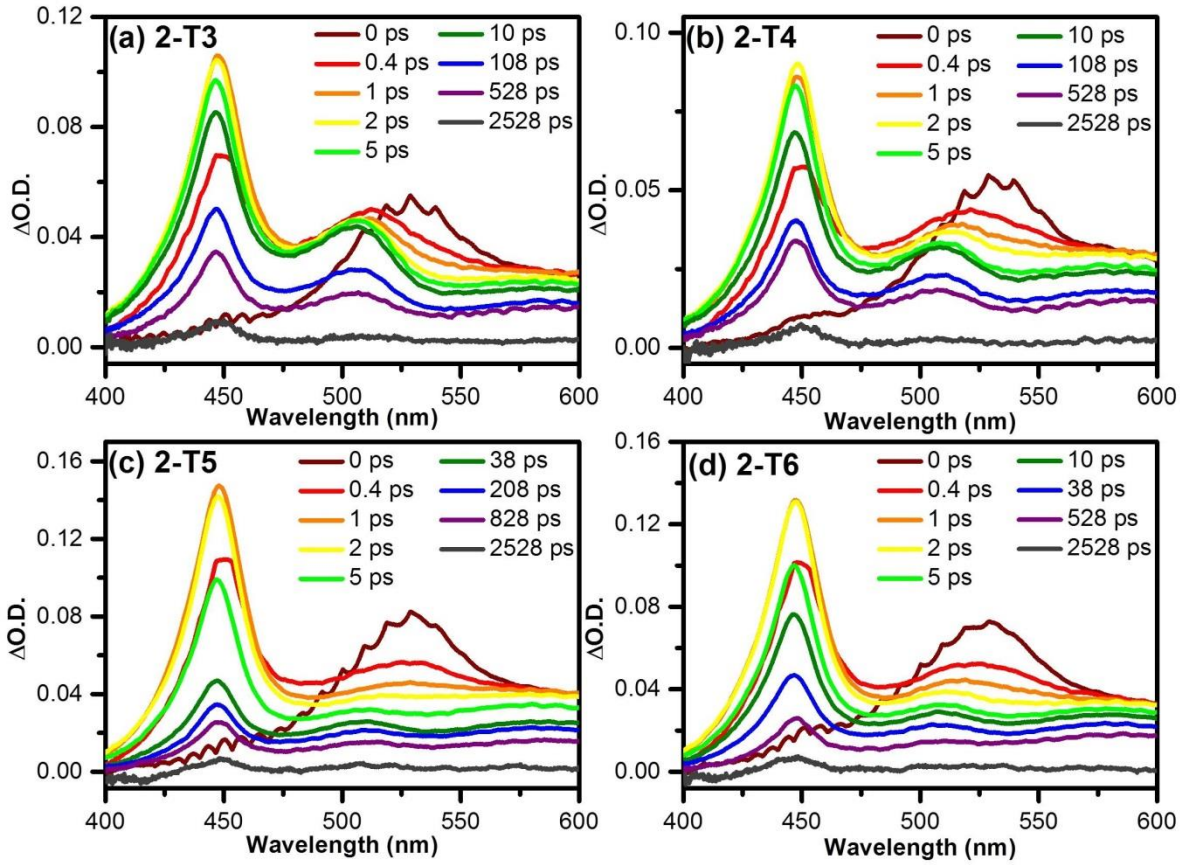

Figure 3-5. Transient absorption spectra (a) **2-T3**, (b) **2-T4**, (c) **2-T5**, and (d) **2-T6** during the laser flash photolysis with 350-nm femtosecond laser pulse at 295 K.

Spectral changes after the generation of **2E**$^{\bullet+}$ were analyzed by global fitting assuming two species (Figure 3-6). The species-associated spectrum for the faster component (τ_1) is attributed to **2E**$^{\bullet+}$−DNA$^{\bullet-}$−**DPA**, and that for the slower component (τ_2) is attributed to **2E**$^{\bullet+}$−DNA−**DPA**$^{\bullet-}$, as is evident from the absorption band around 510 nm. As the number of base pair increases, the absorption intensity of **2E**$^{\bullet+}$−DNA−**DPA**$^{\bullet-}$ decreases. From the ratio of the absorption intensity of **2E**$^{\bullet+}$−DNA−**DPA**$^{\bullet-}$ and **2E**$^{\bullet+}$−DNA$^{\bullet-}$−**DPA**, the generation yield of **2E**$^{\bullet+}$−DNA−**DPA**$^{\bullet-}$ after excess-electron transfer was calculated. To the best of our knowledge, **2-T6** with 6 A:T base pairs is the longest DNA (23.8 Å) that showed excess-electron transfer products by transient absorption measurements during femtosecond laser flash photolysis.

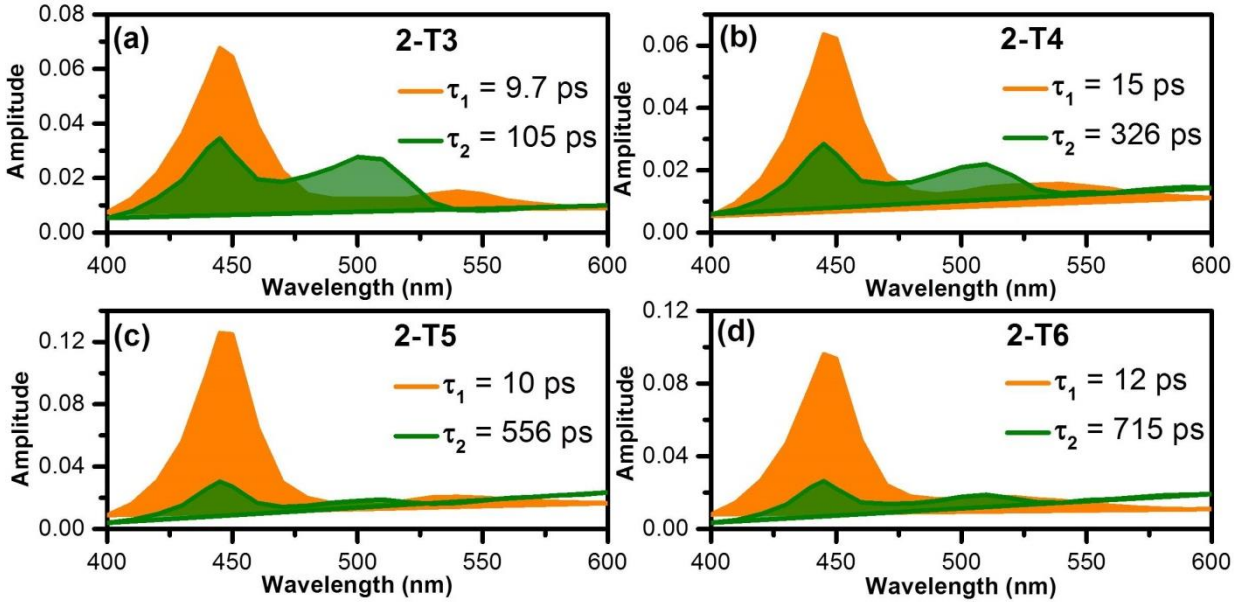

Figure 3-6. Species-associated spectra obtained by global fitting using a double exponential function for (a) **2-T3**, (b) **2-T4**, (c) **2-T5**, and (d) **2-T6** (Black: τ_1, red: τ_2. τ_1 and τ_2 correspond to $(k_{CR} + k_{ET})^{-1}$ and k_{BET}^{-1}, respectively).

The rate constants of excess-electron injection to the adjacent T (k_{CS}), initial charge recombination (CR) between the nucleobase radical anion and $\mathbf{2E}^{\bullet+}$ (k_{CR}), and charge recombination between $\mathbf{2E}^{\bullet+}$ and $\mathbf{DPA}^{\bullet-}$ (k_{BET}) indicated in Figure 3-7 were estimated as follows, and are summarized in Table 3-3. In the case of **2-Tn**, the k_{CS} value is considered equivalent to that of **2-D**. After generation of $\mathbf{2E}^{\bullet+}$, decay profiles can be analyzed by assuming two decaying components. The rate of the fast decaying component can be attributed to the sum of k_{CR} and k_{ET}. The k_{CR} and k_{ET} values were determined by considering the generation yield. The slow decaying component in the DNA oligomers can be attributed to k_{BET}.

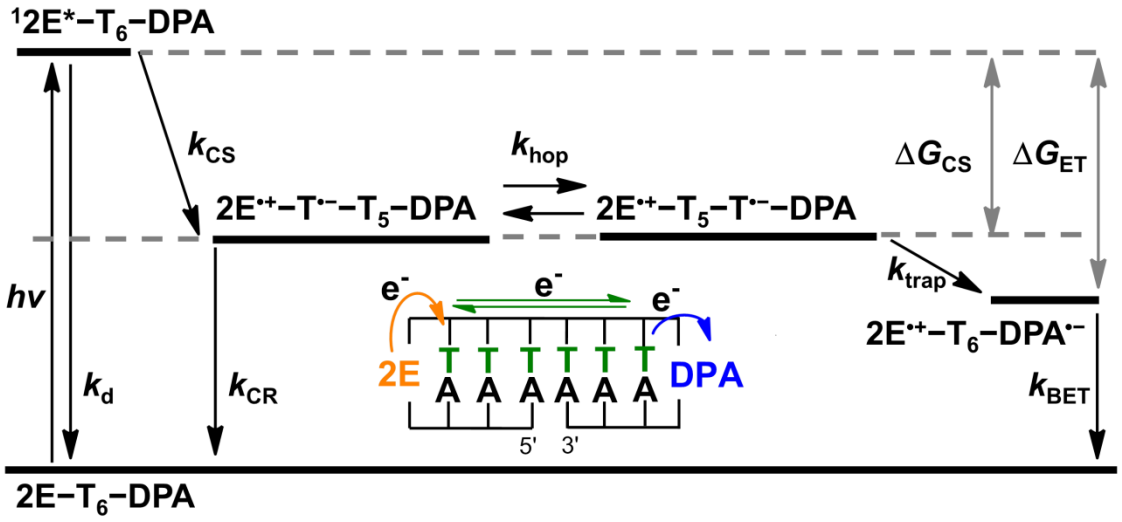

Figure 3-7. Schematic energy diagram for excess-electron transfer from **2E** to **DPA** in **2-T6**.

Table 3-3. Rate Constants (k_{CS}, k_{ET}, k_{CR}, and k_{BET}) in DNA Oligomers.

DNA	k_{CS}[a] (s^{-1})	k_{CR}[a] (s^{-1})	k_{ET}[a] (s^{-1})	k_{BET}[b] (s^{-1})
2-D	1.6×10^{12}	1.3×10^{11}	-[c]	-[c]
2-T3	1.6×10^{12}	5.0×10^{10}	5.3×10^{10}	9.5×10^{9}
2-T4	1.6×10^{12}	4.0×10^{10}	2.7×10^{10}	3.1×10^{9}
2-T5	1.6×10^{12}	7.7×10^{10}	1.9×10^{10}	1.8×10^{9}
2-T6	1.6×10^{12}	6.3×10^{10}	1.9×10^{10}	1.4×10^{9}

[a] Estimation error is less than 10%. [b] Estimation error is less than 5%. [c] Not observed.

It is clear that the k_{CS} values were similar to the reported value for the **2E**−T dyad,[41] which indicates that ^{1}**2E*** was quenched by CS to generate **2E**$^{\bullet+}$ and T$^{\bullet-}$. **DPA**$^{\bullet-}$ generation yields in **2-T5** and **2-T6** were lower than that in **2-T3** because fast CR between **2E**$^{\bullet+}$ and DNA$^{\bullet-}$ cannot be ignored. Therefore, the CR process limits the efficiency of excess-electron transfer through Ts in DNA. Applying eq. (3-1) to k_{ET} of **2-Tn** tentatively, $\beta = 0.10 \pm 0.031$ Å^{-1} of low distance dependence was confirmed. Similar β values have been determined by photochemical product analysis of excess-electron transfer using flavin-sensitized cleavage of the T−T cyclobutane dimer (0.11 Å^{-1}, by Carell et al.),[28] flavin-sensitized cleavage of thymine oxetane (0.16 Å^{-1}, by Diederichsen et al.),[31] Ir(III)-sensitized loss of bromide from 5-bromouracil (0.12 Å^{-1}, by Barton et al.),[32] and pyrene-derivatives-sensitized loss of

bromide from 5-bromouracil (0.22–0.26 $Å^{-1}$, by Lewis et al.).[34,35] These smaller β values indicate that a multi-step hopping mechanism, which shows weak distance dependence, should be operative in **2-Tn**. The author concluded that excess-electron transfer in **2-T6**, as a representative case, occurs by a multi-step hopping mechanism consisting of photoinduced electron injection (k_{CS}), stepwise electron hopping (k_{hop}), and electron trapping by **DPA** (k_{trap}). It should be noted that k_{ET} is expected to be lower than k_{trap} and thus excess-electron hopping is a rate determining step, so k_{hop} can be estimated on the basis of the one-dimensional random walk model (eq 3-2),[27,59]

$$\tau(N) = (1/2k_{hop})N^2 \qquad (3\text{-}2)$$

where $\tau(N)$ is the time required for N hopping steps, i.e., k_{ET}^{-1}, and k_{hop} is the rate constant for a single hopping between neighboring nucleobases. The excess-electron hopping rate constant in **2-Tn** is estimated to be $(2.6 \pm 0.5) \times 10^{11}$ s^{-1}. The estimated k_{hop} is larger than those reported previously.[43-46]

From a series of studies of excess-electron transfer in DNA using **2-Tn** and **1-6**, the author found the k_{hop} values to be in the order of 10^{10}–10^{11} s^{-1}.[43-46] Structural fluctuation of DNA can be pointed out as a factor contributing to the various hopping rates.[33,44,45] For the CS process with larger $-\Delta G_{CS}$, larger thermal energy is expected to deposit on DNA, resulting in larger structural fluctuation of DNA. To verify this point, the $-\Delta G_{CS}$ dependence of $\ln k_{hop}$ was examined by using estimated values (Figure 3-8). The linear nature of these plots indicates that the $-\Delta G_{CS}$ is an essential parameter for k_{hop}. Notably, the intercept of the linear fit ($(3.8 \pm 1.5) \times 10^{10}$ s^{-1}) should correspond to the hopping rate for a non-energy assisted ($-\Delta G_{CS} = 0$) excess-electron transfer in DNA, i.e. intrinsic hopping rate. Interestingly, the intrinsic hopping rate agrees with the reported value for the DNA sugar backbone and base motions, which occur with periods as short as 30 ps at 303 K,[60,61] suggesting that the excess-electron hopping is dominated by the structural dynamics of the DNA.[62,63]

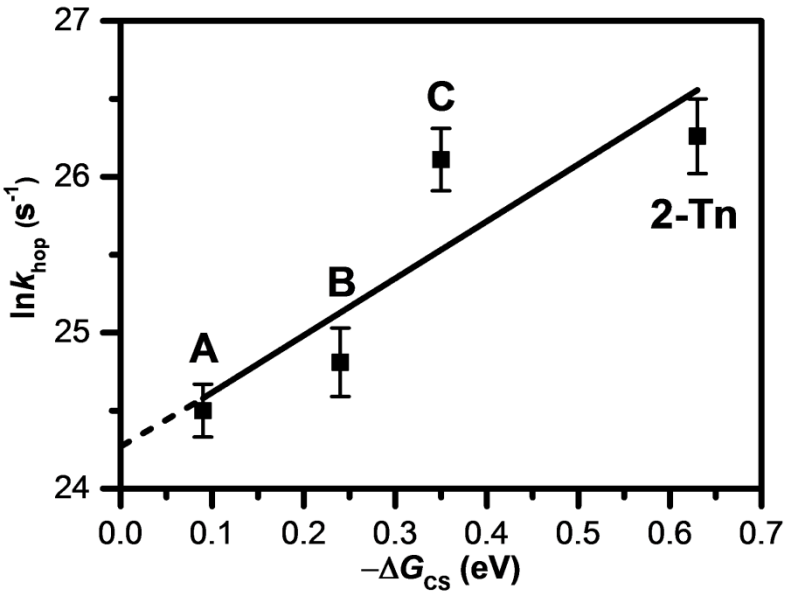

Figure 3-8. Dependence of $\ln k_{hop}$ on $-\Delta G_{CS}$. **A**, **B**, and **C** are data from DNA oligomers **1** and **2**,[43] **3** and **4**,[46] and **5** and **6**,[44,45] respectively.

It should be noted that the structural dynamics of DNA can also be affected by environmental fluctuations such as reorganization of water molecules and/or counter ions surrounding the DNA to stabilize a radical anion nucleobase.[64,65] Both theoretical and experimental results have shown that the time scale of water molecule motions is about 10–30 ps.[66-69] As they reorient for accommodating the DNA including the sugar backbone and the bases, the reported time scale should be similar to the intrinsic hopping rate. Thus, the author concludes that the thermally activated structural fluctuations induce motions of the backbone sugars and bases to propel the radical anion from one nucleobase to the next. These results indicate that structural fluctuation plays an important role in the dynamics of excess-electron transfer in DNA and that the rate of excess-electron transfer can be enhanced by thermally activated structural fluctuations.

In hole transfer in DNA, two mechanisms for hole hopping have been proposed, i.e., migration of localized radical cation of nucleobase and migration of polaron, where a radical cation resides in a delocalized structure comprised of nucleobases.[3] The migration of polaron in DNA was found to be influenced by the motion of the Na^+ ions and the water molecules and was named as the gating mechanism.[70,71] On the other hand, thermal fluctuations were also found to assist hole hopping on each nucleobase via continuous oxidative processes by some research groups including ours.[72-74] Fiebig and colleagues found the time scale for this motion to be 10–100 ps.[74] As mentioned above, the author found that the excess-electron

hopping is dominated by the structural dynamics of DNA with a similar time scale. Thus, it should be preferably agreed that a fluctuation-assisted hopping mechanism prevails in both hole and excess-electron transfer in DNA.

Conclusion

To the best of our knowledge, this is the first study suggesting the role of a fluctuation-assisted hopping mechanism in excess-electron transfer in DNA. The author confirmed that excess-electron transfer in DNA is governed by the hopping mechanism and successfully observed that the rate of excess-electron transfer can be enhanced with an increase in the driving force for CS, which is equivalent to the thermal energy transferred to DNA, which causes structural fluctuation. Thus, a fast charge hopping rate due to structural fluctuation realized a long excess-electron transfer distance in the nicked-dumbbell donor–DNA–acceptor system. Moreover, the estimated intrinsic hopping rate was consistent with the experimental and theoretical results, indicating that the fluctuation-assisted hopping mechanism prevails not only in excess-electron transfer but also in hole transfer in DNA. These results provide new insights into excess-electron transfer in DNA by the hopping mechanism.

References

(1) Wallace, S. S. *Free Radic. Biol. Med.* **2002**, *33*, 1.

(2) Joy, A.; Schuster, G. B. *Chem. Commun.* **2005**, *22*, 2778.

(3) Genereux, J. C.; Barton, J. K. *Chem. Rev.* **2010**, *110*, 1642.

(4) Mallajosyula, S. S.; Pati, S. K. *J. Phys. Chem. Lett.* **2010**, *1*, 1881.

(5) Meggers, E.; Michel-Beyerle, M. E.; Giese, B. *J. Am. Chem. Soc.* **1998**, *120*, 12950.

(6) Giese, B.; Wessely, S.; Spormann, M.; Lindemann, U.; Meggers, E.; Michel-Beyerle, M. E. *Angew. Chem. Int. Ed.* **1999**, *38*, 996.

(7) Giese, B.; Amaudrut, J.; Kohler, A.-K.; Spormann, M.; Wessely, S. *Nature* **2001**, *412*, 318.

(8) Giese, B.; Spichty, M. *ChemPhysChem* **2000**, *1*, 195.

(9) Henderson, P. T.; Jones, D.; Hampikian, G.; Kan, Y.; Schuster, G. B. *Proc. Natl. Acad. Sci. U.S.A.* **1999**, *96*, 8353.

(10) Liu, C.-S.; Hernandez, R.; Schuster, G. B. *J. Am. Chem. Soc.* **2004**, *126*, 2877.

(11) Kawai, K.; Majima, T. *Acc. Chem. Res.* **2013**, *46*, 2616.

(12) Seidel, C. A. M.; Schulz, A.; Sauer, M. H. M. *J. Phys. Chem.* **1996**, *100*, 5541.

(13) Wagenknecht, H.-A. *Nat. Prod. Rep.* **2006**, *23*, 973.

(14) Fujitsuka, M.; Majima, T. *Phys. Chem. Chem. Phys.* **2012**, *14*, 11234.

(15) Carell, T. *Angew. Chem. Int. Ed.* **1995**, *34*, 2491.

(16) Burrows, C. J.; Muller, J. G. *Chem. Rev.* **1998**, *98*, 1109.

(17) Armitage, B. *Chem. Rev.* **1998**, *98*, 1171.

(18) Kanvah, S.; Joseph, J.; Schuster, G. B.; Barnett, R. N.; Cleveland, C. L.; Landman, U. *Acc. Chem. Res.* **2010**, *43*, 280.

(19) Marcus, R. A. *Angew. Chem. Int. Ed.* **1993**, *32*, 1111.

(20) Jortner, J.; Bixon, M.; Langenbacher, T.; Michel-Beyerle, M. E. *Proc. Natl. Acad. Sci. U.S.A.* **1998**, *95*, 12759.

(21) Lewis, F. D.; Zhu, H.; Daublain, P.; Fiebig, T.; Raytchev, M.; Wang, Q.; Shafirovich, V. *J. Am. Chem. Soc.* **2006**, *128*, 791.

(22) Lewis, F. D.; Liu, J.; Weigel, W.; Rettig, W.; Kurnikov, I. V.; Beratan, D. N. Donor- *Proc. Natl. Acad. Sci. U.S.A.* **2002**, *99*, 12536.

(23) Murphy, C.; Arkin, M.; Jenkins, Y.; Ghatlia, N.; Bossmann, S.; Turro, N.; Barton, J. *Science* **1993**, *262*, 1025.

(24) Berlin, Y. A.; Burin, A. L.; Ratner, M. A. *J. Phys. Chem. A* **2000**, *104*, 443.

(25) Berlin, Y. A.; Burin, A. L.; Ratner, M. A. *J. Am. Chem. Soc.* **2001**, *123*, 260.

(26) Takada, T.; Kawai, K.; Cai, X.; Sugimoto, A.; Fujitsuka, M.; Majima, T. *J. Am. Chem. Soc.* **2004**, *126*, 1125.

(27) Conron, S. M. M.; Thazhathveetil, A. K.; Wasielewski, M. R.; Burin, A. L.; Lewis, F. D. *J. Am. Chem. Soc.* **2010**, *132*, 14388.

(28) Behrens, C.; Burgdorf, L. T.; Schwögler, A.; Carell, T. *Angew. Chem. Int. Ed.* **2002**, *41*, 1763.

(29) Behrens, C.; Carell, T. *Chem. Commun.* **2003**, *14*, 1632.

(30) Ito, T.; Rokita, S. E. *J. Am. Chem. Soc.* **2003**, *125*, 11480.

(31) Stafforst, T.; Diederichsen, U. *Angew. Chem. Int. Ed.* **2006**, *45*, 5376.

(32) Elias, B.; Shao, F.; Barton, J. K. *J. Am. Chem. Soc.* **2008**, *130*, 1152.

(33) Grozema, F. C.; Tonzani, S.; Berlin, Y. A.; Schatz, G. C.; Siebbeles, L. D. A.; Ratner, M. A. *J. Am. Chem. Soc.* **2008**, *130*, 5157.

(34) Daublain, P.; Thazhathveetil, A. K.; Wang, Q.; Trifonov, A.; Fiebig, T.; Lewis, F. D. *J. Am. Chem. Soc.* **2009**, *131*, 16790.

(35) Daublain, P.; Thazhathveetil, A. K.; Shafirovich, V.; Wang, Q.; Trifonov, A.; Fiebig, T.; Lewis, F. D. *J. Phys. Chem. B* **2010**, *114*, 14265.

(36) Lewis, F. D.; Liu, X.; Wu, Y.; Miller, S. E.; Wasielewski, M. R.; Letsinger, R. L.; Sanishvili, R.; Joachimiak, A.; Tereshko, V.; Egli, M. *J. Am. Chem. Soc.* **1999**, *121*, 9905.

(37) Lewis, F. D.; Liu, X.; Miller, S. E.; Hayes, R. T.; Wasielewski, M. R. *J. Am. Chem. Soc.* **2002**, *124*, 11280.

(38) Wagner, C.; Wagenknecht, H.-A. *Chem. —Eur. J.* **2005**, *11*, 1871.

(39) Zhang, Y.; Dood, J.; Beckstead, A. A.; Li, X.-B.; Nguyen, K. V.; Burrows, C. J.; Improta, R.; Kohler, B. *Proc. Natl. Acad. Sci. U.S.A.* **2014**, *111*, 11612.

(40) Zhang, Y.; Dood, J.; Beckstead, A. A.; Li, X.-B.; Nguyen, K. V.; Burrows, C. J.; Improta, R.; Kohler, B. *J. Phys. Chem. B* **2015**, *119*, 7491.

(41) Lin, S.-H.; Fujitsuka, M.; Ishikawa, M.; Majima, T. *J. Phys. Chem. B* **2014**, *118*, 12186.

(42) Park, M. J.; Fujitsuka, M.; Kawai, K.; Majima, T. *Chem. —Eur. J.* **2012**, *18*, 2056.

(43) Park, M. J.; Fujitsuka, M.; Kawai, K.; Majima, T. *J. Am. Chem. Soc.* **2011**, *133*, 15320.

(44) Lin, S.-H.; Fujitsuka, M.; Majima, T. *J. Phys. Chem. B* **2015**, *119*, 7994.

(45) Lin, S.-H.; Fujitsuka, M.; Majima, T. *Chem. —Eur. J.* **2015**, *21*, 16190−16194

(46) Park, M. J.; Fujitsuka, M.; Nishitera, H.; Kawai, K.; Majima, T. *Chem. Commun.* **2012**, *48*, 11008.

(47) Lewis, F. D.; Liu, X.; Miller, S. E.; Wasielewski, M. R. *J. Am. Chem. Soc.* **1999**, *121*, 9746.

(48) Takada, T.; Kawai, K.; Fujitsuka, M.; Majima, T. *Angew. Chem. Int. Ed.* **2006**, *45*, 120.

(49) Tainaka, K.; Fujitsuka, M.; Takada, T.; Kawai, K.; Majima, T. *J. Phys. Chem. B* **2010**, *114*, 14657.

(50) McConnell, H. M. *J. Chem. Phys.* **1961**, *35*, 508.

(51) Gorczak, N.; Fujii, T.; Mishra, A. K.; Houtepen, A. J.; Grozema, F. C.; Lewis, F. D. *J. Phys. Chem. B* **2015**, *119*, 7673.

(52) Lewis, F. D.; Liu, X.; Miller, S. E.; Hayes, R. T.; Wasielewski, M. R. *J. Am. Chem. Soc.* **2002**, *124*, 14020.

(53) Fujitsuka, M.; Cho, D. W.; Tojo, S.; Inoue, A.; Shiragami, T.; Yasuda, M.; Majima, T. *J. Phys. Chem. A* **2007**, *111*, 10574.

(54) Yamaguchi, S.; Hamaguchi, H. -O. *Appl. Spectrosc.* **1995**, *49*, 1513.

(55) Turbiez, M.; Frère, P.; Roncali, J. *J. Org. Chem.* **2003**, *68*, 5357.

(56) Lewis, F. D.; Zhang, L.; Liu, X.; Zuo, X.; Tiede, D. M.; Long, H.; Schatz, G. C. *J. Am. Chem. Soc.* **2005**, *127*, 14445.

(57) Vura-Weis, J.; Wasielewski, M. R.; Thazhathveetil, A. K.; Lewis, F. D. *J. Am. Chem. Soc.* **2009**, *131*, 9722.

(58) Patwardhan, S.; Tonzani, S.; Lewis, F. D.; Siebbeles, L. D. A.; Schatz, G. C.; Grozema, F. C. *J. Phys. Chem. B* **2012**, *116*, 11447.

(59) Bar-Haim, A.; Klafter, J. *J. Chem. Phys.* **1998**, *109*, 5187.

(60) Schuster, G. B. *Acc. Chem. Res.* **2000**, *33*, 253.

(61) Borer, P. N.; LaPlante, S. R.; Kumar, A.; Zanatta, N.; Martin, A.; Hakkinen, A.; Levy, G. C. *Biochemistry* **1994**, *33*, 2441.

(62) Dickerson, R. E. *Nucleic Acids Res.* **1989**, *17*, 1797.

(63) Mallajosyula, S. S.; Gupta, A.; Pati, S. K. *J. Phys. Chem. A* **2009**, *113*, 3955.

(64) Voityuk, A. A.; Siriwong, K.; Rösch, N. *Angew. Chem. Int. Ed.* **2004**, *43*, 624.

(65) Furse, K. E.; Corcelli, S. A. *J. Phys. Chem. Lett.* **2010**, *1*, 1813.

(66) Pal, S. K.; Zhao, L.; Zewail, A. H. *Proc. Natl. Acad. Sci. U.S.A.* **2003**, *100*, 8113.

(67) Pal, S. K.; Zhao, L.; Xia, T.; Zewail, A. H. *Proc. Natl. Acad. Sci. U.S.A.* **2003**, *100*, 13746.

(68) Furse, K. E.; Corcelli, S. A. *J. Am. Chem. Soc.* **2008**, *130*, 13103.

(69) Sen, S.; Andreatta, D.; Ponomarev, S. Y.; Beveridge, D. L.; Berg, M. A. *J. Am. Chem. Soc.* **2009**, *131*, 1724.

(70) Barnett, R. N.; Cleveland, C. L.; Joy, A.; Landman, U.; Schuster, G. B. *Science*, **2001**, *294*, 567.

(71) O'Neil, M. A.; Barton, J. K. *J. Am. Chem. Soc.* **2004**, *126*, 11471.

(72) Osakada, Y.; Kawai, K.; Fujitsuka, M.; Majima, T. *Proc. Natl. Acad. Sci. U.S.A.* **2006**, *103*, 18072.

(73) O'Neill, M. A.; Barton, J. K. *J. Am. Chem. Soc.* **2004,** *126*, 13234.

(74) Valis, L.; Wang, Q.; Raytchev, M.; Buchvarov, I.; Wagenknecht, H.-A.; Fiebig, T. *Proc. Natl. Acad. Sci. U.S.A.* **2006**, *103*, 10192.

Comparison of Hole Transfer and Excess-Electron Transfer in DNA

Here, the HT and EET in DNA are compared based on the rate constants reported and obtained in this dissertation (Table 1, *vide infra*). It is necessary to compare HT and EET in DNA each other, since understanding the dynamics of HT and EET is key issue for advance research or application related to DNA electronics. The rate constants of HT and EET in DNA were summarized as shown in Table 1, *vide infra*.

By means of dye-modified DNA oligomers or tuned oxidation potential of nucleobases, HT in DNA have been investigated so far as described in this chapter. The rate constant of single step hole hopping step for G to G (G-hopping) was determined to be 4×10^9 s^{-1} by Lewis group. Our group also determined the rate constant of single step hole hopping step for A to A (A-hopping) to be 2×10^{10} s^{-1}. The rate constant of the A-hopping process is much larger than that of the hopping between consecutive G bases (4×10^9 s^{-1}) because the different oxidation potential of G and A. As mentioned previously in chapter of introduction, the hole hopping rate can be changed depending on its oxidation potential. Moreover, the rate constant can be changed by stacking of nucleobases and sequence difference, too. For example, the rate constant of GTG and GAG were reported considerably smaller than the rate constant for consecutive G bases or A bases (see table 1, *vide infra*). Because the oxidation potential of A is lower than that of T, the hole transfer for GAG sequence is expected to be faster than that for GTG sequence. The rate constant of hole hopping was also reported that comparison between interstrand and intrastrand hole hopping process. The reported intrastrand hole hopping (GCG) rate was somewhat slower than that of GG because the hole hopped across C base, however, that of interstrand hole hopping was faster than that of intrastrand hole hopping process across to C. Lewis and coworkers reported that the tunneling energy gap considerably affect hole hopping process across to C in GCG. They concluded that a small tunneling energy gap is originated by the lower oxidation potential of the intervening bases. These results are consistent with our reported works and shown in Table 1, *vide infra*.

Table 1. Comparison of the hopping rate constants for HT and EET in DNA.

Rate constant of hole hopping				**Rate constant of excess-electron hopping**			
G-hopping	[a] GG	4×10^9 s^{-1} Lewis et al. *JACS* 2010		T-hopping	[a] TT	4×10^{10} s^{-1} Majima et al. *JACS* 2011 6×10^{10} s^{-1} Majima et al. *Chem. Comm*. 2012 2.2×10^{11} s^{-1} Majima et al. *J. Phys. Chem. B* 2015 2.6×10^{11} s^{-1} Majima et al. submitted	
	[b] GAG	5×10^7 s^{-1} Lewis et al. *Nature* 2000 6×10^7 s^{-1} Majima et al. *PNAS* 2004			[b] TGT	1.0×10^{10} s^{-1} Majima et al. prepartion	
					[c] $T_1G\ T_3$ $A\ C_2A$	4.2×10^{10} s^{-1} Majima et al. prepartion	
	[b] GTG	1×10^6 s^{-1} Majima et al. *PNAS* 2004			[b] TCT	4.9×10^{10} s^{-1} Majima et al. *J. Phys. Chem. B* 2015	
					[c] $T_1C_2T_3$ A G A	1.0×10^{11} s^{-1} Majima et al. *J. Phys. Chem. B* 2015	
	$G_1C\ G_3$ $C\ G_2C$	[a] $G_1 \rightarrow G_2$ and $G_2 \rightarrow G_3$ (inter-strand hopping)	4×10^8 s^{-1} Majima et al. *PNAS* 2006		$T_1A\ T_3$ $A\ T_2A$	[a] $T_1 \rightarrow T_2$ and $T_2 \rightarrow T_3$ (inter-strand hopping)	11×10^{10} s^{-1} Majima et al. *Chem. −Eur. J.* 2015
		[b] $G_1 \rightarrow G_3$ (intra-strand hopping)	1×10^8 s^{-1} Majima et al. *PNAS* 2006			[b] $T_1 \rightarrow T_3$ (intra-strand hopping)	not reported
[a] A-hopping (AA)		2×10^{10} s^{-1} Majima et al. *JACS* 2004 1×10^9 s^{-1} Lewis et al. *JACS* 2010		[a] C-hopping (CC)		not reported	

[a] Corresponds to interstrand hopping rate constant through same nucleobases.
[b] Corresponds to hopping rate constant across one nucleobase.
[c] Corresponds to interstrand hopping rate constant through different nucleobases.

However, the rate constants of excess-electron hopping were reported very recently compared to those of hole hopping. Our lab determined the rate constant of excess-electron

hopping through consecutive Ts in DNA to be 4×10^{10} s^{-1} and 6×10^{10} s^{-1} in our previous work and 2.2×10^{11} s^{-1} and 2.6×10^{11} s^{-1} as described in Chapter 2 and 3, respectively. The varied rate constants of excess-electron hopping were originated by increasing the driving force for excess-electron injection from the excited electron donor. The driving force for excess-electron injection can be equivalent to the thermal energy transferred to DNA, which causes structural fluctuation. These results revealed that excess-electron hopping process through consecutive Ts is faster than hole hopping process via consecutive Gs and As. Moreover, C can still be an excess-electron carrier although excess-electron hopping process through consecutive Cs is difficult to be observed due to the competitive proton transfer process in $G:C^{\bullet -}$, described in Chapter 2-1.

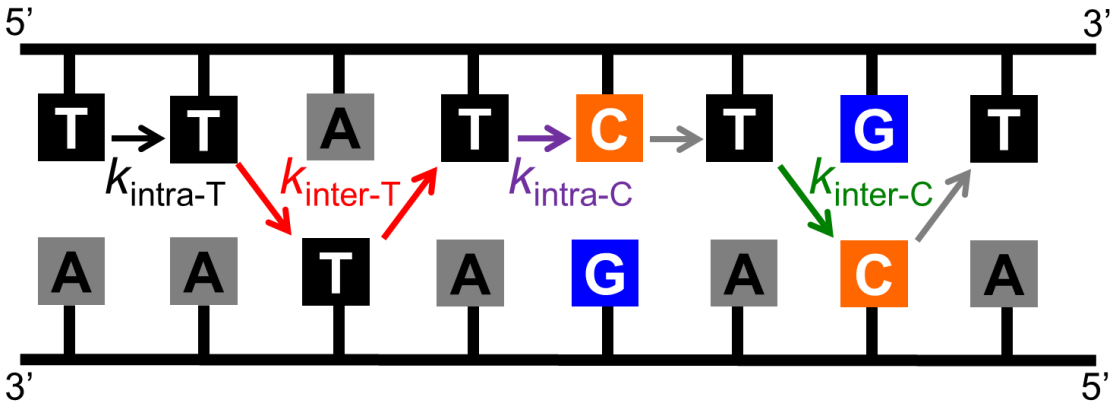

Figure 1. The basic hopping processes of EET in DNA and their rate constants. $k_{intra-T}$ is intrastrand T-hopping. $k_{inter-T}$ in interstrand T-hopping. $k_{intra-C}$ is intrastrand TCT-hopping. $k_{inter-C}$ is interstrand TCT-hopping.

Similar to hole transfer, excess-electron transfer is also sequence-dependent. Thus, the effect of intervening bridge base between primal excess-electron carriers, for example, TCT, TGT, and TAT was studied (Figure 1). Because the reduction potential of C is higher than that of T, the excess-electron transfer for TCT sequence is slower than that for consecutive Ts, described in Chapter 2-1. The rate constant of excess-electron hopping is reported that comparison between interstrand and intrastrand excess-electron hopping process, described in Chapter 2-2. As describing in Chapter 2-3, the interstrand excess-electron hopping (4.2×10^{10} s^{-1}, in TGT) rate is slower than that of intrastrand excess-electron hopping (1.0×10^{11} s^{-1}, in TCT) due to the lack of LUMO interaction. However, in another mechanism, the excess-electron hopping across G and C in TGT (1.0×10^{10} s^{-1}) and TCT (4.9×10^{10} s^{-1}),

respectively, are considerably affected by the tunneling energy gap originally from the reduction potential of G and C, respectively.

To fully understand CT in DNA, it is necessary to investigate both HT and EET in DNA as mentioned previously. However, the comparison values reported in this dissertation can be changed depending chromophores, structural change, which is arrangement of base pairs in DNA, its oxidation or reduction potential and so on. Thus, various dye-modified DNA sequences have to be synthesized and examined by using femtosecond laser flash photolysis and photoelectrochemical technique to determine i) the rate constant of excess-electron hopping through consecutive C's in DNA, ii) the rate constant of excess-electron hopping through non-B DNA, and iii) the temperature dependence of EET in DNA. The mechanisms and dynamics of EET in DNA will become clear in the near future.

General Conclusion

Throughout this dissertation, the mechanism and dynamics of EET (excess-electron transfer) in DNA have been thoroughly examined by photo-induced charge separation using femtosecond laser flash photolysis and photoelectrochemical technique.

In Chapter 1, the author developed various oligothiophenes as electron-donating photosensitizers for investigation EET in DNA using femtosecond laser flash photolysis. By use of strongly electron-donating oligothiophenes as electron donors, a panoramic survey of CS (charge separation) and CR (charge recombination) processes in dyads with all natural nucleobases as electron acceptors was accomplished on the basis of the Marcus theory. In addition, the conformation effect on CR was found, though major contribution of the stacked form was indicated in our results.

In Chapter 2-1, the author studied the role of a G:C base pair in dynamics of EET in DNA and observed sequence-dependent EET through oligonucleobases including G:C pair using a femtosecond laser flash photolysis technique. First, the dynamics of the PT (proton transfer) process of $G:C^{\bullet-}$ base pair were confirmed for the first time ($k_{PT} \sim 10^{10}$ s^{-1}). It suggests the rapid excess-electron trapping by proton transfer in $G:C^{\bullet-}$ base pair limits the participation of consecutive Cs in EET in DNA. Second, the author found the rate constant of single-step hopping in DNA oligomers is affected by the involvement of a G:C base pair: one G:C pair in consecutive Ts decreased the rate constant of single-step hopping to ~50%.

In Chapter 2-2, the interstrand EET dynamics in DNA through alternating A:T base pairs was investigated to clarify the effect of LUMO interaction on EET in DNA. Both rate constant and efficiency of interstrand EET are almost 2 times lower than those of intrastrand EET, due to the lack of π-stacking of Ts.

In Chapter 2-3, the author investigated the sequence dependence of photocurrent generation through long-distance EET in DNA by using photoelectrochemical techniques. According to our results, sequence dependence is essential for the photocurrent generation through DNA films on the Au electrode. Moreover, C was found to be as an electron carrier when a single G:C base pair inserts in consecutive Ts regardless C is next to T or not, though T was expected to play a major role as an excess-electron carrier.

In Chapter 3, the author confirmed that EET in DNA is governed by the hopping mechanism and successfully observed that the rate of excess-electron transfer can be enhanced with an increase in the driving force for charge separation, which is equivalent to

the thermal energy transferred to DNA. The author also found that the estimated intrinsic hopping rate ((3.8 ± 1.5) × 10^{10} s^{-1}) was consistent with the experimental and theoretical results, such as the frequency for DNA sugar backbone and base motions (3.3 × 10^{10} s^{-1}).

In short, the author successfully synthesized new electron donors and used dyad systems for evaluation of their electron donating ability. In addition, the author found the conformation of dyads is important for the CR process. Second, dynamics of EET in DNA has been confirmed to be strongly sequence-dependent. In addition, an agreement obtained between the results of photocurrent generation and those of femtosecond laser flash photolysis indicates electrical conduction in DNA originates from electron transfer through nucleobases via hopping mechanism. Third, the author found that the effect of fluctuation on excess electron hopping in DNA as an important factor, indicating that the fluctuation-assisted hopping mechanism prevails in EET in DNA. Moreover, the author has improved the EET distance to be 23.8 Å in the measurements using femtosecond laser flash photolysis.

To conclude, the author quantitatively studied the dynamics of EET in DNA by using femtosecond laser flash photolysis and photoelectrochemical technique and found that EET in DNA is sequence-dependent. The author believes these significant findings bring new insight into the dynamics and mechanisms of EET in DNA for researcher in the field of DNA and charge transport of conducting materials. Taken the understanding of EET in DNA from these experiments by using femtosecond laser flash photolysis and photoelectrochemical technique, the studies on EET in DNA and further improvements on bioelectronics will be developed over the next few decades.

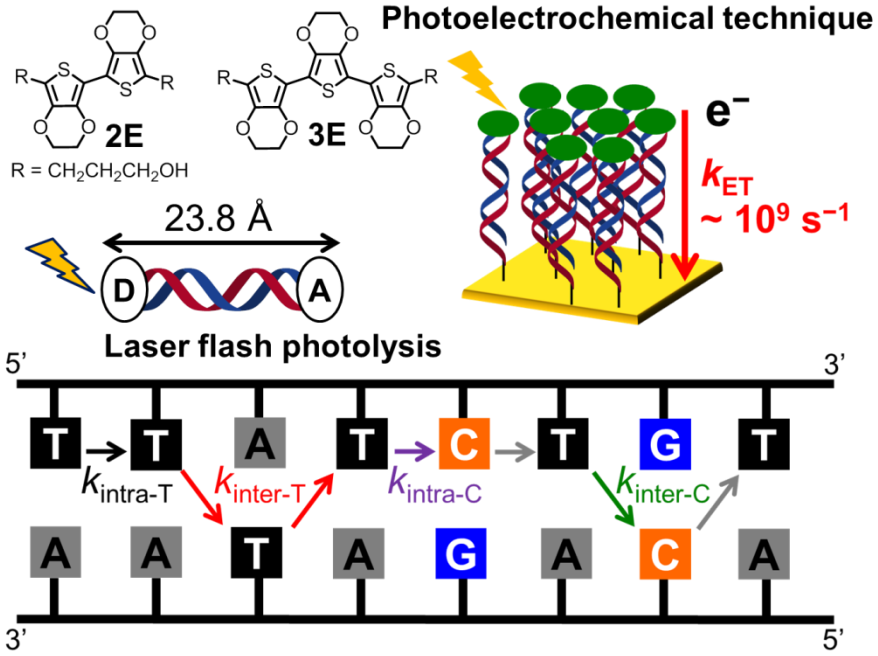

List of Publications

1. Driving Force Dependence of Charge Separation and Recombination Processes in Dyads of Nucleotides and Strongly Electron-Donating Oligothiophenes
   Shih-Hsun Lin, Mamoru Fujitsuka, Mayuka Ishikawa, and Tetsuro Majima.
   J. Phys. Chem. B **2014**, *118* (42), 12186-12191.

2. How Does Guanine−Cytosine Base Pair Affect Excess-Electron Transfer in DNA?
   Shih-Hsun Lin, Mamoru Fujitsuka, and Tetsuro Majima.
   J. Phys. Chem. B **2015**, *119* (25), 7994-8000.

3. Dynamics of Excess-Electron Transfer through Alternating Adenine:Thymine Sequences in DNA
   Shih-Hsun Lin, Mamoru Fujitsuka, and Tetsuro Majima.
   Chem. −Eur. J., **2015**, *21* (45), 16190-16194.

4. Excess-Electron Transfer in DNA by Fluctuation-Assisted Hopping Mechanism
   Shih-Hsun Lin, Mamoru Fujitsuka, and Tetsuro Majima.
   J. Phys. Chem. B, **2016**, *120* (4), 660-666.

5. Sequence-Dependent Photocurrent Generation through Long-Distance Excess-Electron Transfer in DNA
   Shih-Hsun Lin, Mamoru Fujitsuka, and Tetsuro Majima.
   Submitted.

Acknowledgements

The author would like to express the deepest appreciation to Professor Tetsuro Majima for his supervision with valuable suggestions and encouragements during the doctor course.

The author also wishes to express his sincere gratitude to Associate Professor Mamoru Fujitsuka for his helpful advices and deeply discussion. The author is deeply grateful to Associate Professor Kiyohiko Kawai, Assistant Professor Yasuko Osakada, Specially-Appointed Professor Mikiji Miyata, and Specially-Appointed Professor Akira Sugimoto for their helpful suggestions on his research.

The author expresses his appreciation to Professor Ikuya Shibata and Associate Professor Tadashi Mori, and all Professors of Department of Applied Chemistry, Graduate School of Engineering, Osaka University for their fruitful suggestions and comments on this dissertation.

The author sincerely thank to Associate Professor Tadao Takada, Specially-Appointed Assistant Professor Sooyeon Kim, Dr. Man Jae Park, Mr. Atsushi Tanaka, and Miss Mayuka Ishikawa for their kindly supports on his experiments. The author also thanks Miss Sanae Tominaga for her kindly helps on document preparation.

The author is grateful working with Dr. Peng Zhang and sincerely hopes for his brightly future of his research career. It is also his pleasure to work with members of Professor Majima's research group, including Dr. Zaizhu Lou, Mr. Tatsuya Ohsaka, Mr. Chao Lu, Mr. Ossama A. Elbanna, Mr. Xiaowei Shi, Miss Xiaoyen Cai, Miss Ayaka Kuroda, Mr. Kota Nomura, Mr. Yoji Yamamoto, Mr. Yuma Ichinose, Mr. Yang Zhou, Miss Jie Xu, and the past members of Professor Majima's research group.

Finally, the author expresses to sincerely thank to his family for their continuous encouragements enabled him to complete this study.

Shih-Hsun Lin

2016